MINISTRY OF HIGHER EDUCATION AND SCIENTIFIC RESEARCH

Mohamed Boudiaf M'sila University

Faculty of Technology

Civil Engineering Department

Serial number……

Registration Number D.GCM/3C/02/17

Thesis

Submitted for the degree of

Doctorate

Domain ; Civil Engineering

Speciality ; Materials

THEME

CHARACTERIZATION AND MODELING OF SELF COMPACTING CONCRETE (SCC) USING THE NON DESTRUCTIVE TESTING (NDT).

Presented by

ALLALI Ibtissem

Submitted ; 01 /02 / 2024

The jury composition

Surname & Name	Grade	Institution	Quality
KHEMISSA Mohamed	Professor	M'sila University	President
BEDDAR Miloud	Professor	M'sila University	Supervisor
BELAGRAA Larbi	Professor	M'sila University	Co-supervisor
MELLAS Mekki	Professor	Biskra University	Examiner
MEDDAH Abdelaziz	Professor	M'sila University	Examiner
MESBAH Habib Abdelhak	Professor	Rennes University	Invited

Academic year 2023/2024

ACKNOWLEDGEMENT

I would like to express my sincere gratitude to my supervisors professor ***BELAGRAA Larbi*** *and* ***BEDDAR Miloud*** *for their valuable guidance and concerns throughout this work. A particular thank is expressed to professor* ***MESBAH Habib abdelhak*** *for the valuable help given, from the university of Rennes, France. My thanks are extended to professor* ***AMMAR Yahia*** *and* ***MASOUD Hosseinpoor*** *from Sherbrooke university, Canada.*

Further, I would like to thank professor ***KHEMISSA Mohamed*** *the president of the jury as well as professor* ***MELLAS Mekki*** *from the university of Biskra and professor* ***MEDDAH Abdelaziz*** *from the university of M'sila for their interest in the present work by accepting to be examiners and jury members.*

*My acknowledgements and thanks are expressed to the technic staff of the Laboratory of civil engineering and mechanics (****LGCGM****) of the university of Rennes, France.*

My thanks to the laboratory staff and faculty dean and in particular Dr ***Kessal Oussama*** *and Dr* ***Noui Ammar*** *for the technical facilities provided from Bordj Bou Arréridj university to accomplish the experimental part of the research work for the present thesis.*

DEDICATIONS

I dedicate this work to ;

My parents ***Souames Fatima*** *and* ***Mohamed****, my brother* ***Mahfoud*** *and my two sisters* ***Maroua*** *and* ***Nour el houda****; who patiently encouraged and supported me all along the research period of my Ph.D.*

Thus to my friends ; especially ***OMRI Imen Yamina*** *and her family, to all those who love me and to those who have contributed directly or indirectly to the success of this work.*

ALLALI Ibtissem.

Abstract

The use of self compacting concret (SCC) is steadily gaining space and spreading to a variety of applications, thanks to their many technical and socio-economic advantages. However, the formulation of SCC is relatively complex and costly compared to conventional vibrated concrete, This is due to the use of these new constituents: admixtures and mineral additives, whether active such as granulated blast-furnace slag (S) and fly ash (FA) or inert such as limestone (L) and marble powder. The new developed product should guarantee at behavior in the fresh state. Moreover, the formulated SCCs are expected to achieve good mechanical performance and durability at the hardened state. The characterization of SCCs using the experimental design methods alongside with non-destructive testing (NDT) could be beneficial for the formultion of mixtures.

As a first step, the present study aims to the characterization and modeling by design of experimental plans method SCC based on inert limestone [L] and active mineral additions [S], where three degrees of fineness (2000, 3000 and 4000 cm^2/g) and dosages up to 20%) are employed for each type.

In a second approach, static stability (flowability without segregation) is assessed by means of non-destructive testing using a large-scale device (column) and electrical conductivity measurement using time domain reflectometrey (TDR) methods.

Lastly, a Computational Fluid Dynamics (CFD) program is used to model the flow of SCC concrete at the L-box, and a parametric study of SCC based on the addition of fly ash is carried out.

The results obtained in this study show that mathematical models issued from statistical analysis have been derived to predict surface mechanical responses and experimental test results observed in the correlation relationship using non-destructive testing (NDT). Furthermore, it was observed that the use of these additions (L, S) could be advantageous, while the degree of fineness proved to be important factors that affect the mechanical responses of SCC.

The measurement of static stability using the large-scale column test linked by the TDR method enabled us to simulate in site conditions for the flow of SCC.

In the end, the flow of SCC in the L-box is simulated; thus, to assess the effect of internal parameter (viscosity, yield stress, density and shear modulus) and external parameter (reinforcement density, L-box trap velocity and tribology) on the flow behavior, mainly the dynamic stability of SCC is modeled.Consecontly, the results of the present study propose equations to predict flow behavior as a function of these parameters.

Finally, it may be concluded that the proposed models play the role of a numerical laboratory, enabling us to simulate the flow of SCC without recourse to tedious laboratory testing.

Keywords; Self-compacting concrete (SCC), mineral additions, Design of experimental plans method, stability, computational fluid dynamics (CFD).

Résumé :

L'emploi du béton autoplaçant (BAP) ne cesse de gagner du terrain et se généralise à diverses applications grâce à leurs multiples avantages techniques et socio-économiques. Cependant, la formulation des BAP est relativement complexe et coûteuse par rapport à un béton conventionnel vibré par usage de ces nouveaux constituants; les adjuvants et les ajouts minéraux qu'il soit actif comme le laitier granulé de haut fourneau(S) et les cendres volantes (FA) ou inerte comme le calcaire (L) et la poudre de marbre. Ce nouveau produit développé devrait garantir son bon comportement à l'état frais. De plus, les SCC formulés sont supposés atteindre de meilleures performances mécaniques et de durabilité à l'état durci. La caractérisation des SCC en utilisant des méthodes de plans d'expériences à coté des méthodes non destructives (NDT) pourrait être bénéfique pour les BAP.

Dans un premier temps, la présente étude vise la caractérisation et la modélisation par des plans d'éxpériences de bétons autoplaçants à base de calcaire inerte [L] et d'ajouts minéraux actifs [S], lorsque trois degrés de finesse (2000, 3000 et 4000 g/cm^2) et des dosages allant jusqu'à 20 % g/cm^2) sont employés pour chaque type.

Dans une deuxième approche, l'évaluation de la stabilité statique (fluidité sans ségrégation) à l'aide d'un essai non destructif par un dispositif à grande échelle (column) et par la mesure de la conductivité électrique des méthodes de Time domain reflectometry (TDR) est entreprise.

Enfin, la modélisation par un programme Computational fluid dynamics CFD de l'écoulement du béton autoplaçant à la boite en L, ainsi qu'une étude paramétrique du béton autoplaçant basé sur l'ajout de cendres volantes (CV), sont réalisées.

Les résultats obtenus dans le cadre de cette thèse montrent que des modèles mathématiques issus de l'analyse statistique ont été dérivés pour prédire les réponses mécaniques de surface et les résultats des tests expérimentaux observés dans la relation de corrélation en utilisant des tests non destructifs (NDT). En outre, il a été observé que l'utilisation de ces ajouts (L, S) pourrait être avantageuse, tandis que le degré de finesse s'est avéré être un facteur d'influence important, principalement, sur les réponses mécaniques pour les BAP étudiés.

Ainsi la mesure de la stabilité statique par l'essai de la colonne de grande échelle relier par la méthode TDR nous a permis de simuler les conditions réel de l'écoulement du béton autoplaçant.

A la fin, l'écoulement du béton autoplaçant dans la boîte en L ; ainsi pour évaluer l'effet du paramètre interne (viscosité, seuil de cisaillement, densité et module de cisaillement) et du paramètre externe (densité de l'armature, vitesse de la trappe de la boîte L et la tribologie) sur le comportement de l'écoulement, principalement la stabilité dynamique des bétons autoplaçants est modélisée. Par conséquent, les résultats de la présente étude proposent des équations pour prédire le comportement de l'écoulement en fonction de ces paramètres.

Enfin, on pourrait conclure que les modèles proposés jouent le rôle d'un laboratoire numérique où il nous permet de simuler l'écoulement du SCC sans avoir recours au fastidieux test en laboratoire.

Mots clés; Béton autoplaçant (BAP), ajouts minéraux, Méthodes du plan d'expériences, stabilité, computational fluid dynamics (CFD).

ملـخــص
يستمر استخدام الخرسانة القابلة للصب ذاتيًا في الانتشار في التطبيقات المختلفة بفضل مزاياها التقنية والاجتماعية الاقتصادية، رغم ان صياغة هد النوع من الخرسانة معقدة نسبيًا ومكلفة مقارنة بالخرسانة التقليدية لاحتوائه على مكونات جديدة؛ اللملدنات والإضافات المعدنية سواء كانت نشطة مثل حبيبات خبث الافرن العالي والرماد المتطاير أو خاملة مثل الحجر الجيري ديمومة؛ ومسحوق الرخام يجب أن يضمن هذا المنتج المطور حديثًا خصائص جيدة في الحالة السائلة ،الحالة الصلبة وكذل تعتبر دراسة سلوك الخرسانة القابلة للصب ذاتيا باستخدام طرق تصميم التجارب جنبا الى جنب مع الطرق الغير مدمرة مفيدة للخلائط المُصاغة.
في البداية، تهدف الدراسة الحالية إلى التوصيف والنمذجة من خلال الخطط التجريبية للخرسانة القابلة للصب ذاتيًا على أساس الحجر الجيري الخامل والإضافات المعدنية النشطة لخبث الافرن عند ثلاث درجات من النعومة (2000، 3000 و4000 غ / سم ^{2}) وجرعات تصل إلى 20٪ غ / سم ^{2}) لكل نوع.
وفي المقاربة الثانية، يتم تقييم الاستقرار الساكن (قابلية التدفق دون الفصل) باستخدام الاختبار غير المدمر باستخدام جهاز واسع النطاق (عمود) بطرق قياس انعكاس المجال الزمني وعن طريق قياس الناقلية الكهربائية.
اخيرًا، يتم تنفيذ النمذجة بواسطة برنامج ديناميكية الموائع الحسابية لتدفق الخرسانة القابلة للصب ذاتيًا في العلبة ل، بالإضافة إلى دراسة حدودية للخرسانة القابلة للصب ذاتيًا على أساس إضافة الرماد المتطاير.
تظهر النتائج التي تم الحصول عليها في هذه الرسالة أن النماذج الرياضية من التحليل الإحصائي تم اشتقاقها للتنبؤ بالاستجابات الميكانيكية السطحية ونتائج الاختبارات التجريبية التي لوحظت في علاقة الارتباط باستخدام الاختبار غير المدمر. علاوة على ذلك، لوحظ أن استخدام هذه الإضافات يمكن أن يكون مفيدًا، بينما تم العثور على درجة النعومة كعامل مؤثر مهم، بشكل أساسي، على الاستجابات الميكانيكية للخرسانة القابلة للصب ذاتيًا.
أيضا إن قياس الاستقرار الساكن عن طريق اختبار العمود الكبير المتصل بطريقة قياس انعكاس المجال الزمني سمح لنا بمحاكاة الظروف الحقيقية لتدفق الخرسانة القابلة للصب ذاتيًا.
في النهاية، تدفق الخرسانة القابلة للصب ذاتيًا في العلبة ل؛ وبالتالي لتقييم تأثير العوامل الداخلية (اللزوجة وعتبة القص والكثافة ومعامل القص) والعوامل الخارجية (كثافة التسليح وسرعة باب العلبة ل والترايبولوجي) على سلوك التدفق، تمت نمذجته لتصميم الاستقرار الديناميكي للخرسانة القابلة للصب ذاتيًا بشكل أساسي.
الخرسانة القابلة للصب ذاتيًا وفقًا لهذه المعاملات تقترح نتائج الدراسة الحالية معادلات للتنبؤ بسلوك تدفق
أخيرًا، يمكن أن يستنتج أن النماذج المقترحة تلعب دور المخبر الرقمي حيث تسمح لنا بمحاكاة تدفق دون اللجوء إلى الاختبار المخبري الشاق.

الكلمات المفتاحية؛
الخرسانة القابلة للصب ذاتيًا، الإضافات المعدنية، طرق التصميم التجريبية، الاستقرار، ديناميكيات السوائل الحسابية.

TABLE OF CONTENTS

PART TWO. Experimental part.

PART THREE. Modeling part.

LISTE OF FIGURES

LIST OF TABLES

Abbreviations

SCC Self-compacting concrete.

SF Slump Flow.

VF V funnel.

t_{VF} V funnel time.

AFGC French Civil Engineering Association.

HA High adhesion.

CSH Hydrated calcium silicate

CEM II A 42.5 Compound Portland cement CPJ.

CEM I 52.5 N Portland cement.

S Granulated blast-furnace slag.

FA Fly ash.

L Limestone.

SP Super plasticizer.

BSS Specific Surface of Blaine.

D Content of filler (%).

ρ_s Absolute density (g/cm^3).

ρ Bulk density (g/cm^3).

P Porosity (%).

C Compactness (%).

E Void Index (%).

E_s Sand modulus (%).

Ab Water absorption (%)

W Water content (%)

LA Los Angeles(%).

τ The shear stress[Pa].

τo Shear yield stress [Pa].

μp Plastic viscosity [Pa.s].

γ The shear rate [s^{-1}].

Rc Compressive strength (MPa).

FS Flexural strength (MPa).

Ft Flexural tensile strength (MPa).

NDT Non-destructive testing.

UPV Ultrasonic Pulse Velocity (m/s).

I Sclerometer index.

TDR Time domain reflectometry.

EDM Experimental design methods.

ANOVA Analysis of variance.

SI Stability index.

BI Bleeding index.

HI Homogeneity index.

CFD Computationalfluid dynamics.

VOF Volume of fluid method.

GMO Moving object technique.

NSE Navier -Stokes equations.

STL **St**ereo-**L**ithography.

General Introduction

Self-compacting concrete (SCC) requires a specific formulation that contains two components more than an ordinary concrete ; these two components are the admixtures and the mineral additions that it is active such as silica fume, granulated blast furnace slag and fly ash or inert such as limestone and marble powder; this complicates the mix dosages for SCC formulation.

This innovative concrete differs from other types of concrete by its high fluidity which allows it to be placed without any vibration ; this serves to limit the laboriousness of the workers and to reduce noise pollution on the building sites. Moreover, this new devolped product ensure its capacity of passage in the strongly reinforced environments and presents a good quality of the facads outlook. Nevertheless, its high fluidity can make it more susceptible to dynamic or static instability or even bleeding.

Firstly, the main objective of the use of inert (limestone) or active (slag) mineral additions in our research subject is to propose formulations of SCC with better performance by relying on an experimental approach based on design of experiments software. As well as a correlation study between the different properties by means of non-destructive tests in order to find a relation for the prediction of the mechanical response according to the other variables (percentage of the mineral addition and their specific surface of Blaine (BSS), is envisaged. This quality of SCC ensures good rheological characteristics at the fresh state, good mechanical strength and durability in the hardened state. Further, its economical and ecological advantages by the recovery of industrial waste as mineral additiond could be evaluated with much more beneficial use.

Secondly, the characterization and modeling of the stability (limited segregation) of SCC as a primary characteristic not only to have a flow, a capacity of passage and suitable implementation, but also to have good mechanical characteristics and achieve better transport properties and satisfactory durability.

A considerable effort has been made by civil engineering researchers to develop reliable tests to characterize the resistance of SCC to static segregation and to bleeding. In spite of the diversity of the tests developed specifically to evaluate the stability of these concretes, it remains that none of these tests allows an evaluation of the dynamic and static stability of SCC in an optimal way. Because, these tests are on a reduced model and do not simulate real flow conditions, in this case the concrete might have a higher risk of segregation which could lead to blocking during flow in casting operation.

The objective of this second approach is to experimentally characterize the stability of SCC concrete by means of non-destructive testing (NDT); static stability using a column of 1.5 m height, by associating the method of electrical conductivity according to the principle of TDR (Time Domain Reflectometry).

Thus, numerical simulations of the SCC flow are established by the Flow 3D software using dynamic flow models. The results of the numerical simulations are compared to the experimental results.

The numerical modeling is used to better characterize and predict the flow performance of this SCC formulated ; therefore, in the end it plays the role of a numerical laboratory.

A parametric study is consiedred through numerical simulations; in order to evaluate the effect of rheological parameters (plastic viscosity and shear yield stress), density, tribology as well as density and arrangement of reinforcements on the stability of the SCC. Our current contribution is concretized by new formulations based on the correlation models between the various factors by means of NDT tests. Consequently ; recommendations in the case for the flow of SCC at the fresh state as well as the mechanical response at the hardened state are proposed in the present numerical analysis study.

Structure of the thesis

The thesis is devided into seven chapters as follows ;

- General Introduction.
- **PART ONE. Literary review on SCCs ;**
  - Chapter I. General concepts on SCC ;

    Definition, history, advantages, disadvantages, formulation, and technical recommendations for SCC. Also the mineral additions.

  - Chapter II. Rheology, flow, dynamic and static stability of SCC at the fresh state;

    This chapter presents notions of rheology, dynamic and static stability of SCC. Further, it describes parameters affecting the stability of SCC.
  - Chapter III. This chapter provides details on desrtuctive and non destructive tests (NDT) as well as a state of the art on destructive and NDT applied to SCC at fresh and hardened state.

- **PART TWO. Experimental part ;**
  - Chapter IV. Materials, Formulations and Tests carried out on SCC ;

    Caracterisation of the basic materials, description the methods of formulations and tests carried out on SCC.

- Chapter V. Experimental Results and Discussion;

Presentation and interpretation of the results obtained from the experimental testing program is given in this chapter.

- PART THREE. Modeling part;

- Chapter VI. Experiments design plan methods (JMP) ;

This chapter highlights the principle of Experimental Design Plans method (EMD). Also, the presentation and the interpretation of the results obtained from the modeling of the mechanical responses by (JMP) software method is provided.

- Chapter VII. Computational fluid dynamics CFD (FLOW 3D) ;

In this part principles of Computational fluid dynamics are presented. Further, the presentation and interpretation of the results obtained from the modeling of the flow of SCC using FLOW 3D software is detailed.

- General conclusion.

The thesis ended with a general conclusison that includes the main outcome of the present study.

PART ONE.

Literature review on SCCs.

Chapter I.

General concepts on SCC.

I.1 General concepts on SCC

I.1.1 Definition

Self-compacting concrete also called easy placing concrete, self-leveling concrete or self-consolidating concrete; is an innovative concrete which differs from other types by its higher fluidity.This allows it to be placed without any vibration.

I.1.2 History

Concrete is the most widely used construction material in the world, both in the civil engineering and public works sectors.

Concrete has existed for thousands of years and its oldest form dates back to 7000 BC when the Egyptians and Romans developed a material similar to concrete; but the real appearance of concrete in its present form is due to the invention of cement by Joseh Aspidin in 1824 (Belagraa, 2015). Later the creation of the first cement factory by Dupont and Demarle in Boulogne sur mer in France toke place.

Since the discovery of ordinary concrete and for many decades, this material had not been developed much, but from the 1970s-1980s, significant advances have been made that have allowed the diversity its field of use. Looking for good mechanical strength and durability different family of concrete appeared in this period such as high performance concrete HPC, the concrete with very high performance VHPC, fiber metal concrete FMC and reactive powder concrete RPC (Belghit, 2009).

In the late 1980s, SCC was developed by a group of researchers at the University of Tokyo in Japan (Okamura and al, 1999). The idea was to develop a fluid concrete to solve the problem of excessive reduction in the number of skilled workers in Japan to ensure proper placement.

Ten years later, self-compacting concrete was introduced in Europe by Sweden, and then it was rapidly integrated in other Scandinavian countries, as well as in other European countries such as France, Netherlands, Germany and the United Kingdom, and even in North America and Canada (Goodier, 2003). Today, SCC is being developed all over the world and tends to replace ordinary concrete.

I.1.3 Advantages and disadvantages

I.1.3.1 Advantages

SCC has not only technical advantages but also socio-economic and ecological advantages (Djebri, 2018).

a) Technical advantages

- Placing by pumping and without any vibration.
- Capacity of passage in the denser mediums areas.
- Possibility of realization of elements of complex geometrical form.
- Ensures a resistance and a durability superior to that of an ordinary concrete.
- Presents a good quality of facades.

b) Socio-economic benefits

- Increasing the rate of productivity and time saving.
- Limitation of the laboriousness of workers and the building sites safety ensurance.
- Reduction of noise pollution on the construction sites and in the manufacturing plants.
- Eliminating costly tasks that require a qualified workforce.

c) Ecological advantages

- Valorization of the waste which enters in the formulation of the SCC.
- Limition of the cement production that depletes natural resources further to CO_2 emission that causes the greenhouse effect.

I.1.3.2 Disadvantages

Complication in the dosages of designed mixtures due to the specific and expenssive formulation. The additional components are the admixtures and the mineral additions as new constituents compared to ordinary concrete.

I.1.4 The constituents of SCC

SCC contains six components; which are ;

a) Aggregates

Aggregates are inert grains with dimension varies from 0 mm to 40 mm; it can be sand, gravel. The origin of such materials can be natural or artificial.

The rolled or crushed aggregates in accordance with the standard EN 12620 (NF EN 12620+A1, 2008) is suitable for the confection of SCC and this alows to avoid the risks

of blockage (AFGC, 2008) and limits the maximum diameter of the gravel between 10 mm and 20 mm.

b) Cement

Cement is a hydraulic binder capable of setting with water; it contains mainly clinker which is obtained by firing at high temperature above 1450°C a mixture of 80% limestone and 20% clay, and possibly additions such as granulated blast furnace slag, pozzolan ... etc.

In fact, all types of cement conforming to the NF EN 197-1 standard (NF EN 197-1, 2020) are suitable for making SCC; but the portland cement CPA-CEM I 42.5 containing at least 95% of clinker remains the most suitable for varying and controlling efficiently the introduction of mineral additions in SCC.

c) Water

The mixing water must be clean and it must not contain an excess of impurities that can affect the strength of the concrete, the aesthetic behavior and cause corrosion of the reinforcement.

The quantity of water in a SCC mix must be well determined in order to obtain the desired workability without segregation or bleeding.

d) The admixtures

d.1) Superplasticizer

Superplasticizers are additive products with very long macromolecular chains defined by the standard NF EN 934-2 (NF EN 934-2+A1, 2012); their main action is to deflocculate the cement grains by electrostatic repulsion acts, that is by neutralizing the electric charges present on the surface of the grains and / or by steric repulsion, that is by separating the grains from each other (Baron J and al, 1999).

The use of superplasticizer allows to obtain a very fluid concrete with a low W/C ratio, nevertheless, it is necessary that the superplasticizer is compatible with the cement.

d.2) Viscosity agents

Viscosity agents are organic products that make SCC less sensitive to bleeding and segregation. These colloidal suspensions have an action opposite to that of superplasticizers, so it is recommended to use a coupled compatible viscosity agent ad superplasticizer.

e) Mineral additions

Mineral additions are fillers that do not exceed 80 micrometers. Fillers comes from the English word "to fill" (Djebri, 2018). There are inert mineral additions that do not present any chemical reaction during the mixing (Belagraa, 2015), and active mineral additions that present pozzolanic reactions or hydraulic reactions during the mixing.

The mineral additions is a primary component in the formulation of SCC. These fillers are used to improve the characteristics in the fresh and hardened state of the SCC according to their size, their geometry and their chemical compositions (El hilali, 2009).

I.1.5 Formulation approaches of SCC

There are several approaches to formulating SCC througout the word. All these approaches aim to produce a homogeneous and stable SCCs without bleeding and static or dynamic segregation.

According to literature the following could be cited;

a) Japanese approach

Japanese approach or method based on mortar optimization; this approach is developed by Japanese researchers (Okamura and al, 1999), Okamura and Ozawa (Okamura and al, 2000), (Okamura and al, 2003) at Kochie University.

The principle of this approach is to keep the quantity of aggregate as a fixed amount. The quantity of chippings is limited to 50% of their compactness and the quantity of sand is limited to 40% of the volume of mortar.The dosage of water and superplasticizer is determined experimentally by the spreading test and the funnel flow test (V-funnel). The Japanese method leads to formulate very expensive SCC because of the need for a large quantity of paste.

b) Swedish approach

Swedish approach or optimization approach of the volume of paste (Van Khanh and al, 1999); in this approach the concrete is considered two-phase with a solid phase (aggregates) and a liquid phase (paste). The paste of a SCC plays a double role; it fluidizes the mixture to avoid the intergranular friction and it allows to avoid the risk of blocking. The principle of this method is

to determine the minimum volume of paste to achieve a good filling rate to the L-box and the minimum volume of paste to achieve an acceptable workability spread of the produced concrete mix.

c) French approach

French approach or optimization approach of the granular skeleton proposed by Sedran and De Larrard (Sedran and al, 1999) (Sedran, 1999) (De Larrard, 2000). The principle of this approach is based on a mathematical model "Solid suspension model". This model is implemented in the software Rene-LCPC. The data introduced in the software are: the granulometry, the density, the compactness specific to each constituent and the dosage of saturation in superplasticizer. The dosage of viscosity agent is not taken into account. This approach has been validated for SCC that have the following rheological conditions (Chekireb, 2015) ;

- A shear yield stress less than or equal to 400 Pa.
- A plastic viscosity less than or equal to 200 Pa.s.

This approach leads to an economical formulations in a short time and does not require much trial tests.

d) North American Approach

The principle aim of the North American approach is to ensure a low shear rate and moderate viscosity. The first method is a combination of the Japanese approach and the high performance concrete (HPC) mix design method. It is based on a low W/L ratio and the use of mineral additives to increase the mechanical performance of the HPC, while the second method is based on the use of viscosity agents (Bonen and al, 2005).

I.1.6 Technical recommendations for SCC Formulation

The recommendations and standards concerning the formulation of SCC require certain technical specifications. It is necessary that all these specifications are met for the formulated concrete to be defined as SCC.

I.1.6.1 At the fresh state

The various technical quality control tests of SCC in the fresh state are ;

a) Slump flow test

The slump flow test allows to evaluate the fluidity and the capacity of passage of the concrete in the unconfined media; the larger the diameter of the spreading, the more fluid the concrete is and thus able to pass in the unconfined media.

The acceptability criteria related to the slump flow test are presented in the following table

Table II-1. Conformity criteria for fresh SCC according to their slump flow (NF EN 12350-8, 2019).

Spread class	Criteria
SF1	520 mm ≤ SF ≤ 700 mm
SF2	640 mm ≤ SF ≤ 800 mm
SF3	740 mm ≤ SF ≤ 900 mm

SF ; Slump Flow.

b) The V-funnel test

The V-funnel test allows us to estimate the viscosity of the concrete and the filling capacity. The longer the time to empty the funnel, the more viscous the concrete is. A low viscosity means a risk of segregation, but a high viscosity reduces the filling capacity. The acceptability criteria for the funnel test are presented in the following table.

Table II-2. Criteria of conformity of fresh SCC according to their viscosity (NF EN 12350-9, 2010).

Viscosity Class for V-funnnel test	Criteria
Class viscosity VF1	$t_{VF} \leq 8$ s
Class viscosity VF2	9 s ≤ t_{VF} ≤25 s

VF ; V funnel, **t_{VF} ;** V funnel time.

c) L-box test

The L-box test allows us to evaluate the dynamic stability and flow capacity in confined environments. The higher the L box ratio H2/H1 recorded, the concrete is considered to be as much more homogeneous with a good flow capacity and better dynamic stability. The acceptability criteria related to the L-box test are presented in the following table.

Table II-3. Compliance criteria for fresh SCC according to their flow in the L-box (NF EN 12350-10, 2010).

Class	Criteria
Flow class PL1 (2 bars)	PL ≥ 0,80
Flow class PL2 (3 bars)	PL ≥ 0,80

d) Sieve stability test

The sieve stability test evaluates the static segregation of concrete; the higher the segregation rate, the more static instability the SCC is occuring in mixtures. The acceptability criteria for the sieve stability test are presented in the following table.

Table II-4. Conformity criteria for fresh SCC according to their resistance to segregation (NF EN 12350-11, 2010).

Class	Criteria
Resistance ségrégation class RS1	RS ≤ 20 %
Resistance ségrégation class RS2	RS ≤ 15 %

RS ; resistance to segregation.

I.1.6.2 At the hardened state

The various technical quality control tests of SCC at the hardened state are compressive strength, tensile strength and Young's modulus at 28 days of age. However, the compressive strength is the only property commonly tested, it varies between 30 and 60 MPa at 28 days (Zied, 2021).The compressive strength of a SCC is higher than an ordinary concrete and the tensile strength presents 10% of the compressive strength (Bensalem and al, 2014).

I.2 Mineral additions

I.2.1 Active mineral additions

a) Silica fume

Silica fume is a by-product of the manufacture of silicon, it is composed mainly of silica (SiO_2).These fumes have pozzolanic properties that is, silica reacts with lime during the hydration of cement and produce hydrated calcium silicates (C-S-H).

Silica fume has been used in high performance concretes HPC and very high performance concretes UHPC, currently silica fume is widely used in different types of self-compacting Concretes SCC, namely fibrous self-compacting concretes FSCC (Hilal and al, 2022), recycled aggregate SCC (Zhanggen Guo and al, 2022) and geopolymer SCC (Velrajkumar G and al, 2022).

Silica fume used as blending cement improves the mechanical properties and durability of SCC (Qin and al, 2022) and decreases the brittleness (Wang and al, 2022).Nevertheless, silica fume decreases the spread ability of SCC (Çelik and al, 2022).

b) Blast furnace slag (S)

Blast furnace slag is a by-product of the steel industry that comes from the manufacture of iron.Itis composed of four elements: Lime (CaO), magnesia (MgO), silica (SiO_2) and alumina (Al_2O_3).

The slag is produced by melting iron ore, cokes, mineral additions and a flux during the firing process. The slag is isolated by flotation. When cooled rapidly, the slag is vitrified (granulated) and has a glassy structure, and when cooled slowly, the slag is crystallized and has a stable crystal structure.

An average proportion of 300 kg of slag for one ton of cast iron can be produced (Laifa, 2015).

Today slag has become a valuable construction material and not just an industrial waste product. Slag is used as a partial replacement of cement alone (Faraj and al, 2022) or combined with other filler such as fly ash (Mohammed and al, 2022) (Elsayed and al, 2022) (Vivek, 2022) or even as a total replacement of cement in geo-polymer SCC (Rautaray, 2022).

The use of slag in SCC improves workability, mechanical performance such as compressive strength, tensile strength or even flexural strength (Al-Oran and al, 2022) (Bharathi and al, 2022).

I.2.2 Inert mineral additions

a) Limestone fillers (LF)

The limestone filler is an inert addition. It does not react chemically or little with the cement in the presence of water, this fine mineral contains mainly $CaCO_3$ and is obtained by grinding a natural limestone rock for the production of aggregates (Kherraf, 2018).

Limestone filler is widely used in SCC and fibrous composites (Karimipour and al, 2021) (Kavitha and al, 2022).

The shape, the percentage of addition of filler to cement and the fineness of these filler influence the SCC properties (Benjeddou and al, 2021).

The use of limestone filler in the SCC improves their performance (Daoud and al, 2020) whether it is the rheological properties (Yang and al, 2021) or mechanical (Alani and al, 2021). Moreover, it improves the durability of SCC (Rahman and al, 2023).

I.3 Conclusion

This chapter includes the main notions on SCC, definition, history, essentiel properties and advantages as well as inconvenients. The aprroaches used so far for SCC formulations, its constituents beside the additions and admixtures to be incorporated in the SCC compositions are descibed in the sections above.

Chapter II.

Rheology, flow, dynamic and static stability of SCC at the fresh state.

II.1 Rheology

II.1.1 Definition

Rheology is a branch of continuous media mechanics that is used to study the deformation and flow of material following an applied stress. This science is used to characterize materials in the fresh state such as (paint, cementitious materials and concretes...etc).

II.1.2 Rheological behavior

- Newtonian fluid; the fluid is Newtonian if its viscosity remains always constant and does not vary with the variation of the shear rate.

- Non-Newtonian fluid; the fluid is non-Newtonian if its viscosity is variable. Among the non-Newtonian fluids we find;

A-Pseudo-plastic fluid (Rheofluidifiant); the fluid is pseudo-plastic if its viscosity decreases with the increase shear rate.

b- Dilatant fluid (Rheo-thickening); the fluid is dilatant if its viscosity increases with the increase of the shear rate.

c- Thixotropic fluid; the fluid is thixotropic if its viscosity decreases as long as a constant shear stress is applied. This deformation is reversible. The fluid is restructured after acertain time, when the applied stress is removed.

d- Rheopectic fluid (anti-thixotropic); rheopectic fluid is the opposite of thixotropic fluid. But very rare, its viscosity increases when a constant shear stress is applied. This deformation is reversible.

II.1.3 Rheological parameters

-Viscosity; the viscosity is a physical quantity used to describe the behavior of fluids [Pa.s]. It is an intrinsic property of the material that depends on the morphology and internal attraction forces of the chemical structure of the material, as well as external forces applied.

The viscosity **μ;**

$$\mu = \tau / \gamma \qquad [Pa.s] \qquad \text{(Eq II-1)}$$

Where;

τ : Shear applied stress **;** is the resulted due to the application of force **F** on the surface of area **A**

$$\tau = F / A \quad [Pa] \qquad \text{(Eq II-2)}$$

γ; the shear rate; it is the difference in velocity **DV** between the layers of the fluid in a distance **d**.

$$\gamma = DV / d \quad [s^{-1}] \qquad \text{(Eq II-3)}$$

-Shear yield stress; the shear is a shear stress above which the fluid begins to flow. The static shearis obtained at a zero shear rate and usd to evaluate the effort needed to initiate the flow.The dynamic shear is determined on a material at rest or when the shear rate is very low, it is determined to evaluate the stop of the fluid flow. The static shear is always higher than the dynamic shear (Daddy Kabagire and al, 2018).

II.1.4 Behavioral law

There are several mathematical models to describe the rheological behavior of cementitious materials. The simplest and therefore the most used is the Bingham model.

The Bingham model ;

$$\tau = \tau o + \mu p \gamma \qquad \text{(Eq II-4)}$$

Where; **τ;** The shear stress [Pa].

τo ; Shear yield stress [Pa].

μp ; The plastic viscosity [Pa.s].

γ; The shear rate [s^{-1}].

In the case of highly viscous fluids where the Bingham model provides negative shear threshold values, we must use other nonlinear and more complex models such as the Herschel-

Bulkley model or the modified Bingham model; but these two models provide only one parameter (the shear threshold).

Herschel-Bulkley model;

$$\tau = \tau o + K \gamma^n \quad \text{(Eq II-5)}$$

where; **K ;** consistency coefficient.

n ; Flow index;

if ;

n< 1 ; Pseudo-plastic fluid.

n> 1 ; dilatant fluid.

n = 1; Bingham fluid.

Bingham modified model; $\tau = \tau o + \mu p \gamma + C \gamma^2$ (Eq II-6)

Where; **C;** Second order parameter [$Pa.s^2$].

II.1.5 Rheology of SCC

SCC is a non Newtonian elastoviscoplastic fluid; where a yield stress is required to intiate their flow. SCCs require a yield strees less than the ordinary concrete which facilitates the flowability of the mixes.

The rheological parameters of ordinary concrete can vary from 500 to 2000 Pa and 50 to 100 Pa.s for yield stress and plastic viscosity values, respectively. However, SCC yield stress and plastic viscosity values are in the range of 50 to 200 Pa and 20 to 100 Pa, respectively (Hosseinpoor, 2016),

At the same time SCC is a thixotropic material; where the thixotropy is the increase of their viscosity over time and in function of the history of the flow. Thixotropy is a physical reversible phenomenon or sufficiently vigorous mixing can erase the consequences of a long rest time on the state of structuring of SCC. But, no mixing can not reverse chemical reactions. The viscosity may also increase due to the cement hydration process.

Thixotropy has a positive effect on vertical casting where the increase in the viscosity of the SCC reduces the hydaustatic pressure exerted by the concrete on the formwork. But the thixotropy can cause a multi-layer in horizontal casting because the SCC freezes rapidly due to the increase of theire viscosity and discontinuity in casting time could result in heterogeneity of mixtures (Roussel, 2008).

II.2 Flow of SCC

The flow performance of concrete can be evaluated by measuring the flow and filling capacity.

II.2.1 Filling capacity

Filling capacity is the ability of concrete to flow under its own weight through unconfined media. Standardized tests developed to evaluate the flow capacity such as the Slump flow test (NF EN 12350-8, 2019) and the V-funnel test (NF EN 12350-9, 2010).

a) Slump flow test [NF EN 12350-8]

The test is performed using the Abrams cone. The same cone used to perform the slump test. The procedure for this test is to place the cone on a clean, moistened plate of sufficient diameter, then fill it with SCC, after that we lift the cone and let the concrete flow under its own weight. Finally, we measure the average diameter of the cake on two orthogonal diameters d moy = (d1+d2)/2 the bigger the diameter the more fluid the concrete (NF EN 12350-8, 2019).

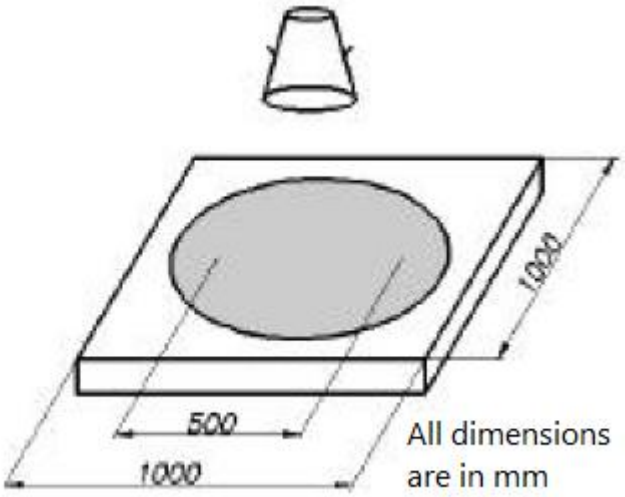

Figure II-1. Slump flow test (EFNARC, 2002).

b) Funnel flow test (V-funnel) [EN 12350-9]

The V-funnel test consists of filling the funnel with SCC and then opening the valve at the bottom and timing the time required for the SCC to flow completely out of the funnel (NF EN 12350-9, 2010).

Figure II-2. V-funnel test (NF EN 12350-9, 2010).

II.2.2 Flowability Ease of passing

Flowability is the ability of concrete to flow under its own weight through confined spaces. Several tests have been developed to evaluate flow capacity such as the L-box test (NF EN 12350-10, 2010), the ring flow test (NF EN 12350-12, 2010) and the U-box test (EFNARC, 2002).

a) L-box test [EN 12350-10]

The L-box test consists of filling the vertical part of the box with SCC then opening the trap door and letting the concrete flow to the horizontal part. The difference in height in the vertical and horizontal parts is measured and the result is expressed by the blocking ratio B_R=H2/H1. According to the French Civil Engineering Association (AFGC) for the SCC to be accepted. The filling ratio (H2/H1 ratio) of the L-box must be higher than 0.8 (NF EN 12350-10, 2010).

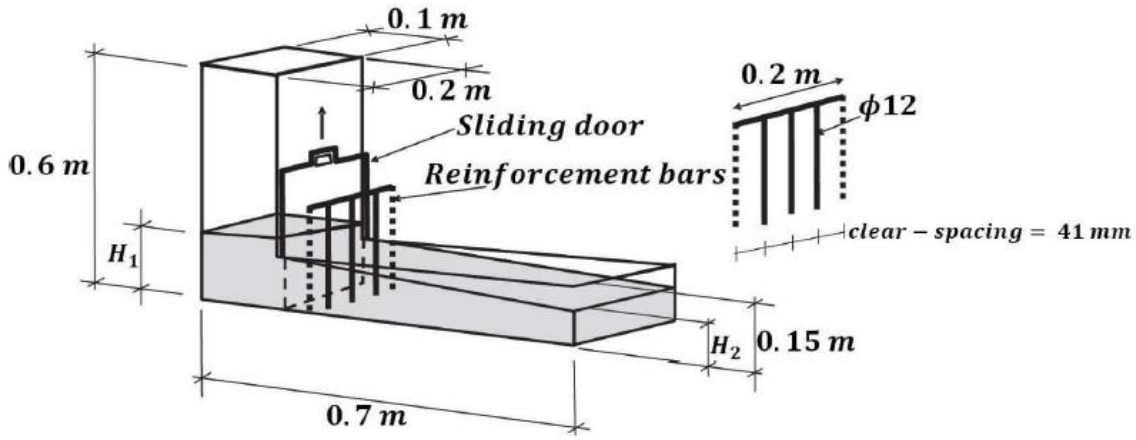

Figure II-3. L-box test (EFNARC, 2002).

b) Ring flow test (J-ring) [EN 12350-12]

The ring flow test, also known as the modified spread test, is carried out using a ring fitted with 16 or 18 high adhesion (HA) reinforcing rods with a diameter of 16 mm spaced 5 cm apart. At the end of the test, the diameter of the cake obtained is measured. Thus we measure the heights at the center (hint) and outside (hext) of the ring (NF EN 12350-12, 2010).

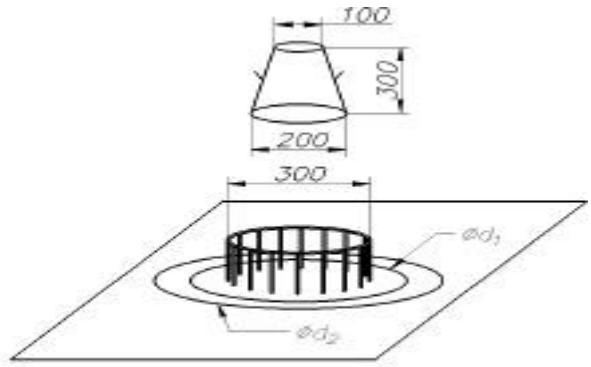

Figure II-4. J-ring test (EFNARC, 2002).

c) Testing the U-box

The U-box test consists of filling the upper part of the U-box with concrete and then opening the trap door so that the concrete can pass through the 13 mm reinforcement to the second part of the box. For the concrete to qualify as self-compacting, it must reach a fill height greater than or equal to 30 cm (EFNARC, 2002).

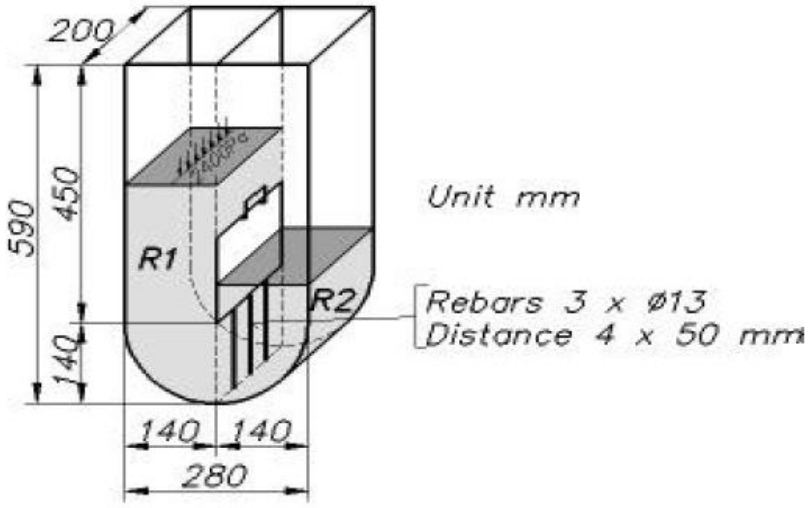

Figure II-5. U-box test (EFNARC, 2002).

II.3 Dynamic and static stability of SCC

SCC has a very high fluidity which makes it more sensitive to segregation during flow (dynamic segregation) and in the resting state after placement (static segregation).

II.3.1 Dynamic Segregation

Dynamic segregation is the separation of aggregates from the mortar in suspension during the flow of SCC. Dynamic segregation can manifest it self either vertically by the accumulation of aggregate at the bottom of vertical structures (veil, column etc...) or horizontally by the decrease in the percentage of aggregate as a function of the length of horizontal structures (slab, beam...etc) (Hosseinpoor, 2016).

The non-uniform distribution of aggregates makes the SCC structure more permeable due to dynamic segregation. This causes a decrease in mechanical strength and durability.

It is necessary to characterize the stability of the concrete upstream to avoid this instability phenomenon.

Many tests have been developed to measure the dynamic stability of SCC, but the visual stability index (VSI) is the only standardized test. But it is a qualitative evaluation that is not precise and depends on the operator's judgment (ASTM C1611/C1611M-18, 2021).

Other researchers have modified some standardized tests to be able to measure dynamic stability such as the modified spread test (Tregger, 2012), the 3-compartment sieve test (Gökçe and al, 2018), the modified L-box test (Paki Turgut and al, 2012) and the dynamic sieve segregation test (Mohammad Musa Alami, 2014).

- The Modified Spreading Test (Tregger, 2012)

The dynamic stability assessment consists of measuring the aggregate content in three concentric zones.

- The 3-compartment sieve test: H. SüleymanGökçe and ÖzgeAndiç-Çakır (Gökçe and al, 2018) introduced a new dynamic segregation measurement device. The test consists of determining the aggregate content using the 3-compartment sieve.

- The modified L-box test

Turgut, Turk and Bakirci (Paki Turgut and al, 2012); modified the L-box test to assess dynamic stability. The test consists of calculating the volume of the aggregate in the different partitions.

II.3.2 Static segregation

Static segregation is a loss of homogeneity of concrete under the effect of gravity alone; this heterogeneity is mainly due to the large difference between the density of aggregates and the fluid in suspension (Spangenberg and al, 2012). As a result, aggregates accumulate at the bottom and cementitious paste manifests at the surface causing bleeding. This can lead in the long term to cracking and even consequent shrinkage, as well as a lower resistance of the concrete to various chemical aggressions.

The evaluation of the static segregation of SCC has been the interest of several researchers since the appearance of Among the tests designed to measure static stability, there are standardized tests such as the visual stability index (VSI) (ASTM C1611/C1611M-18, 2021), the penetration test (ASTM C1712-20, 2020), the sieve stability (NF EN 12350-11, 2010) and the segregation column test (ASTM C1610/C1610M-19, 2021).

- Visual Stability Index [ASTM C16 11]

The visual stability index (VSI) provides a qualitative assessment of segregation resistance. The test consists of visually inspecting the condition of the SCC spreding after the slump flow test; this evaluation depends on the observation and judgment of the test operator (ASTM C1611/C1611M-18, 2021).

Table II-1. Visual stability index values (VSI), criteria (ASTM C1611/C1611M-18,2021).

Valeur de (VSI)	Criteria
0 = Very stable	No evidence of segregation or bleeding.
1= stable	Stable no evidence of segregation and slight bleeding observed as a chip on the concrete mass.
2 = unstable	At hin10 mm mortar layer halo and/or a pile of aggregates in the concrete mass.
3 = Very unstable	Segregation by evidence of a large mortar halo of > 10 mm and/or a large aggregate pile in the center of the concrete mass.

The hardened visual stability index (HVSI), allows to qualitatively evaluate the resistance to segregation of concrete in the hardened state. The test consists in visually observing the granular

distribution in a longitudinal section of a cylinder of (150 mm X 300 mm) size (Lin Shen and al, 2005). The evaluation criteria are presented in table II-2 (Fang and al, 2020).

Table II-3. Stability index for hardened concrete (Fang and al, 2020).

Evaluation	Description
0- Stable	No mortar layer at the top of the cutting plane and no variation in size and percentage of the overall aggregate distribution area from top to bottom.
1- Stable	No mortar layer at the top of the cutting plane but slight variation size and percentage of the coarse aggregate distribution area from the top to the bottom.
2- Unstable	Thin mortar layer, less than 25 mm thick at the top of the cut plane and distinct variance in size and percentage of surface Overall distribution from top to bottom.
3- Very unstable	A layer of mortar greater than 25 mm thick and or considerable variance in size and percentage overall aggregate range from top to bottom.

Based on the hardened visual stability index (HVSI), the digital image analysis procedure (Panesar and al, 2012) consists of scanning the hardened concrete profile and obtaining images that are used to estimate the static stability of the concrete by observing the distribution of aggregates and the thickness of the mortar stagnate at the top surface of the sample.

- The penetration test [ASTM C1712]

The penetration test consists of pouring SCC into the inverted Abrams cone; then inserting a probe carefully and measuring the initial indentation d1 and the final indentation d2 after 80 seconds (ASTM C1712-20, 2020).

Pd = d2 –d1.

Table II-4. Degree of resistance to static segregation.

Penetration depth (Pd) (mm)	Degree of static segregation
Pd ≤10 mm	Resist
10 mm < Pd < 25 mm	Moderate resistance
Pd ≥25 mm	No Resistance

Based on the same principle of measuring the penetration test Lin Shen and al (Lin Shen and al, 2014) introduced a modified segregation probe that is used to rapidly assess static segregation. The symmetry of the designation of the modified probe avoids the tilt problem presented by the original probe.

Table II-5. Segregation probe evaluation criteria (Lin Shen and al, 2014).

Probe penetration depth (Pd) mm)	Stability index
<4	very stable
4–<7	Stable
7–25	Unstable
>25	Very unstable

Thus, based on the same principle of measurement of the penetration test Hassan El-Chabib and Moncef Nehdi (Hassan El-Chabib and al, 2006) have developed an improved penetration device with four penetration heads instead of one head.

- Sieve stability test [NF EN 12350-11]

The sieve stability test allows to evaluate the resistance to static segregation of SCC. In fact, the principle of this test is to measure the amount of laitance passed through the mesh of a 5 mm sieve of a concrete sample (4.8 ± 0.2 kg). The acceptability criteria are set by the AFGC (NF EN 12350-11, 2010) as follows;

The percentage of laitance $= \frac{laitance\ mass}{Sample\ mass} * 100\% = \Pi$ (Eq II-7)

The stability criteria of SCC ;

- ✓ $0 \leq \Pi \leq 15\%$, Satisfactory stability.
- ✓ $15 < \Pi \leq 30\%$, Critical stability.
- ✓ $\Pi > 30\%$, Unstable (Bad stability).

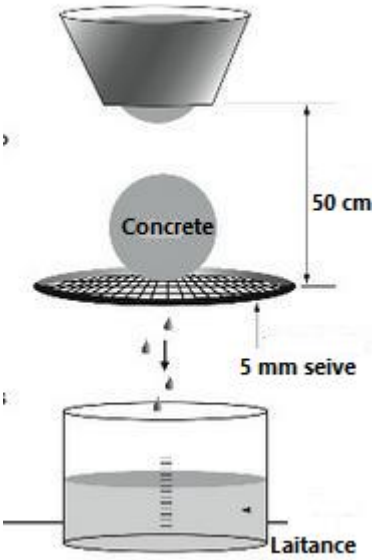

Figure II-6. Sieve stability test.

- The segregation column test [ASTM C1610]

The segregation column test; consists of pouring the SCC into a column of 200 mm diameter and 660 mm height. After 15 min of rest; a sieving (on sieve, size 4) and a washing of the upper and lower section of the SCC is performed. Then, the aggregates are dried and weighed. Finally, the segregation rate is deduced (ASTM C1610/C1610M-19, 2021).

$$Seg = 2 \cdot (m_{inf} - m_{sup}) / (m_{inf} + m_{sup}) \quad \text{(Eq II-8)}$$

Where ;

m_{inf} ; The aggregate mass of the lower SCC section.

m_{sup} ; The aggregate mass of the upper SCC section.

The column test has inspired many researchers to develop non-destructive tests either by measuring electrical resistivity (Nili and al, 2017) (Yim and al, 2020) or by measuring electrical conductivity (Mesbah and al, 2011).

Other researchers have relied on wave analysis as a non-destructive method to assess the static stability of concrete either in the fresh state by measuring the ultrasonic wave velocity (Benaicha and al, 2015), and the shear wave velocity (Naji and al, 2017). Or in the hardened state by measuring the compression wave velocity (Tenza-Abril and al, 2020), or even by X-ray

computed tomography and fractal analysis analysis accompanied by image analysis (Erdem, 2014).

Nevertheless, other researchers have developed tests to measure static stability and dynamic stability simultaneously (Esmaeilkhanian and al, 2014) (Nili and al, 2018).

II.3.3 Parameters affecting the stability of SCC

The design parameters of SCC and external disturbances cause a change in rheological properties of cement, mortar and SCC; which in turn affects the static and dynamic stability of SCC (Zhang and al, 2021).

SCC is a very fluid concrete, and in order to obtain a very good quality SCC it is necessary to make a trade-off between fluidity and stability by studying the influence of different components of self-compacting concrete. Aggregates, admixtures, mineral additions and the W/C parameter on their stability (Libre and al, 2010). Thus, it is necessary to take into account the influence of external disturbances on the SCC such as the agitation during the transport of the self-compacting concrete and the flow during the implementation of the SCC.

The segregation phenomenon remains the least understood property of self-compacting concrete (Hassan El-Chabib and al, 2006). According to the literature, the influence of mix design parameters and external disturbances on static and dynamic stability are not well determined and remain contradictory.

Some researchers show that the design parameters have both the same influence on static and dynamic stability except that the degree of influence is different (Zhang and al, 2021). Other researchers prove that the effect of design parameters is completely different in the static and dynamic stability of self-compacting concrete (Ghoddousi and al, 2014) (Amini, 2016).

II.3.3.1 The influence of formulation parameters

a)Aggregates

The different properties of the aggregates entering the formulation of the SCC; such as density, packing density, maximum diameter, gradation and shape have an influence on the static and dynamic stability of SCC.

- Aggregate density

Higher aggregate density widens the density difference between the aggregate and the mortar in suspension, and this causes static segregation by stagnation of the heavy aggregate at the bottom. Thus, in the case of higher aggregate density; the drag force provides lower acceleration

to advance the aggregates in addition to higher friction and deceleration provided by the flow surface which prevents the aggregate advancement and causes dynamic segregation (Lin Shen and al, 2009). Nevertheless, a lower density of aggregates causes dynamic segregation but in a reverse way where light aggregates appear on the surface instead of the mortar (Esmaeilkhanian and al, 2014), Thus the lower density of aggregates even affects the static stability of the SCC by the appearance of light aggregates on the surface after the flow during rest.

- Packing density

High packing density can increase the network effect or smaller particles slow down the movement of medium-sized particles, which slows down the movement of larger ones, which can lead to lower deposition of aggregates at the bottom and therefore improves static stability (Aïssoun and al , 2016) (Ghoddousi and al, 2014).

- Maximum aggregate diameter

SCC with coarser aggregate diameters is susceptible to static and dynamic segregation. The coarse aggregate leads to an increased speed of aggregate deposition to the bottom and causes static segregation so the deposition of coarse aggregate to the bottom prevents the aggregate from flowing at the same speed as the mortar and this causes dynamic segregation (Esmaeilkhanian and al, 2014) (Lin Shen, 2009) (Lin Shen and al , 2016).

-Aggregate grading

SCC formulated with narrow (Esmaeilkhanian and al, 2014), discontinuous (Mesbah and al, 2011) or even with a single granular fraction (Lin Shen and al, 2009) shows segregation. This is due to the reduction in the surface to mass ratio of the aggregate that decreases the drag force leading to more granular separation and causing static segregation. In addition, a weak aggregate network effect leads to higher dynamic segregation compared to a broad and well graded particle distribution or in which smaller particles slow down the movement of medium sized particles, which slows down the movement of larger particles thus preventing shear induced migration and settling of coarser aggregates, which leads to higher dynamic stability (Esmaeilkhanian and al, 2014) (Lin Shen and al, 2009).

- Aggregate shape

Research on the influence of aggregate shape on stability is contradictory; some researchers prove that whatever the shape of the aggregate rolled or crushed, it has no significant influence on dynamic segregation. This is because the specific surface area of the aggregate and the surface-to-volume ratio does not change significantly with the shape of the aggregate (Esmaeilkhanian and al, 2014). Nevertheless, other researchers prove that crushed aggregates contribute to a better adhesion with the hydrated cement matrix and therefore cause a high

viscosity resulting a high static and dynamic stability. On the contrary, the rolled aggregates which are smooth presents a poor adhesion with the cement causing a low viscosity and leading to a static and dynamic instability (Aïssoun and al, 2016). Thus, crushed aggregates with high aggregate specific surface area leads to good stability in contrast to rolled aggregates, which have low aggregate specific surface area, which leads to less stability (Navarrete and al, 2017). Otherwise, needle-shaped aggregates are prone to getting stuck in the reinforced areas of the formwork and this produces arches and may even stop the flow (Cui and al, 2020).

b) The W/C parameter

The strength of SCC against static and dynamic segregation improves by decreasing the W/C ratio (Hassan El-Chabib and al, 2006). However, beyond a certain value of the W/C parameter; the decrease will not have any influence on the stability of the SCC (Esmaeilkhanian and al, 2014). The excessive decrease can lead to a negative effect on the stability, the void index increases resulting in low cohesion and consequently low resistance to segregation (Wong and al, 2008) (Zhang, 2021).

c) The superplasticizer

The role of superplasticizer is to flocculate the cement grains by electrostatic repulsion acts by neutralizing the electrical charges present on the surface of the grains and/or by steric repulsion by moving the grains away from each other. This increases the fluidity of the SCC and therefore decreases their static and dynamic stability. Increasing the percentage of superplasticizer decreases the dynamic stability of SCC (Lin Shen and al, 2016) (Koura and al, 2020). Increasing the superplasticizer affects both the static and dynamic stability; Nevertheless that the dynamic stability is the most influenced (Hassan El-Chabib and al, 2006). It is conceivable to use superplasticizer instead of increasing the W/C parameter in order to achieve the desired fluidity (Libre and al, 2010).

d) Mineral additions

The influence of mineral additives used in the formulation of SCC on stability depends on their characteristics. Additions with a spherical and smooth shape such as fly ash, decrease the friction between aggregates resulting in a high fluidity and consequently a low resistance to segregation (Amini, 2016). On the other hand, mineral additions with a higher specific surface and fine particle content cause a reduction of the water content resulting in less fluidity and a high resistance to segregation (Amini, 2016) mineral additions with a particle size close to that of cement such as granulated blast furnace slag affect the stability causing a dilution effect and reducing the amount of cement around the aggregate (Ghoddousi and al, 2014) (Zhang, 2021).

II.3.3.2 The influence of external disturbances

The very prolonged mixing of SCC in the mixer truck during its transport to a construction site can disperse the cement grains and consequently, the fluidity increases and therefore the risk of instability increases (Mehdipour and al, 2013).Thus the use of vibration of the SCC in some cases during the casting destroy the granular connection which leads to a reduction of the shear yield stress and the viscosity of the concrete and influences the homogeneity and stability of the SCC mixtures (Petrou and al, 2000).

II.4 Conclusion

Many methods have been proposed to evaluate the static and dynamic stability of SCC, but none of them really simulates the real conditions because of their reduced model. Many researchers have devoted their work to the study of the influence of the formulation parameters and the external disturbances as well as the rheological parameters on the static and dynamic stability of SCC. But, the influence of some formulation parameters remains contradictory or still insufficient in the case of the effect of external disturbances or even the effect of rheological parameters.

Chapter III.

Destructive and non-destructive testing (NDT) methods.

III.1 Introduction

The control of the static stability in fresh state and the mechanical resistance of SCC later in hardened state, always remains an essential factor of first interest. Hence, two categories of tests can be used ; destructive tests and non-destructive test methods (NDT).

Destructive tests are known by those test based on the deterioration of the controlled samples. However, Non-destructive tests are those not harmful and do not cause any damage for the controlled samples.

III.2 Destructive and (NDT) method in fresh state

The segregation column test [ASTM C1610] as reported in chapter II is used to evaluate static segregation by a destructive method because it is based on the division of the different parts for sieving and the determination of the coefficient of segregation after. On the other hand, other researchers have developed non-destructive tests to evaluate static stability (segregation index) of the SCC such as the electrical conductivity method (Mesbah and al, 2011) or the electrical resistivity method (Nili and al, 2017) (Yim and al, 2020); where the segregation coefficient is evaluated by resorting to the division of different parts of the column, and the test presents a good correlation with the destructive method.

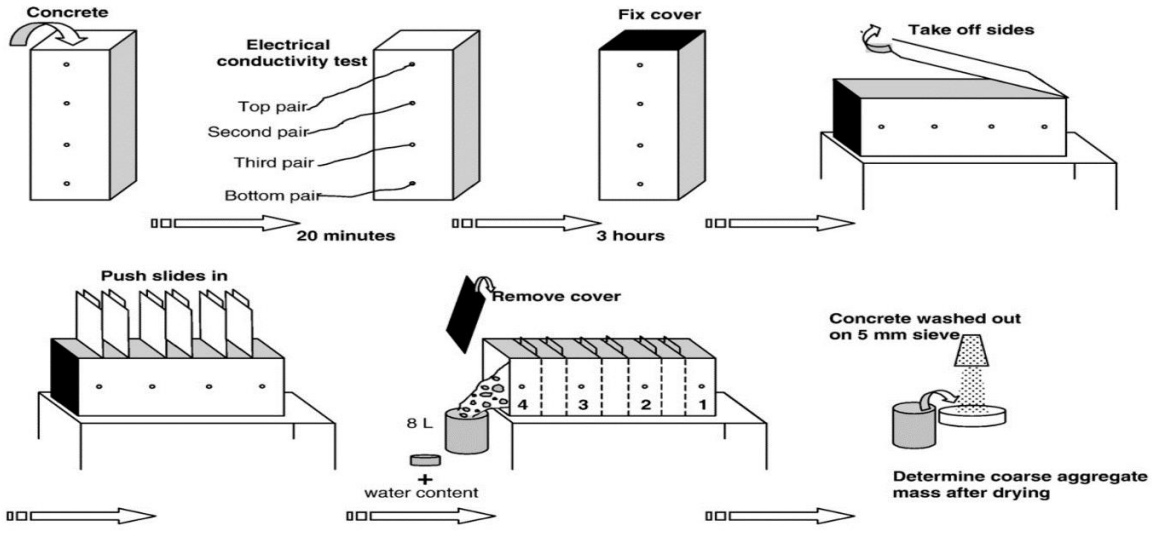

Figure III-1. Physical Stability measurements (Destructive method) (Mesbah and al, 2011).

Figure III-2. Stability measurements NDT (method) (Mesbah and al, 2011).

III.3 Destructive and (NDT) method at hardened state

III.3.1 Destructive test methods

a) Compression test [NF EN 12390-3]

The measurement of compressive strength is carried out by a hydraulic press machine, according to the standard (NF EN 12390-3, 2019) on cylindrical specimens (16x32) cm^2 or cubic specimens (10x10x10 cm^3) with water curing till the age of the due test.

Crushing is done at 3.7, 14, 28, and 90 days of age; the strength obtained each time is the average of three measurements on three different specimens.

The compressive strength is given by the following formula ;

$$R_c = F/S \qquad \text{(Eq III-1)}$$

Where ;

Rc: compressive strength (MPa).

F: Failure load (N).

S : Area section of the specimen (mm^2).

b) Flexural strength [NF EN 12390-5]

The measurement of flexural strength is carried out by a hydraulic press, according to the standard (NF EN 12390-5, 2019) on prismatic specimens of dimensions (7 x 7 x 28) cm^3 water cured. The measurement is made often at the age of 28 days; f_{t28}.

The expression of the results is given by the formula ;

$$f_t = 0,6 + 0,06\, f_{cj} \qquad \text{(Eq III-2)}$$

For $f_{cj} < 60$ MPa

F_{c28} days > 60 MPa

Where ; $f_{cj} > 60$ MPa $\qquad f_t = 0,273.\sqrt[3]{fcj}$ (Eq III-3)

The flexural tensile strength is defined as (f_{tj}) cocentionnaly by limit state design for concrete (Dreux G and al, 1995), (BAEL, 1991).

c) Splitting tensile testing [NA EN 12390-6]

The measurement of tension by splitting is carried out by a hydraulic press, according to the standard [NF EN 12390-6] (NF EN 12390-6, 2012) on cylindrical specimens (16x32 cm^2), walled with water, where, the specimen is placed horizontally between the plates of the press.

III.3.2 Non-destructive testing methods

a) Rebound hammer test [NA EN 12504-2]

The rebound hammer index test was developed in the 1940s (John and al, 2006). The principle of this test is to measure the surface hardness of concrete according to the standard (NF EN 12504-2, 2021), with the Shimdt hammer (sclerometer test).

The test is carried out on cylindrical or cubic specimens fixed in a hydraulic press, the measurement is carried out at several points spaced at least by 2 cm, and an average of the sclerometer index is obtained. The test can be done vertically, horizontally or at an angle; depending on the position of the operation and the sclerometric index obtained. The value of the compressive strength is deduced using a chart for the different measurement angles adopted.

Figure III-3. Rebound hammer test (Sclerometer).

b) Ultrasonic Pulse Velocity test (UPV) test [NA EN 12504-4]

The ultrasonic test was developed in the 1950's (WescheK, 1955). This dynamic auscultation test consists in determining the propagation velocity of ultrasonic pulses passing through concrete according to the standard (NF EN 12504-4, 2021), using a sonic auscultation device (ultrason).

Figure III-4. Ult rasonic pulse velocity test device.

The test consists in placing the two probes in a direct, indirect or semi-direct way, we obtain a numerical display on screen indicating the time of passage of the longitudinal ultrasonic waves through the concrete; then we deduce the speed by the formula V=d /t (Km/s).

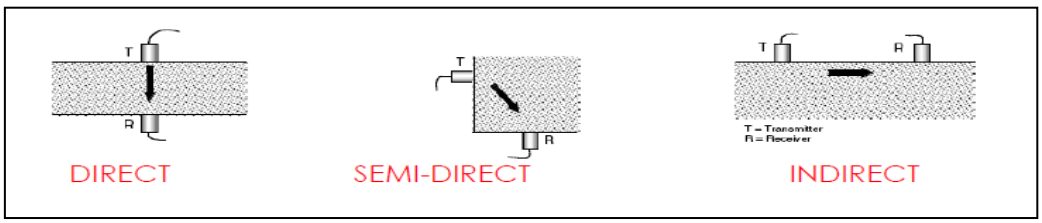

Figure III-5. Measurement positions for ultrasonic test (Kenai, 2018).

Table III-1. Concrete quality and velocity for ultrasonic test (Solis and al, 2008).

Quality	**Excellent**	**Good**	**Fairly good**	**Poor**	**Very poor**
Velocity [m/s]	Superior to 4000	3200-4000	2500-3200	1700-2500	Inférieure à 1700

c) Combined (NDT) methods

It is sometimes reliable to combine the two non-destructive methods ; the sclerometer test and the ultrasonic test, which leads to evaluate the compressive strength.

Non-destructive testing is sometimes questionable ; then the combination of two methods eliminates this concern and leads to more reliable results. This solution is advantageous when variations in concrete properties lead to contradictory results, such as increasing the moisture content increases the sound velocity. However they decrease the sclerometer index (Hannachi and al, 2011).

The most used combined method is the SonReb method developed by RILEM (RILEM Draft recommendation, 1993), according to the literature there are many formulas to determine the compressive strength of concrete with the SonReb method (Cristofaro and al, 2020).

It could be quote for example, a linear formula developed by (Giuseppe and al, 2011) ;

$$R_C = 0.26511 \cdot I + 0.01385 \cdot UPV/ - 34.51583 \qquad \text{(Eq III-4)}$$

Where ;

R_c ; the compressive strength [MPa].

I ; Sclerometer index.

UPV ; Ultrasonic velocity [m/s].

III.3.3 State of the art on NDT at hardened state in the case of SCC based on mineral additions

Non-destructive testing has been widely used to estimate the mechanical strength in ordinary concrete, currently they have been used even in the case of SCC to assess their mechanical performance; Some scientific works on the use of non-destructive testing in SCC are cited ;

(Nepomuceno and al, 2019); found a good correlation of the mechanical resistance to compression with the ultrasonic velocity and rebound hammer index; either in the case of ordinary concrete or in the case of SCC.

(Singh and al, 2018); Found good correlation between compressive strength and ultrasonic velocity and rebound hamer index in the case of SCC based on recycled aggregates.

(Allali and al, 2020); have shown that the non-destructive tests (Ultrasonic test and the rebound hammer test) could be reliable to evaluate the mechanical resistance in the case of the SCC. When, the SCC mixtures has low content of silica fume as mineral addition incorporated.

(Tripathi and al, 2022); proved the feasibility of non-destructive testing in the measurement of mechanical strength in the case of SCC based on fly ash.

Furthermore, (Ashteyat and al, 2014) ; developed statistical models to estimate the mechanical properties of SCC exposed to fire without the recourse to tedious laboratory testing.

(Revilla-Cuesta and al, 2021) ; have managed to develop reliable numerical models to predict the compressive strength as a function of the ultrasonic beside the rebound hammer index.Also, they proposed models as a function of these two combined parameters simultaneously.

III.4 Conclusion

In this chapter a state of the art on the characterization of the static stability in fresh state and mechanical resistance of SCC in the hardened state by destructive and non-destructive tests has been described.

The destructive tests lead to more precise results, nevertheless the non-destructive tests are advantageous in certain cases, moreover they are more flexible and more economic in terms of ease of use and time saving. It is possible to establish several tests on the same sample; sometimes the concrete of the specimens differs from that of the structure because of the difference in the curing method or the compaction and once the structure is built it is possible to establish simply non-destructive tests better than the go back again to the destructive core operations on the built constructed element (Bouakkaz, 2012).

According to the literature there are few studies that deal with of the convenience of NDT for the measurement of mechanical strength in the case of SCC. Therefore, it is worth undertaking essential research works to evaluate the effectiveness of these tests especially in the case of SCC based on mineral additions.

PART TWO.

Experimental part.

Chapter IV.

Materials, Formulations and Tests carried out on SCC.

IV.1 Introduction

This chapter will be devoted to the characterization of the basic materials and the description of the two methods of formulations. Also, a presentation of the tests used in the development of the experimental program of the present study.

IV.2 Basic materials

Concerning the materials, we used a range available locally in Algeria or abroad in France for the confection of the various mixture of SCC;

a) Cement

Two types of cement were used; for the experimental part carried out in Algeria a compound Portland cement CPJ CEM II A 42.5 from the Ain Lekbira Setif cement factory was used.

For the part carried out in France, a Portland cement CEM I 52.5 N from Lafarge was used.

The different chemical and physical characteristics of the cements used are presented in the following table;

Table IV-1. Chemical and physical characteristics of the cements used.

	Chemical characteristics of the cements used.								
Element	Cao	Sio_2	Na_2O	Mgo	Al_2O_3	K_2O	T_iO_2	Fe_2O_3	SO3
CEM II A 42.5	62.7	17.7	0.05	1.90	4.6	0.67	/	2.99	/
CEM I 52.5 N	65.4	20.6	0.2	0.9	3.6	0.3	0.2	4.1	2.7
	Physical characteristics of the cements used								
	Specific density (g/cm^3)						Fineness (cm^2/g)		
CEM II A 42.5	3.10						3800		
CEM I 52.5 N	3.16						3950		

c) Aggregates

Local crushed gravels from the region of Bordj Bou Arreridj at two fractions (3/8) and (8/15); with a specific gravity of around 2.6 were used. The silicious sand used comes from the Oued

Souf region (South-east of Algeria); its specific gravity of 2.64 and equivalent sand modulus of 0.80.

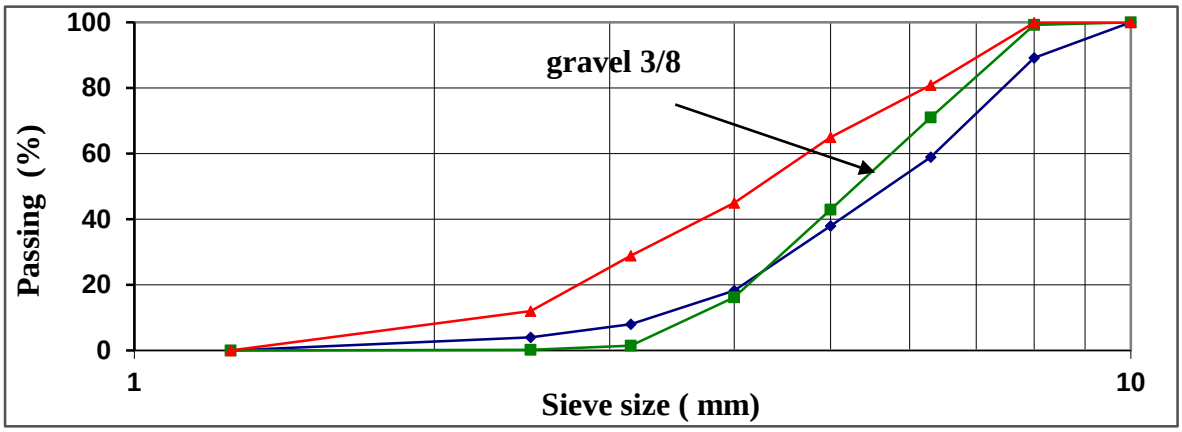

Figure IV-1. Particle size analysis of gravel (3/8).

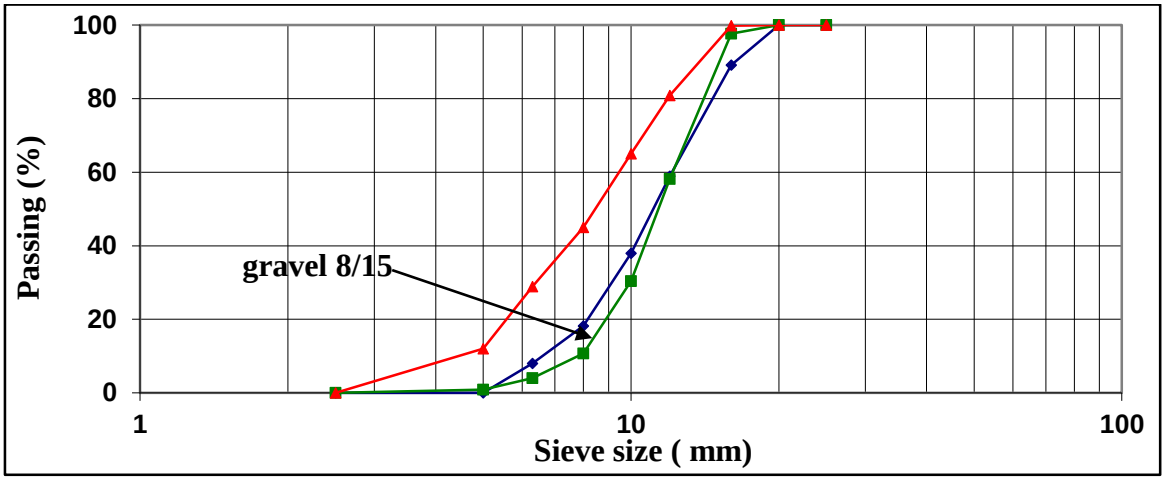

Figure IV-2. Particle size analysis of gravel (8/15).

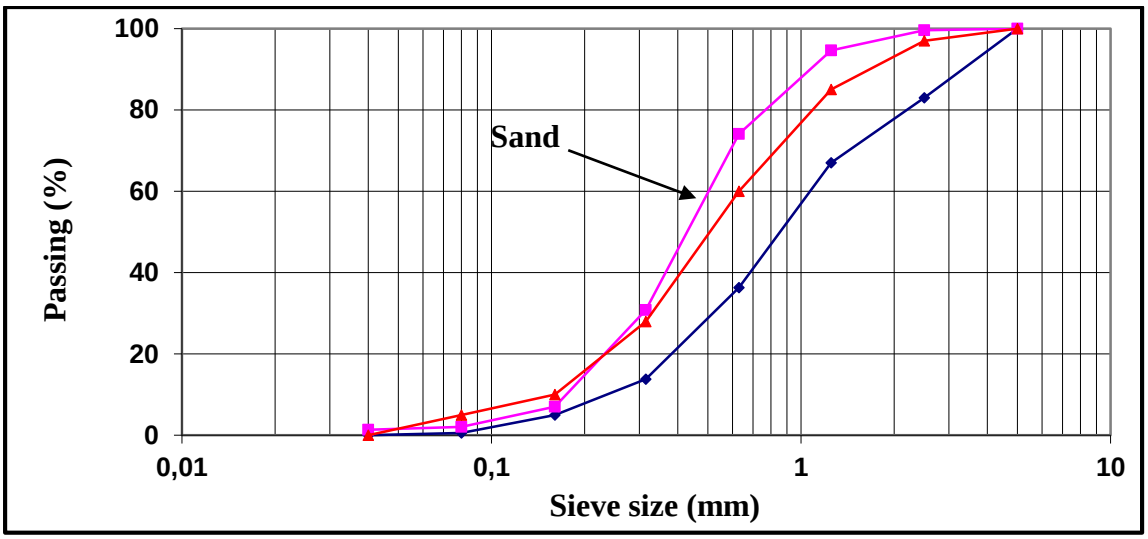

Figure IV-3. Particle size analysis of Oued Souf sand.

d) Mineral additions

The mineral additions used in our study were characterized by a granulometry lower than 80 micrometer. Limestone fillers (UF5, UF 10 and F20) were provided from ENG lekhroub Constantine and granulated blast furnace slag from El hadjar Annaba iron production plant. While, fly ash was deliverd in the laboratory LGCGM, Rennes, France.

Figure IV-4. Limestone Fillers.

Figure IV-5. Slag (S).

Figure IV-6. Fly ash (FA).

The chemical and physical characteristics of these different additions are presented in the following table;

Table IV-2. Physical and Chemical composition of additions.

Element	SiO_2	Al_2O_3	Fe_2O_3	CaO	MgO	SO_3	K_2O	Na_2O	Cl	TiO_2
Limestone Fillers UF05	0.10	0.00	0.01	58.21	0.013	0.04	0.01	0.06	0.00	0.00
Limestone Fillers UF10	0.18	0.00	0.01	58.29	0.11	0.03	0.01	0.05	0.002	0.00
Limestone Fillers F20	0.15	0.01	0.00	58.22	0.13	0.08	0.00	0.06	0.003	0.00
Slag	36.77	7.77	0.85	37.31	13.91	1.02	0.4	0.31	0.36	0.00
Fly Ash	52.7	32.7	6.4	3.1	0.8	0.9	1.2	0.7	00	1.5
	Physical properties of additions									
Limestone Fillers	SSB=2000, 3000, 4000 (g/cm^3)			Density=2,7						
Slag	SSB=2000, 3000, 4000 (g/cm^3)			Density=2,8						
Fly ash	4350 (g/cm^3)			Density=2,5						

e) Admixtures (Superplastizier)

Admixtures are water-soluble products, they are incorporated into concrete at dosages below 5% of the weight of cement. For the studied mixes prepared in Algeria the admixture used is a Super plasticizer (SP), a high water reducer (MEDAFLOW 30). It is designed based on polyether carboxylates which considerably improves the properties of concretes.The different characteristics of the SP (Medaflow 30) are presented in the following table.

Table IV-3. Superplastizier characteristics (MEDAFLOW 30).

Aspect	**Color**	**PH**	**Density**	**chlorine content (g/l)**	**Extract dry (%)**
Liquid	Light brown	6-6.5	1,078 ± 0,01	< 0,1	30

For the mixtures prepared in France we used a superplasticizer high water reducer SIKA ViscoCrete TEMPO 12 with a specific gravity of 1.07 and a solid content of 30%. Further to a viscosity agent SIKA STABILIZER were used. The different characteristics of these two products are presented in the attached technical data sheets (annex, 5&6).

IV.3 Formulation of SCC

IV.3.1 Design method

There are several approaches to formulating SCC. In this study two formulation methods are adopted. For mixes made in Algeria an empirical method according to the recommendations of AFGC is utilized. However, for those mixtures econfected in France the LCPC method is used.

a) Empirical method

The empirical formulation is established according to the recommendations of the AFGC (AFGC, 2008);

A ratio: G/S=0.9

A ratio: E/(C+F) =0.4

A cement dosage of: 400 kg/m^3

Addition (5%, 10%, 20% of the weight of cement).

The following tables present the mixing proportions of SCC developed by this method;

- SCC based on limestone; as an inert addition;

F2 (UF05) =2000 (cm^2 /g), F3 (UF10) =3000 (cm^2 /g), and F4 (F20) =4000 (cm^2 /g)

Table IV-4. Composition of one cubic meter of SCC concrete based on limestone; formulated by the AFGC method.

Mixes	S Kg /m3	Gr (3/8) kg/m3	Gr (8/15) kg/m3	C kg/m3	W kg /m3	SP Kg /m3	L Kg /m3
SCC_{10F2}*	828	446	446	400	185	5.6	40
SCC_{10F3}	828	446	446	400	185	5.6	40
SCC_{10F4}	828	446	446	400	185	5.6	40
SCC_{20F2}**	811	439	439	400	183	5.5	80
SCC_{20F3}	811	439	439	400	183	5.5	80
SCC_{20F4}	811	439	439	400	183	5.5	80

*SCC_{10F2}:10% Limestone fillers (L) with fineness of 2000 cm^2/g
**SCC_{20F2}:20% Limestone fillers (L) with fineness of 2000 cm^2/g

- SCC based on granulated blast-furnace slag; as an active addition;

S2 =2000 (cm^2 /g), S3=3000 (cm^2 /g), and S4 =4000 (cm^2 /g)

Table IV-5. Composition of one cubic meter of SCC concrete based on slag ; formulated by the AFGC method.

Mixes	S Kg /m3	Gr (3/8) kg/m3	Gr (8/15) kg/m3	C kg/m3	W kg /m3	SP Kg /m3	L Kg /m3
SCC_{5S2*}	835	450	450	400	187	5.6	20
SCC_{5S3}	835	450	450	400	187	5.6	20
SCC_{5S4}	835	450	450	400	187	5.6	20
SCC_{10S2**}	828	446	446	400	185	5.6	40
SCC_{10S3}	828	446	446	400	185	5.6	40
SCC_{10S4}	828	446	446	400	185	5.6	40

*SCC_{5S2}:5% Slag (S) with fineness of 2000 cm^2/g
**SCC_{10S2}:10% Slag (S) with fineness of 2000 cm^2/g

b) LCPC method

The LCPC method was developed in the « Laboratoire Central des Ponts et Chaussées » (LCPC) (De Larrard and al, 1999). The present study has applied this method using the model established by the software Bétonlabpro3. This model optimizes the granular skeleton and minimizes the amount of water in the SCC. The following table shows the mixing proportions of the SCC developed by this method.

Table IV-6. Composition of one cubic meter of SCC concrete formulated by the LCPC method.

Mixture	SCC_{FA1}	SCC_{FA2}	SCC_{FA3}
Cement (Kg)	350	350	350
Fly ash (Kg)	100	100	100
Water (Kg)	212	242	212
W/C	0.47	0.54	0.47
Volume paste (%)	37%	40%	37%
Coarse aggregates content (%)	33%	33%	30%
Sand (Kg)	748	670	830
$G_{10/14}$(Kg)	-	-	81.2
$G_{4/8}$(Kg)	179	180	-
$G_{8/12.5}$(Kg)	715	720	-
Superplasticizer (l/m^3)	5	3.5	3.7
Viscosity modifying agent (l/m^3)	1	1	-

*SCC_{FA}: Concrete with Fly ash

IV.3.2 Mixtures preparation

The mixer used for the manufacture of SCC in the civil engineering department is avertical axis type. However the mixer used for the manufacture of SCC in the laboratory in France is a mixer equipped with blades at their end.

The mixing sequence consists in homogenizing the sand and the gravel during 1 minute before introducing 1/3 of the mixing water. Then, the cement and admixture are introduced with the diluted admixture in the second 1/3 of water. Later, the concrete is then mixed for an additional five minutes adding the third (1/3) remainning part of water gradually. The fresh characterization tests are performed immediately and the SCC cast into specimens without vibration for hardened state testing.

IV.3.3 Specimen conservation (curing)

After the mixing of the SCC, the moulds are kept in a room at ambient temperature, and demoulded after 24 hours. Once removed from the mold, to ensure proper curing of the concrete, the specimens are kept in a water tank at a temperature of 20°C, to avoid water loss and to ensure the normal hydration process of the cement.

Figure IV-7. Curing of SCC specimens.

IV.4 Performed tests

a) Fresh state

- Slump flow test diameter [NF EN 12350-8].
- Sieve stability test [NF EN 12350-11].
- L-box test [EN 12350-10].
- V-funnel test [EN 12350-9].
- Column test as a non destructive test.

- **Column test**

The static stability of SCC is measured by a non-destructive method using a 1.5 m high column, and by measuring the electrical conductivity according to the TDR (Time Domain Reflectometry) principle. The method consists in pouring 100 liters of SCC in a column of 1500 mm height and 250 X 250 mm cross section; the column is equipped with four pairs of electrodes placed at different depths. These probes are used to monitor local ionic changes for 150 min; at the end of this test, we deduce the bleeding index, segregation index and homogeneity index that gives us an idea on the static stability.

Figure IV-8. Column test (Civil Engineering and Mechanical Engineering Laboratory LGCM, Rennes, France).

Index	Formula	Schematic sketch
Bleeding index	$BI = \frac{Cumulative\ area\ top\ pair\ to\ mean}{T_{End} - T_{initial}}$	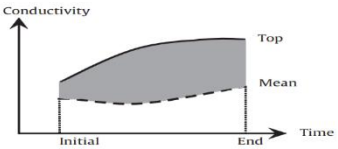
Segregation index	$SI = \frac{Cumulative\ area\ mean\ to\ bottom\ pair}{T_{End} - T_{initial}}$	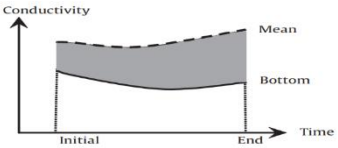
Homogeneity index	$HI = \frac{Cumulative\ area\ top\ pair\ to\ bottom\ pair}{T_{End} - T_{initial}}$	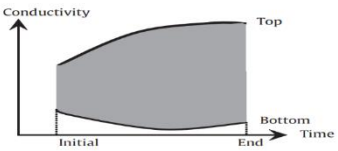

Figure 0IV-9. Stability indices (Mesbah and al, 2011).

b) Hardened state

b. 1) Standars Destructive tests

- Compression test [NF EN 12390-3].
- Flexural test [NF EN 12390-5].

b.2) Non destructive tests (NDT)

- Ultrasonic pulse Velocity test UPV [NA EN 12504-4].

IV.5 Conclusion

In this chapter the different materials used for the formulation of SCC in the experimental program research work are presented of our research work. Further, the two methods of formulations used in Algeria and in France and the different tests carried out either in the fresh state or in the hardened state are explained.

Chapter V.

Experimental Results and Discussion.

V.1 Introduction

This chapter is devoted to the presentation and interpretation of the results obtained from the testing experimental program. Firstly, the characterization of SCC based on inert and active mineral additions (Limestone, Slag) at fresh and haredened state. The evaluation of the static stability by a non-destructive test using a large-scale device by the measurement of the electrical conductivity with TDR method is undertaken for formulated SCC mixtures based on (FA) in a later step.

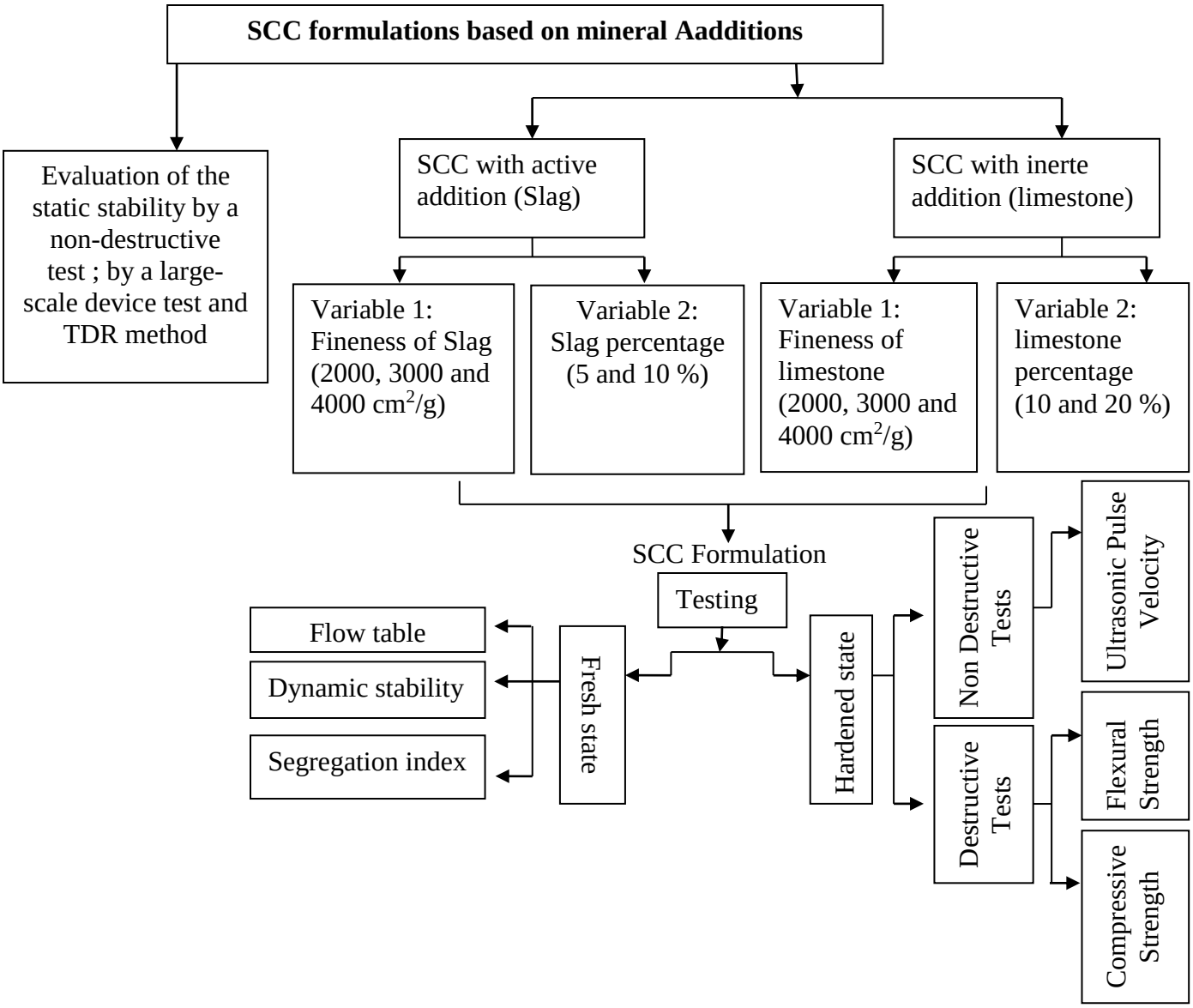

V.2 Part 01

V.2.1 Effect of limstone on SCC

a) Fresh state

a.1) Slump flow test

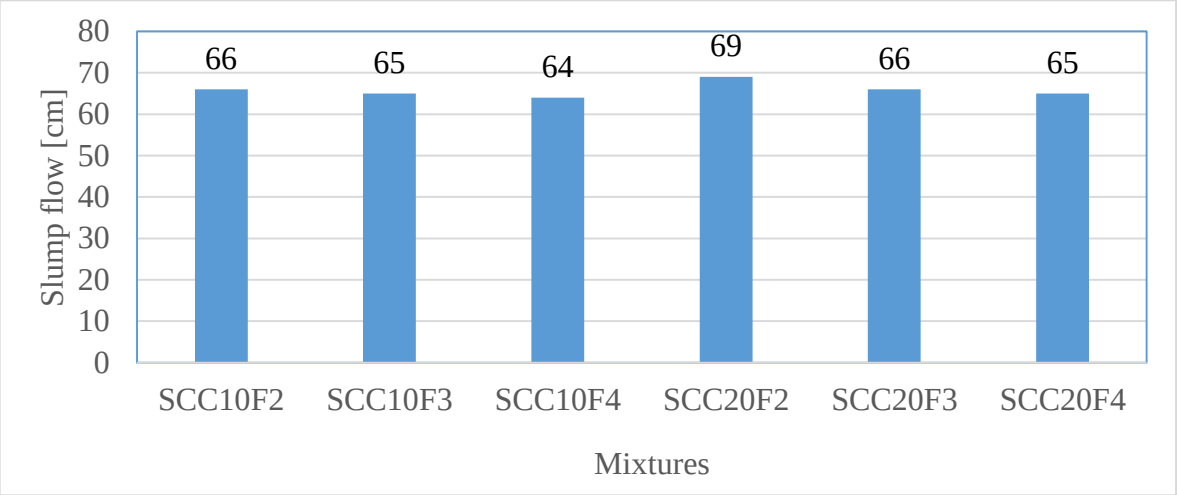

Figure V-1. Slump flow test results for SCC limestone mixtures.

In regards to standard value of the flow diameter are usually in the range between 60 and 75 cm for SCC mixtures. It could be observed from figure V-1 that the higher percentage of the fineness of the limestone filler increases the water demand, which causes a decrease of workability expressed in the slow spread of the SCCs (Bensalem and al, 2014) (Benjeddou and al, 2017) (Alyousef and al, 2019). It is observed that the fluidity is slightly greater by increasing the SSB of limestone for allmost the mixes.

However, the higher dosages of limestone filler increases the fluidity ; this can be explained by the inert effect of the limestone filler its grain nature and shape (Benaicha M and al, 2019). So, the increase in the volume of paste by the addition of limestone filler reduces the intergranular friction by improving the flow of the SCC. The fine particles integrate in the voids and release the trapped water which improves the fluidity (Kherraf, 2018).

Thus, the SCC with incorporation of limestone fillers are with higher workability that is related to fillers dosage of such mixtures which are much more fluid with a good mobility.One could conclude that the introduction of the limestone fillers at the percentages of 10 and 20 % has a meaningful effect on the workability of the tested SCC’s types.

a.2) Dynamic stability (L-box test)

It is noted that the incorporation of limestone filler in mixtures up to 20% ensures an ease of casting for such mixtures. Furthermore, the variation of the fineness of limestone fillers with BSS that ranges from 2000 to the maximum value 4000 cm^2/g and the dosage of filler 20% does not negatively affect the passage and filling capacity of SCC and consequently permit the ease of casting in confined zones that contribute to the dynamic stability (Skender and al, 2021).

a.3) Static Stability (Segregation index)

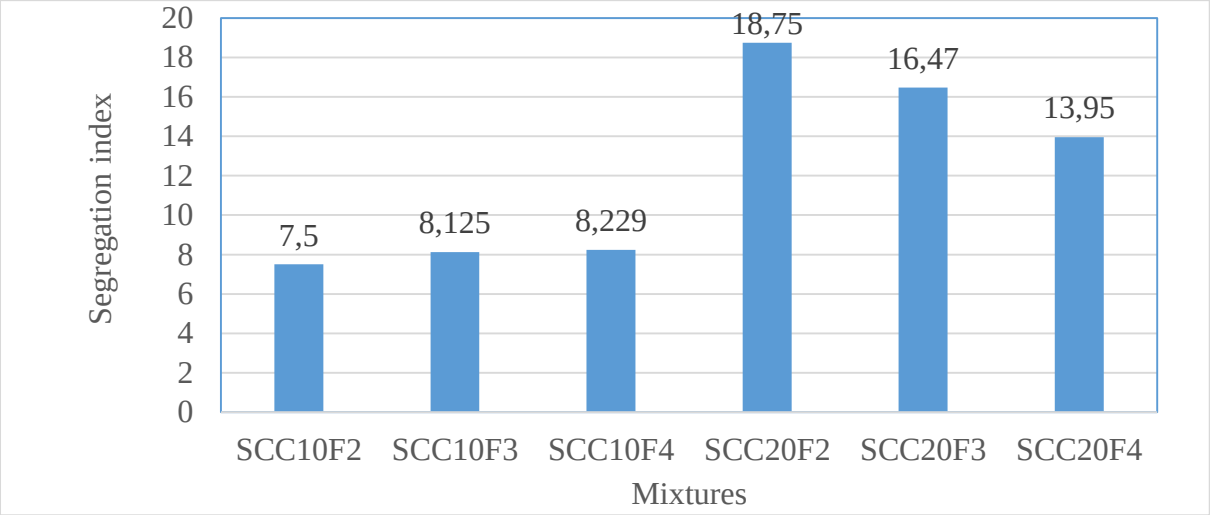

Figure V-2. Segregation index test results for SCC limestone mixtures.

It is noticed in figure V-2 that all the SCCs with 10% of calcareous filler have a segregation rate lower than 15%, synonymous of a correct stability; thanks to the good compactness and the granular distribution that gives these filler to the cement matrix of the mixtures.On the other hand, at greater percentage with 20% these show a critical segregation rate ranging from around 14 to 18 %, which is explained by a bad cohesion between the cement particles and the filler once the dosage of the calcareous filler exceeds 10%. Above 15% fines, the water demand decreases and the fillers begin to behave as a water-reducing admixture and the interaction of cement-fines-aggregates causes a recovery of the occluded air (Benjeddou and al, 2017) (Alyousef and al, 2019).

b) Hardened state

b.1) Compressive strength (CS)

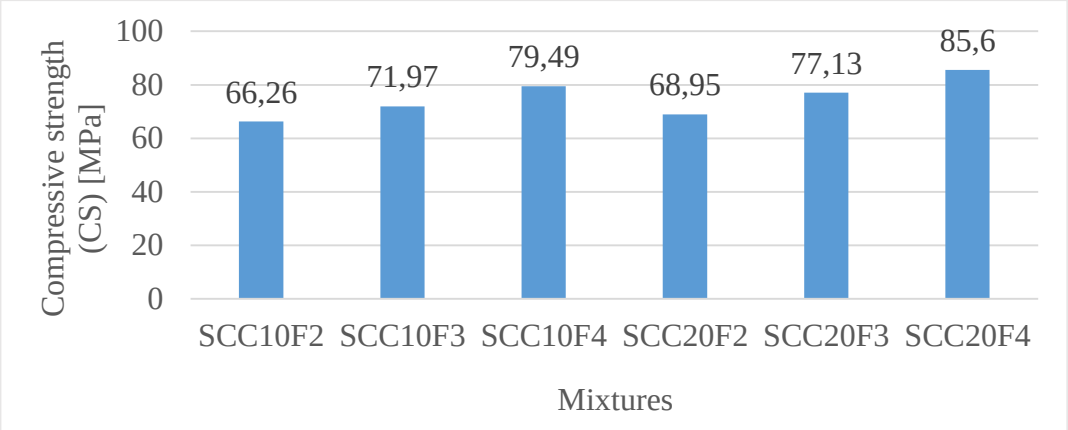

Figure V-3. Compressive strength of SCC limestone mixtures.

The compressive strength 66.26, 71.97, 79.49, 68.95, 77.13 and 85.6 Mpa its refer to 55, 60, 70, 60 ,70 and 70 Mpa respectively according to concrete class (C55/67), (C60/75), (C70/85), (C60/75), (C70/85) and (C70/85) (NF EN 206+A2/CN, 2022).

The compressive strength (CS) is estimated at 28 days of hardening and presented in the Figure V-3. The minimum value of the mechanical strength is 66.26 MPa (SCC10F2); it refers to the SCC which presents the minimum value of SSB 2000 cm^2/g and dosage of filler 10%. Mechanical resistance increases with increasing BSS and dosage of filler up to a value equal to 85.6 MPa (SCC20F4); the SSB that presents the maximum value of the BSS 4000 cm^2/g and the dosage of filler 20%. It is noted that the increase in the SSB of the limestone filler ; increases the compressive strength thus the increase greater dosage of limestone filler increases the compressive strength. Indeed, the obtained values for CS at a dosage of 10 % for limestone show a percentage of improvement up to around 20 % for SCC10F2 (BSS= 2000 cm^2/g) compared to SCC10F4 (BSS= 4000 cm^2/g). Furthermore, the percentage of 20 % limestone fillers incorporation register an increase of up to 25 % for SCC20F2 and SCC20F4, respectively.

This, could be explained by the filling effect of the limestone powder which enhances the mechanical resistance. The increases in strength are related to the improvement of the compactness obtained by the addition of fines, on the other hand the decreases are mainly due to the increase of the W/C as more water content negatively affect the strength which is a synonym of higher porosity and lower compact cementitious matrix. The optimum content of limestone fines which allows the highest strength to be obtained is around 15 % (Khan and al, 2016) (Benjeddou and al, 2017).

b.2) Flexural Strength (FS)

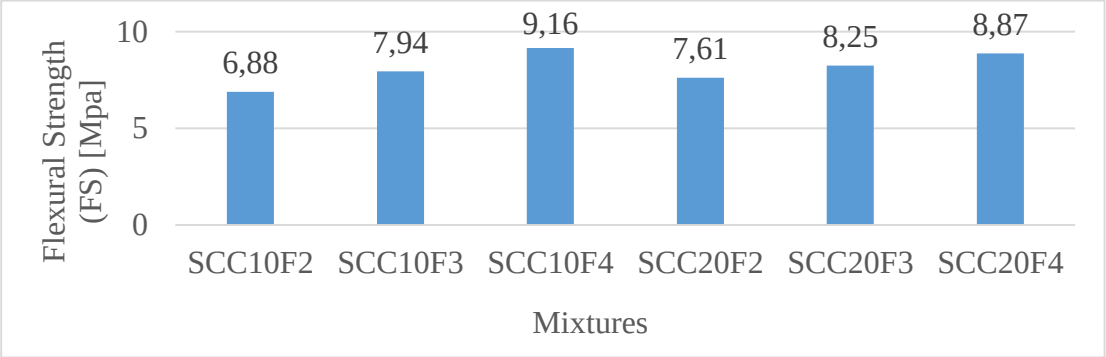

Figure V-4. Flexural strength of SCC limestone mixtures.

Figure V-4 presents the flexural strength (FS) at 28 days age of hardening for the different SCC studied mixtures. The minimum value of the flexural strength is 6.88 MPa for SCC10F2 and increases up to 9.16 MPa for SCC20F4, respectively. It is mainly depending on the degree of fineness and dosage of limestone filler. Again, It is noted that important fineness (BSS) of the limestone filler increases the flexural trength, thus the higher is the dosage of limestone filler the greater is the flexural strength recorded overall the studied SCCs. This percentage reaches 20 % once comparing SCC10F2 with SCC20F4 mixes ; this is in accordance with other research study (Beeralinge gowda B and al, 2007).

b.3) Ulrasonic Pulse Velocity (UPV) - NDT test

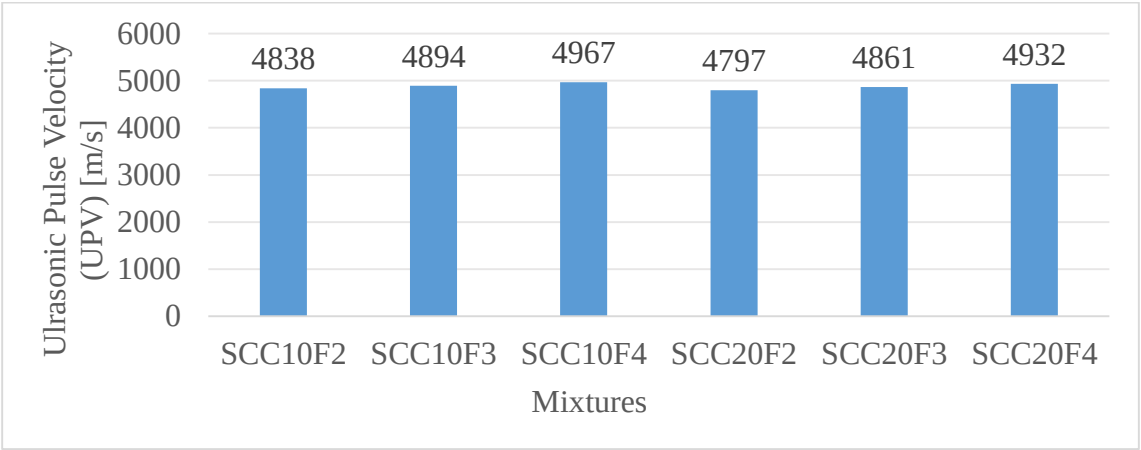

Figure V-5. Ulrasonic Pulse Velocity of SCC limestone mixtures.

The Ulrasonic Pulse Velocity is determined at 28 days age of hardening and presented in the Figure V-5. The Ulrasonic Pulse Velocity values of all the SCC are greater than 4000 m/s which means excellent resistance and proves the good quality of the confected SCC concrete based on limestone addition. It can be seen that combined higher SSB of the limestone filler or the dosage increases the ultra-sonic velocity. Which reflected the increase in the mechanical resistance of almost SCC studied mixtures. One can conclude that these results of NDT test correlated well with compression test previously discussed and judged to be more reliable in assessing the concrete of the SCC with limestone incorporation filler in the present study as reported by other researcher work (Belouadah and al, 2021).

V.2.2 Effect of granulated blast-furnace slag.

a) Fresh state

a.1) Slomp flow test

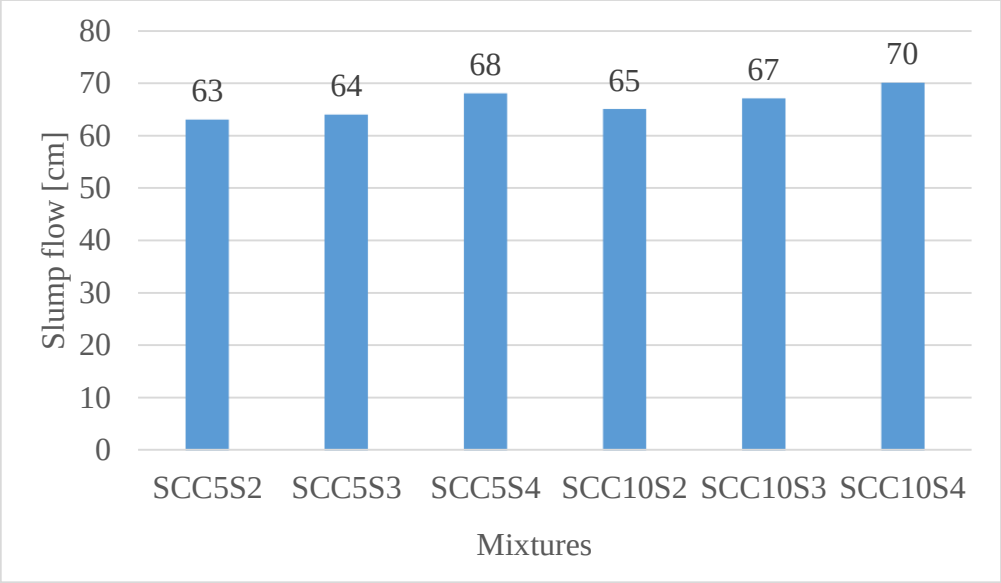

Figure V-6. Flow table test results for SCC slag mixtures.

In regards to standard value ; the flow diameter are usually in the range between 60 and 75 cm of all the SCCs as illustrated in figure V-6.

Nevertheless, higher dosages of granulated blast furnace slag increase fluidity,this can be explained by the increase in paste volume by the addition of granulated blast furnance slag which reduces intergranular friction by improving the flow of the SCC. The fine particles with a spherical shape fit into the voids and release trapped water which improves fluidity (Bensalem and al, 2014) (Zhao and al, 2015)

Thus the higher percentage of the fineness of the granulated blast furnance slag reduces the demand for water, which causes an increase in workability this is explained by the spherical shape of the slag grains wich allowed better intergranular slip (Bensalem and al, 2014).

a.2) Dynamic stability (L-box test)

It is noted that the incorporation of granulated blast furnace slag in mixtures up to 10% ensures ease of casting for such mixtures. In addition, the variation in the fineness of the granulated blast furnace slag with BSS which goes from 2000 to the maximum value 4000 cm^2/g and the dosage of filler 10% does not negatively affect the passage and the filling capacity of the SCC and therefore allows ease of casting in confined areas which contributes to dynamic stability (Bensalem and al, 2014) (Mohammed and al, 2022) (Karakurt and al, 2022).

a.3) Static Stability (Segregation index)

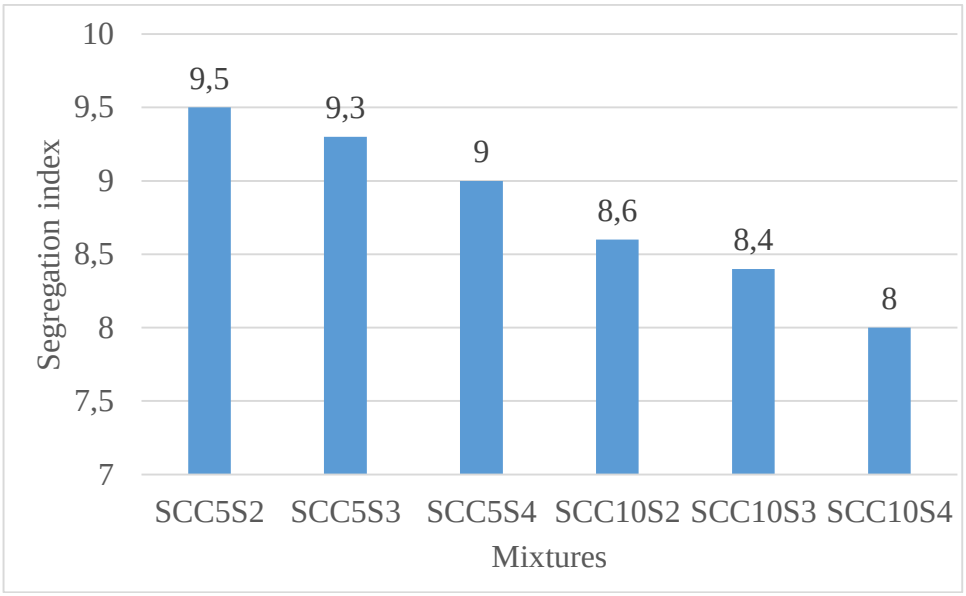

Figure V-7. Segregation index test results for SCC slag mixture.

It can be seen in Figure V-7 that all the SCCs, based on granulated blast-furnace slag have a segregation rate of less than 15%, synonymous with correct static stability; thanks to the good compactness and granular distribution that fillers give to the cementitious matrix of the mixtures (Bensalem and al, 2014) (Zhao and al, 2015).

b) Hardened state

b.1) Compressive strength (CS)

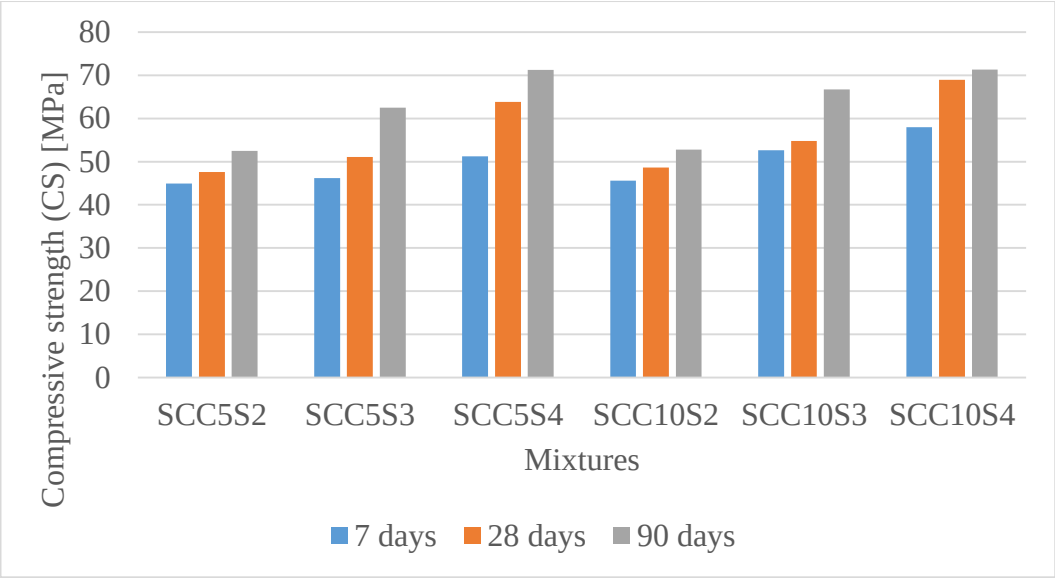

Figure V-8. The compressive strength of SCC slag mixtures.

The compressive strength (CS) is estimated at 7, 28 and 90 days of hardening and presented in FigureV-8. It was observed that the compressive strength of the specimens increases with the maturation for SCC based granulated blast furnace slag.

It can be seen in Fig V-8 that, the minimum value of the mechanical resistance is (44.94, 47.59 and 52.50) MPa for 7, 28 and 90 days respectively; it refers to the SCC5S2 which has the minimum value of SSB 2000 cm^2/g and the dosage of filler 5% of the granulated blast furnace slag. The mechanical strength increases with BSS higher fineness and dosage up to a value equal to (57.95, 68.96 and 71.34) MPa for 7, 28 and 90 days respectively (SCC10S4); the SSB which has the maximum BSS value of 4000 cm^2/g and the dosage of 10% of granulated blast furnace slag. It is noted that the increase in the SSB of the granulated blast furnace slag; increases the compressive strength, so the important dosage of granulated blast furnace slag gives a higher compressive strength. This could be explained by the hydraulic reaction which produces hydrated calcium silicate (CSH) and the portlandite $Ca(OH)_2$, and the pozolanic effect of the granulated blast furnace slag which silica reacts in the presence of water with the portlandite formed during the hydration of cement and form hydrated calcium silicate (CSH).This increases the mechanical resistance (Bensalem and al, 2014) (Karakurt and al, 2022).

$3CaO.SiO_2+H_2O$ —> CSH + $Ca(OH)_2$ (hydraulic reaction). (Eq V-1)

$Ca(OH)_2 + SiO_2 + H_2O$ —> CSH (pozzolanic reaction). (Eq V-2)

b.2) Flexural Strength (FS)

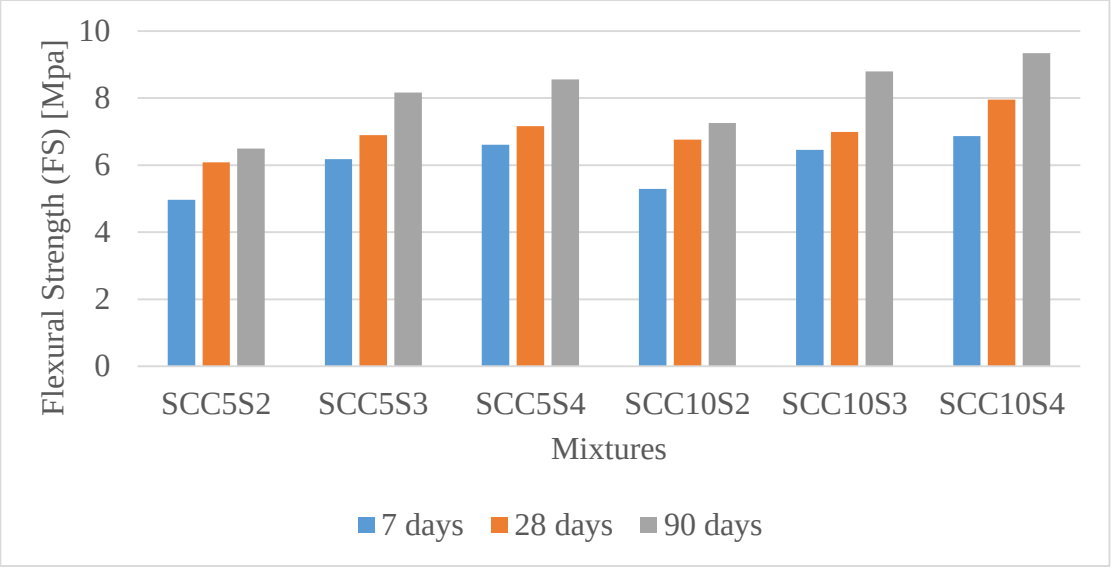

Figure V-9. The flexural strength of SCC slag mixtures.

Figure V-9 presents the flexural strength (FS) at 7, 28 and 90 days of hardening for the different SCC mixtures studied based on granulated blast furnace slag.

The minimum value of bending strength is (4.97, 6.09 and 6.50) MPa for 7, 28 and 90 days respectively, in the case of SCC5S2 these values increase to reach (6.87, 7.96 and 9.34) MPa for 7, 28 and 90 days respectively compared SCC10S4 at higher dosage of slag content. It is evident that this rise mainly depends on the degree of fineness and the dosage of the granulated blast furnce slag. Here again, it should be noted that a high fineness (BSS) of the granulated blast furnace slag increases the resistance to bending, so the higher the dosage of granulated blast furnce slag, the higher the resistance to bending. This percentage reaches 20% when comparing SCC5S2 blends with SCC10S4; this is in correlation with other research studies (Bensalem and al, 2014) (Mohan and al, 2018).

b.3) Ulrasonic Pulse Velocity (UPV) - NDT test

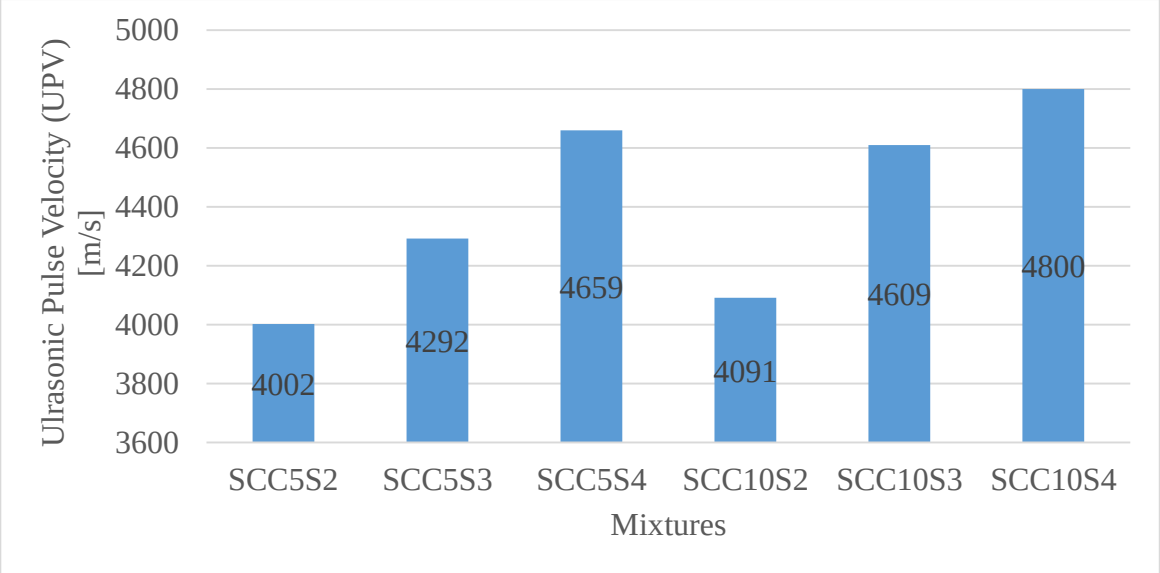

Figure V-10. Ulrasonic Pulse Velocity of SCC slag mixtures.

The Ulrasonic Pulse Velocity is determined at 28 days age of hardening and presented in the Figure V-10. The Ulrasonic Pulse Velocity values of all the SCC are greater than 4000 m/s which means excellent resistance and proves the good quality of the confected SCC concrete based on granulated blast furnce slag. It can be seen that the higher SSB of granulated blast furnace slag or the dosage of such mineral active addition; this increases the ultrasonic velocity . Which reflected the improvment of the mechanical resistance of almost SCC slag confected mixtures. One, could conclude that these results of NDT test correlated well with compression test previously discussed and judged to be more reliable in assessing the concrete of the SCC with granulated blast furnce slag filler incorporation. The present study as reported above is in accordance with results found by other research works on the subject (Belouadah and al ,2021).

V.3 Part 02 ; Measurement of static stability by a large-scale device and electrical conductivity

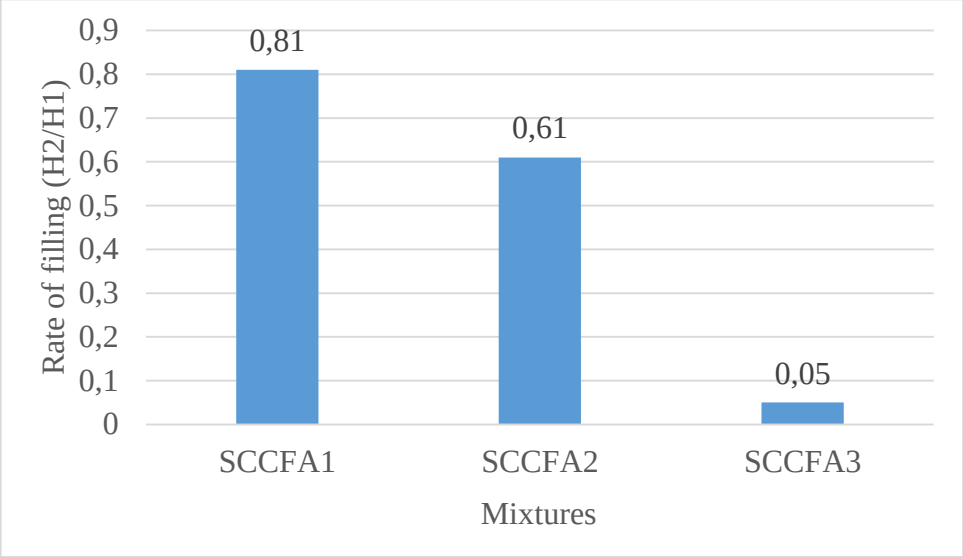

Figure V-11. L-box test results (H2/H1) for SCC fly ash mixtures.

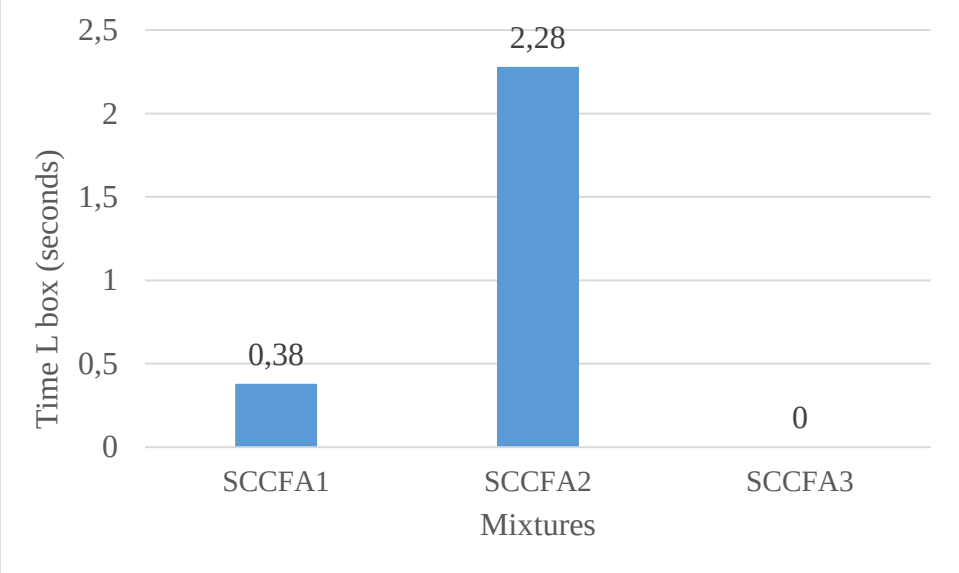

Figure V-12. L-box test results (Arrival Time) for SCC fly ash mixtures.

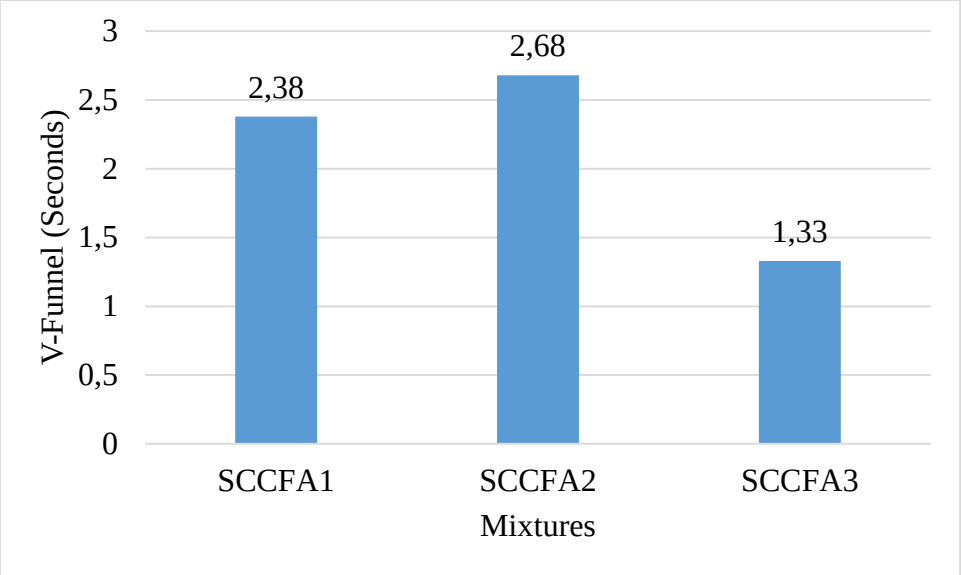

Figure V-13. V-Funnel test results for SCC fly ash mixtures.

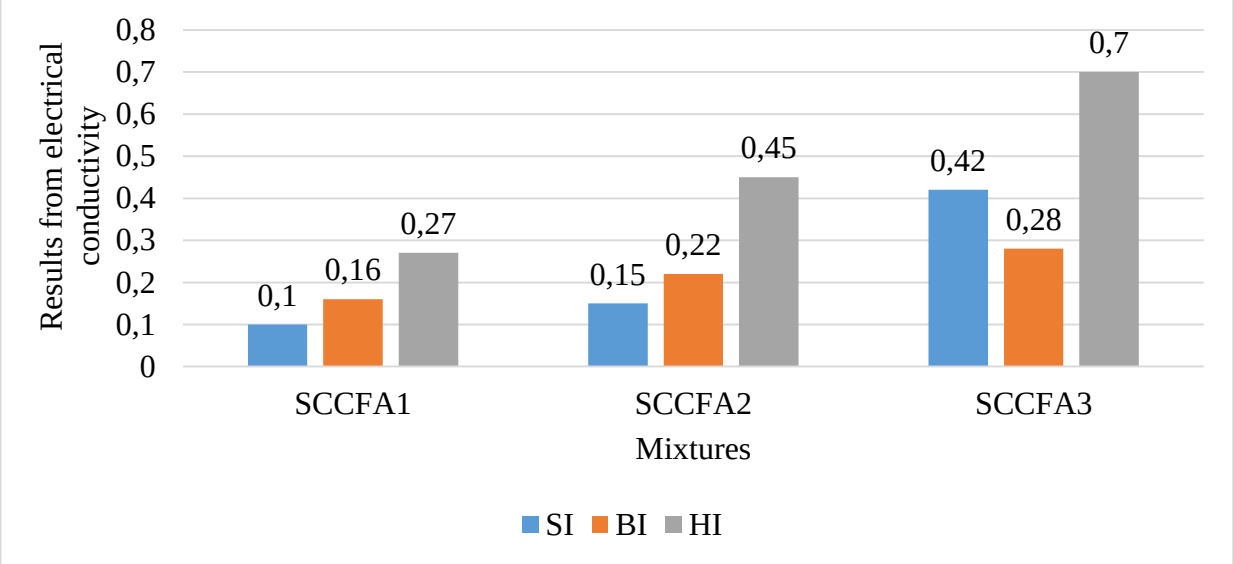

Figure V-14. Results from electrical conductivity test for SCC fly ash mixtures.

V.3.1 Effect of granular distribution and viscosity modifying agent on dynamic and static stability

According to the two figures V-11 and V-12. It is deduced that the concrete with a granular discontinuity and without viscosity modifying agent (SCC_{FA3}) presents a dynamic instability and a blocking with a critical H2/H1 ratio of 0.055, thus the two other Concrete (SCC_{FA1}) and (SCC_{FA2}) of granular continuity incorporating viscosity modifying agent present a dynamic stability with an H2/H1 ratio of 0.81 and 0.61 and an L Box passage capacity time of 0.38 second and 2.28 second for SCC_{FA1} and SCC_{FA2} respectively.

Nevertheless, according to figure V-13, it is noted that the concrete with granular discontinuity and without viscosity modifying agent (SCC_{FA3}) has a good filling capacity at the V Funnel of 1.33 second compared to the two other concretes with granular continuity and which contains viscosity modifying agent with a time of V Funnel filling of 2.38 s and 2.68 s for SCC_{FA1} and SCC_{FA2}, respectively.

From figure V-14, it can be seen that the concrete with granular discontinuity and without Ad (SCC_{FA3}) presents a static segregation index and a bleeding index at values of (SI 0.42, BI 0.28 and HI 0.70). These are higher than the two other concretes with granular continuity and which contains Ad with values of (SI 0.10, BI 0.16 and HI 0.27) and (SI 0.15, BI 0.22 and HI 0.45) for SCC_{FA1} and SCC_{FA2}, respectively. This is in accordance with other previous research study (Mesbah and al, 2011).

Figure V-15. Blockage of SCCFA3 based on fly ash.

V.3.2 Effect of the volume paste on dynamic and static stability

According to the two Figures V-11 and V-12; it could be deduced that increasing the volume paste from 37 % to 40 % decreases the dynamic stability of H2/H1 from 0.81 for SCC_{FA1} to 0.61 for SCC_{FA2}, respectively. Thus, the decrease in the ability to pass through the L box from 0.38 s for SCC_{FA1} at 2.28 s for SCC_{FA2} is noticed again.

From Figure V-13; , it is deduced that increasing the paste volume from 37% to 40% decreases the filling capacity at the V Funnel from 2.38 s for SCC_{FA1} to 2.68 for SCC_{FA2}.

From Figure V-14, It could be observed that increasing of the volume paste from 37% to 40% gives a lower static stability and increases the bleeding and the heterogeneity by (SI 0.10, BI 0.16 and HI 0.27) for SCC_{FA1} to (SI 0.15, BI 0.22 and HI 0.45) for SCC_{FA2}. The obtained results in the present investigation correlate well with other research study (Mesbah and al, 2016).

V.3.3 Effect of the coarse aggregate content on dynamic and static stability

Increasing the coarse aggregate content from 30% for SCC_{FA3} to 33% for SCCFA1 improves dynamic stability from H2/H1 0.05 for SCCFA3 to 0.81 for SCC_{FA1}; this resulted an improved static stability and reduced bleeding (SI 0.42, BI 0.28 and HI 0.70) for SCC_{FA3} compared to SCC_{FA1} at values of (SI 0.10, BI 0.16 and HI 0.27). Indeed, this is in agreement with other research study carried out on the subject previously (Mesbah and al , 2016).

V.4 Conclusion

The obtained results in the experimental program of all the testes are reported in two parts. Firstly, The limestone filler and granualated blast furnace slag incorporation at percentages up to 20 % improves the rheological properties at fresh state mainly, the fluidity, the dynamic stability and the static stability (limited segregation) of the SCC. Dosages of 20 % (L) and to 10 % (S) additions in the formulation of SCC enhance the mechanical performances (compressive and flexural strengths). Furthermore, the effect of fineness for both additions (L, S) is noticed.

Secondly, for mixtures incorporating fly ash (FA) once measuring the static and dynamic stability and bleeding using large scale device and electrical conductivity. The effect of intrinsic parameters is appreciated in improved homogeneity and reduced bleeding index for higher content of coarse aggregate. Moreever, granular discontinuity cause a decrease in the static stability and a rise in the bleeding index. The viscosity modifying agent proved to give improved static and dynamic stability. However, the increase in volume paste decreases the dynamic and static stability as well as the capacity of passage and filling for confected SCC (FA) mixtures.

PART THREE.

Modeling part

Chapter VI.

Experimental design plan methods (JMP).

VI.1 Experimental design methods

In order to better organize the tests that accompany an experimental program dedicated to a parametric study by minimizing both the number of tests and increasing the accuracy; whether it is in the case of optimizing the formulation of a SCC to obtain a SCC of better performance, screening the parameters that do not influence its characteristics, predicting the effects of different parameters on the properties of the formulated SCC; or even deducing the effect of interaction of several parameters at once on the produced SCC. For such purpose, the experimental design modeling methods are used.

VI.1.1 Definition

The experimental design methods (EDM) is a branch of applied statistics whose purpose is to plan experiments and to analyze and interpret their results. The appearance of the (EDM) go back to 1925 with the introduction of Fisher's work in the agricultural field followed by the introduction of Taguchi's method in Japan for the improvement of the quality. Nevertheless, since 1980, many design of experiments softwares are developed such as MINITAB, EXPERT DESIGN and JMP.

Design of experiments can be used in the case of a technical study, the optimization of a manufacturing process, the best adjustment of a machine, the improvement of the quality of a product or the development of a new product.

There are several types of experimental designs such as full factorial design, fractional factorial design, Plackett and Burman design, Taguchi tables, star design, Koshal design, and Dohlert design (Goupy JACQUES L, 1990).

- Full factorial design Plans ;

Full factorial designs are inspired by Fisher's work; where each factor takes only two levels (values) a lower level takes the sign (-1) and a higher level takes the sign (+1).

Full factorial designs are easy to construct, the risk of error is minimized because each factor takes only two values, as well as the interpretation of the results and the calculation of the effects of the interactions is easy and the mathematical modeling is immediate. Nevertheless, their only disadvantage is that it forces the experimenter to do a large number of trials which sometimes requires a lot of time, energy and money.

- Fractional factorial design ;

Fractional factorial designs are applicable when the number of factors is large; these designs are used to reduce the number of trials to 50% or more without reducing the number of factors to be studied.

Fractional factorial designs lead to an economical experimental program; however, the only disadvantage is that the experimenter has to make an effort to develop these designs and interpret the results.

- Plackett and Burman design ;

Plackett and Burman design are used to study the effect of several factors by designing few trials where each factor takes only two values and the interaction between the factors is neglected.

- Taguchi's tables ;

Taguchi tried to simplify the use of factorial designs by providing tables and graphs that are themselves factorial designs.

- Koshal's design plans ;

The principle of the Koshal design is to establish a design of experiments whose the number of experiments is equal to the number of coefficients of the polynomial of their mathematical model; where each factor is studied alone "one factor at a time"; therefore the study of interaction effect between the different factors is impossible.

Most experimenters use this design without knowing that it is a Koshal design of experiments.

- Star design plans ;

Star designs are complementary models to factorial designs or can be established in a progressive way ; first a fractional factorial design is implemented and then a complementary design if the results are doubtful or insufficient.

The principle of this type of design is to give at least three levels to each factor while using a minimum number of tests.

- Dohlert's designs ;

Dohlert proposed a design of experiments of a uniform distribution or all experimental points are at the same distance from the center of the study domain.

VI.1.2 The principle of Experimental Design method

VI.1.2.1 Terminology

- Factor ;

A factor is a variable that is assumed to have an influence on the studied system; the factor may be quantitative or qualitative.

- Level of factor ;

This is the quantitative or qualitative value given to a factor.

- Response ;

The response is a quantity measured after each experiment.

- Effect of factor ;

The effect of a factor is the observed variance of the response according to different factors.

- Study domain ;

The study domain or experimental domain ; it is an interval bounded by the lower and upper levels of each factor.

- Interaction ;

Interaction occurs when the impact of one factor on the response depends on the value of a second factor; means that the combination of factors are not acting independently.

- Mathematical Modeling ;

Mathematical modeling is a function in the form of a polynomial that; best describes the variation of the response depending on the values of the factors. These models will allow us to calculate the responses of the study domain without the return to the realization of the experiments.

$$Y = a_0 + a_1x_1 + a_2x_2 + a_{12}x_1x_2 + C$$

Y ; response.

Xi ; factor level i.

a_0 ; Response in the domain centre.

a_1 ; Factor 1 effect.

a_2 ; Factor 2 effect.

a_{12} ; Factors 1 and 2 interaction.

C ; The gap.

VI.1.3 Step of modeling by experimental design plans method

Step 1 ; Clearly identify the problem to be solved and determine the objective to be achieved.

Step 2 ; Choose the factors to study and fix their level.

Step 3 ; Choose the type of experimental design that is appropriate and build it.

Step 4 ; Carry out the experimental program provided by the experimental design and measure the responses at the end of each trial.

Step 5 ; Analyze the results and deduce the effect of each factor, the interaction between the different factors and a mathematical model that is used to predict the results without resorting to the experimental test in the laboratory.

The effect of the factors is deduced by calculating the coefficients of the polynomial of the mathematical model; thus the interaction effect between the factors is calculated by the t-test or the ANOVA test.

VI.1.4 State of the art on the modeling of SCC by experimental design methods

According to the literature, many researchers have used design of experiments as a tool to predict results in advance, to study the effect of certain parameters and to optimize mixtures in order to achieve a better performance of SCC (Sonebi, 2004).

(Sonebi, 2004.) ; Used a factorial design of experiments to model mathematically the influence of the parameter W/C, the dosage of superplasticizer, the cement content and the fly ash content on the filling capacity, passage, segregation and compressive strength of a self-placing concrete of medium strength.

(Bouziani T, 2013) ; proposed a statistical approach to evaluate the effect of different type of sand on the properties of SCC.

(Al qadi and al, 2016) ; developed by experimental design a model to predict the compressive strength at 28 days age of self-compacting concrete.

(Al qadi and al, 2017) ; used design of experiment modeling to predict the J -Ring test results of a self-compacting concrete.

(Habibi and al, 2018) ; used Taguchi's design of experiments method for the design of an optimal mix of a self-compacting concrete.

Other researchers used the design of experiment method in other type of concrete.

(Ahmed and al, 2015); used a statistical program by JMP design of experiments to propose a modeling to predict the slump and compressive strength of a high strength concrete.

(Bederina M and al, 2016) ; used the design of experiments method to model the main physical-mechanical properties of a lightweight sand concrete.

(Yan and al, 2019) ; established a statistical model based on design of experiments to evaluate the effect of W/C parameter and S/A (sand/aggregate) parameter on the properties of desert sand concrete, thus a mixture optimization of desert sand concrete.

(Cotto-Ramos and al, 2020) ; used experimental designs to study the effect of adding silica fume, nano silica and recycled plastic on the cost and mechanical strength of conventional intoxicant-friendly concrete.

(Solouki and al, 2022) ; optimized the mix design of concrete paver production by design of experiment modeling.

(Hamla and al, 2022); modeled by experimental design the physical and mechanical characteristics of roller compacting concrete.

VI.1.5 Conclusion

In regards to the the evolution of digital technology, it has become necessary to use EDM as a reliable tool, less expensive and more accurate than the tedious laboratory experiments, to better organize the tests, or predict the characteristics and study the effect of certain parameters on the behavior of SCC.

The bibliographic research undertaken so far, let us deduce that many researchers have used and proved the reliability of these experimental design plans in the case of self-compacting concrete and other concrete types.

VI.2 Modeling of the mechanical response (CS-FS-UPV) of SCC based on limestone

VI.2.1 Correlation of (CS, FS – UPV)

The results of the experimental tests characterizing the mechanical behavior of SCC with different Specific Surface of Blaine (BSS) and content of limestone powder (D%) are reported, in the table VI-1. The six (3*2) experiments proposed by full factorial design were performed are put in the table VI-2 summarizes the values of each factor and their respective levels.

The correlations between the observed and the predicted values of compressive strength, flexural strength, and Ultrasonic Pulse Velocity (UPV) (m/s) are given in Figure VI-1. It can be observed that the generated points dissipated along the trend line, in this way, the models yielded a good expectation power.

Table VI-3 collects the Summary of Fit results which shows a high correlation coefficients value.The R square for CS, FS, and UPV is 0.997,0.998, and 0.997, respectively.

Table VI-1. Observed results of mehanical response for statistical modeling of studied SCC mixtures.

Mixes	SSB (cm^2/g)	(L) (%)	Comp-Strength CS(MPa)	Flex-strength FS(MPa)	Ultrasonic Velocity UPV(m/s)
SCC_{10F2}	F2=2000	10	66	6.8	4838
SCC_{10F3}	F3=3000	10	71	7.9	4894
SCC_{10F4}	F4=4000	10	79	9.2	4967
SCC_{20F2}	F2=2000	20	68	7.6	4797
SCC_{20F3}	F3=3000	20	77	8.2	4861
SCC_{20F4}	F4=4000	20	85	8.8	4932

Table VI-2. The experimental ranges and factors level.

Levels	D (%).	BSS (cm2/g)
-1	10	2000
0	-	3000
+1	20	4000

Table VI-3. Summary of Fit.

	CS(MPa)	FS(MPa)	UPV(Km/s)
R^2	0.997	0.998	0.997
Adjusted R^2	0.994	0.997	0.992
RMSE	0.529	0.044	5.307
Mean of response	74.9	8.122	4881.5

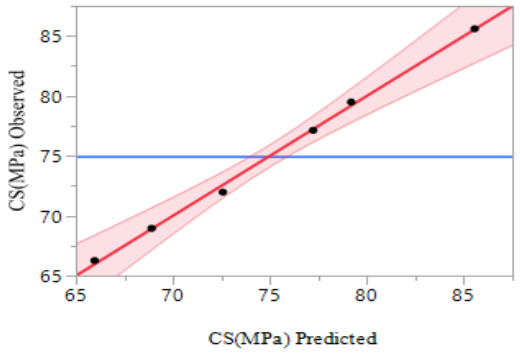

(a) Compressive strength

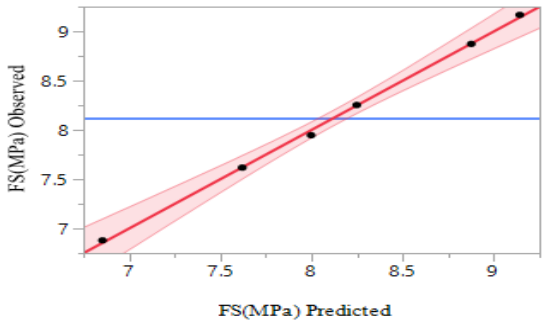

(b) Flexural strength

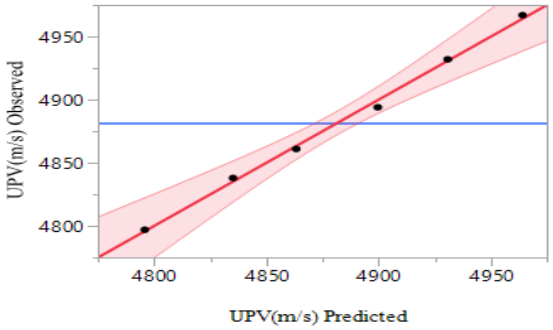

(c) Ultrasonic Pulse Velocity.

Figure VI-1. Correlation between actual and predicted values. a-compressive strength, b-flexural strength, c- Ultrasonic Pulse Velocity.

VI.2.2 Analyse of variance

Table VI-4. Shows the results of ANOVA (Analysis of Variance) in which we present the degrees of freedom, the Sum of Squares, mean square, F-ratio, and the probability.

The probability (Prob.> F) values for CS, FS, and UPV is 0.0032, 0.0017, and 0.0043, respectively (Prob. > F) are lower than 5% that allowed and considered evidence that there is at least one significant effect in the model.

Table VI-4. Analysis of variance (ANOVA) for derived models.

	Source	degree of freedom	Sum of squares	Mean square	F -ratio
CS(MPa)	Model	3	258.60797	86.2027	307.8483
	Error	2	0.56003	0.2800	Prob. > F
	Total	5	259.16800		0.0032*
FS(MPa)	Model	3	3.4965095	1.16550	587.9636
	Error	2	0.0039645	0.00198	Prob. > F
	Total	5	3.5004741		0.0017*
UPV (m/s)	Model	3	19413.167	6471.06	229.7416
	Error	2	56.333	28.17	Prob. > F
	Total	5	19469.500		0.0043*

Table VI-5. Effect of test.

	Model term	Estimation	standard Error	t ratio	Prob. > |t|
CS(MPa)	Constante	74.9	0.216031	346.71	<.0001*
	BSS(cm^2/g)	7.47	0.264583	28.23	0.0013*
	D (%)	2.3266667	0.216031	10.77	0.0085*
	BSS(cm^2/g)*D(%)	0.855	0.264583	3.23	0.0839
FS(MPa)	Constante	8.1229583	0.018176	446.90	<.0001*
	BSS(cm^2/g)	0.8855	0.022261	39.78	0.0006*
	D (%)	0.1250417	0.018176	6.88	0.0205*
	BSS(cm^2/g)*D(%)	-0.258	0.022261	-11.59	0.0074*
UPV (m/s)	Constante	4881.5	2.166667	2253.0	<.0001*
	BSS(cm^2/g)	66	2.653614	24.87	0.0016*
	D (%)	-18.16667	2.166667	-8.38	0.0139*
	BSS(cm2/g)*D(%)	1.5	2.653614	0.57	0.6288

a) Compressive strength (CS)

Figures VI-2 and VI-3, illustrated the graphical results of compressive strength of SCC with different content and finesse of limestone powder.According to the effect test, Table VI-5,p-values are lower than 0.05 thus, revealing that all of the independent variables considered contrariwise the interaction is not statistically significant. (p-values bigger than 0.05).

From figures VI-2-a,VI-2-b, it can be noted that an increase in the Blaine Specific Surface (BSS), led to increasing the compressive strength, While, the increase in the content of limestone

powder has a slight influence on the compressive strength. The interaction plots of compressive strength are presented in Figure VI-3-b. The intersection of the two lines Indicates that interaction of factors has no considerable effect on this response. The empirical equation for the compressive strength is given in equation (Eq VI-1).

$$\mathbf{CS(MPa)} = \mathbf{74.9} + \mathbf{7.47}\frac{\mathbf{BSS-3000}}{\mathbf{1000}} + \mathbf{2.32}\frac{\mathbf{D-15}}{\mathbf{5}} + \mathbf{0.855}\frac{\mathbf{BSS-3000}}{\mathbf{1000}}.\frac{\mathbf{D-15}}{\mathbf{5}} \qquad \text{(Eq VI-1)}$$

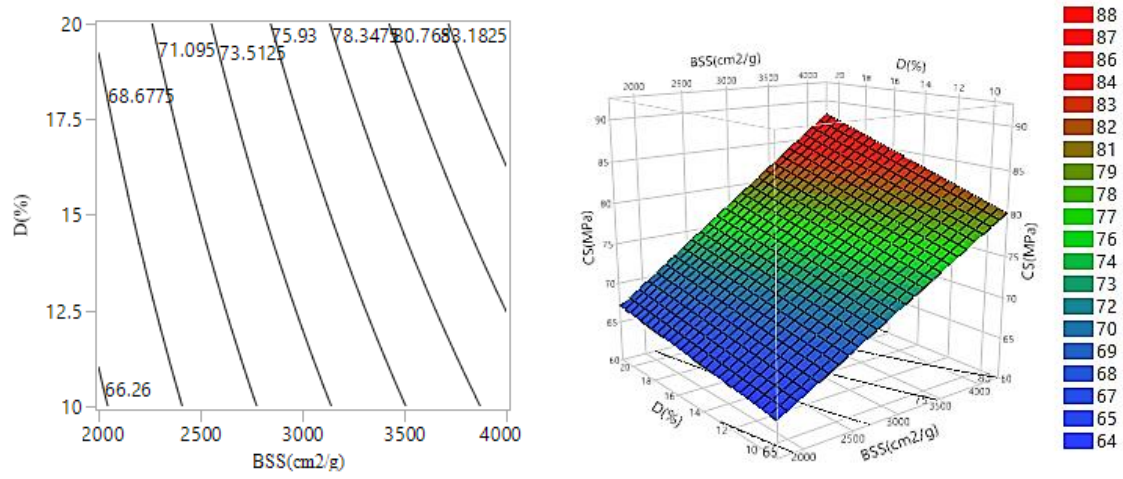

(a) (b)

Figure VI-2. (a) Isoresponse curves and (b) response surfaces of compressive strength.

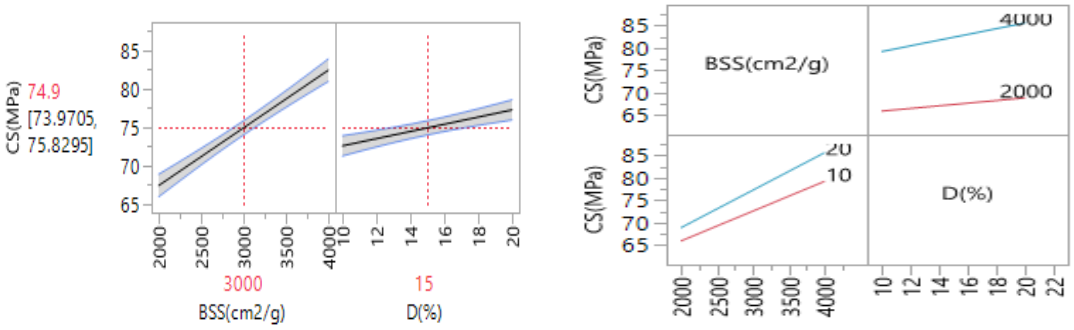

(a) (b)

Figure VI-3. (a) Main effect plots and (b) interaction plots of compressive strength.

b) Flexural strength (CS)

Figure VI-5-a (Main effect) describe the effect of the two factors on the flexural. Figure VI-4- (a) and (b) show the iso-response and surface response for flexural strength SCC specimens.

The Iso-response figure shows that the flexural strength increases from 6.88 to 8.90 with increasing limestone powder BSS.It can be also noted from the surface response that the increase in the (BSS), led to increasing the flexural strength.While, the increase in the content of limestone powder has a small influence.

Strength it may be noted that the BSS of limestone powder reproduces a stronger positive effect on the flexural strength, in the same context, the limestone powder content has a small positive effect on this response. These results are dependable with the estimated coefficients (table VI-5) and equation (Eq VI-2);

Figure VI-5-b shows interaction plots of flexural strength, it can be observed that the two lines intersect with each other, Which indicates that interaction effects of factors have a considerable effect on response.

$$\mathbf{FS(MPa)} = \mathbf{8.12} + \mathbf{0.885}\frac{\mathbf{BSS-3000}}{\mathbf{1000}} + \mathbf{0.125}\frac{\mathbf{D-15}}{\mathbf{5}} - \mathbf{0.258}\frac{\mathbf{BSS-3000}}{\mathbf{1000}}.\frac{\mathbf{D-15}}{\mathbf{5}} \qquad \text{(Eq VI-2)}$$

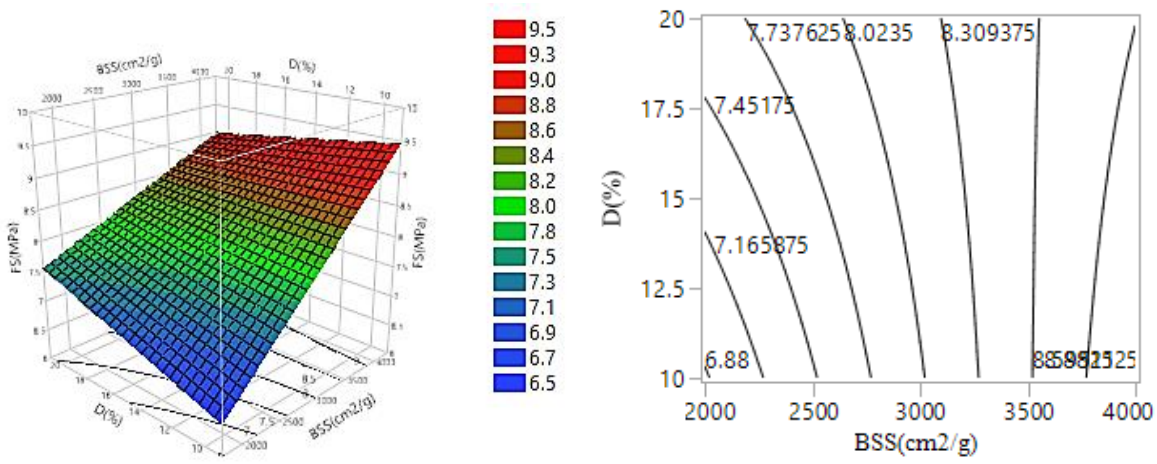

(a) (b)

Figure VI-4. (a) Isoresponse curves and (b) response surfaces of flexural strength (a) Main effect plots and (b).

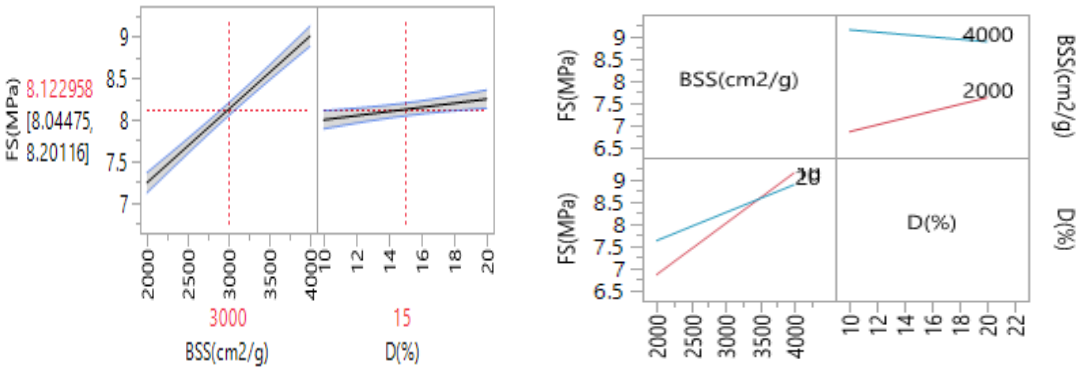

(a) (b)

Figure VI-5. (a) Main effect plots and (b) interaction plots of flexural strength.

c) Ultrasonic Pulse Velocity (UPV) - NDT test

Figure VI-6 (a) and (b) show the iso-response and surface response show clearly that the increase of BSS of limestone powder increases the Ultrasonic Pulse Velocity, remarkably.Indeed, the content of powder presents a slight negative effect on the response.

The optimum conditions of UPV were 10% limestone powder and the fineness 4000 cm^2/g.

In the same context, and according to the test effect table VI-5 above, it has been observed that the BSS of limestone powder is the most influencing factor in the Ultrasonic Pulse Velocity. While the content shows a second-order effect; the interaction does not affect the response.These results were confirmed by the main effect and interaction plots figure VI-7.

The mathematical model of Ultrasonique Pulse Velocity is written in equation (Eq VII-3).

$$\mathbf{UPV}\left(\frac{\mathbf{cm2}}{\mathbf{g}}\right) = \mathbf{4881.5} + \mathbf{66}\frac{\mathbf{BSS-3000}}{\mathbf{1000}} - \mathbf{18.16}\frac{\mathbf{D-15}}{\mathbf{5}} + \mathbf{1.5}\frac{\mathbf{BSS-3000}}{\mathbf{1000}}.\frac{\mathbf{D-15}}{\mathbf{5}} \qquad \text{(Eq VI-3)}$$

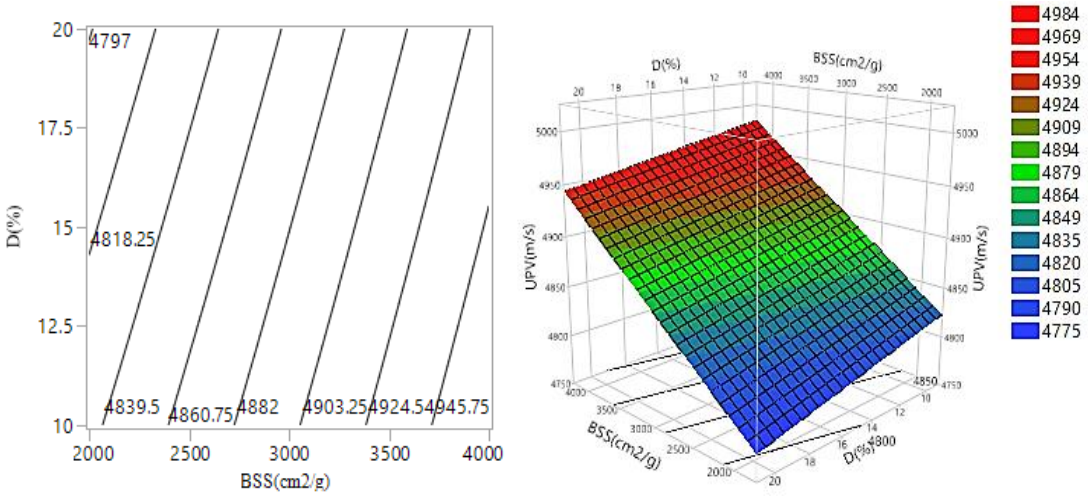

(a) (b)

Figure VI-6. (a) Isoresponse curves and (b) response surfaces of UPV (m /s).

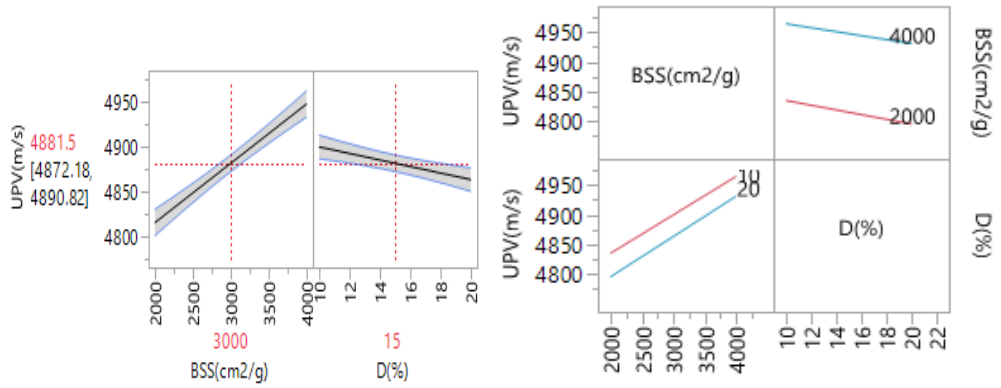

(a) (b)

Figure VI-7. (a) Main effect plots and (b) interaction plots of UPV (m /s).

VI.3 Modeling of the mechanical response (CS-FS-UPV) of SCC based on slag

VI.3.1 Correlation of (CS, FS – UPV)

The results of the experimental tests characterize the mechanical behavior of SCC with different Specific Surface of Blaine (BSS) and content of granulated blast furnce slag (D%) Table VI-6. The six (3*2) experiments proposed by full factorial design were performed;Table VI-7 summarizes the values of each factor and their respective levels.

The correlations between the observed and the predicted values of compressive strength, flexural strength, and Ultrasonic Pulse Velocity (UPV) (m/s) are given in Figure VI-8. It can be observed that the generated points dissipated along the trend line, in this way, the models yielded a good expectation power.

Table VI-8 collects the Summary of Fit results which shows a high correlation coefficients value. The R square for CS, FS, and UPV is 0.988,0.997, and 0.998, respectively.

Table VI-6. Observed results of mehanical response for statistical modeling of studied SCC mixtures at 28 days.

Mixes	SSB (cm^2/g)	(S) (%)	Comp-Strength CS(MPa)	Flex-strength FS(MPa)	Ultrasonic Velocity UPV(m/s)
SCC_{5S2}	F2=2000	05	47	6.1	4002
SCC_{5S3}	F3=3000	05	51	6.9	4292
SCC_{5S4}	F4=4000	05	64	7.2	4659
SCC_{10S2}	F2=2000	10	48	6.8	4091
SCC_{10S3}	F3=3000	10	55	6. 9	4609
SCC_{10S4}	F4=4000	10	69	7.9	4800

Table VI-7. The experimental ranges and factors level.

Levels	D (%).	BSS (cm2/g)
-1	5	2000
0	-	3000
+1	10	4000

Table VI-8. Summary of Fit.

	CS(MPa)	FS(MPa)	UPV(Km/s)
R^2	0.988	0.997	0.998
Adjusted R^2	0.983	0.996	0.998
RMSE	1.290	0.041	16.443
Mean of response	57.255	6.992	4388

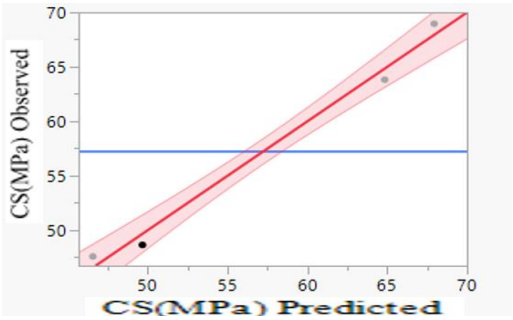

(a) Compressive strength

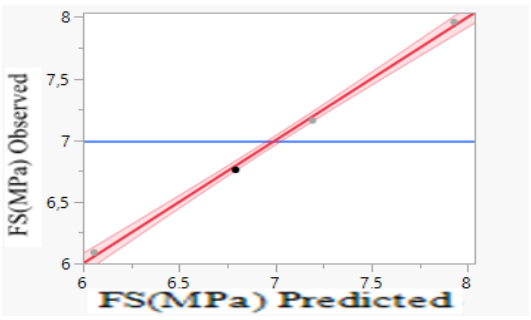

(b) Flexural strength

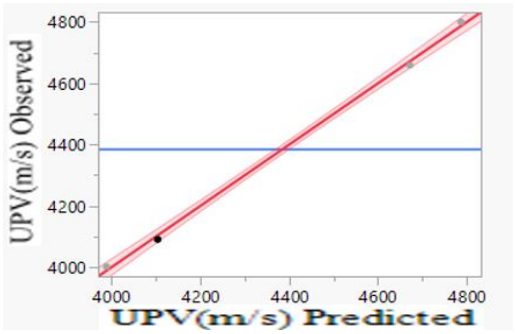

(c) Ultrasonic Pulse Velocity.

Figure VI-8. Correlation between actual and predicted values. a-compressive strength, b-flexural strength, c- Ultrasonic Pulse Velocity at 28 days.

VI.3.2 b) Analyse of variance

Table VI-9 shows the results of ANOVA (Analysis of Variance) in which we present the degrees of freedom, the Sum of Squares, mean square, F-ratio, and the probability.

The probability (Prob.> F) values for CS, FS, and UPV is <.0001* (Prob. > F) are lower than 5% that allowed and considered evidence that there is at least one significant effect in the model.

Table VI-9. Analysis of variance (ANOVA) for derived models.

	Source	degree of freedom	Sum of squares	Mean square	F -ratio
CS(MPa)	Model	2	686.80580	343.403	206.2926
	Error	5	8.32320	1.665	Prob. > F
	Total	7	695.12900		<.0001*
FS(MPa)	Model	2	3.6569000	1.82845	1081.923
	Error	5	0.0084500	0.00169	Prob. > F
	Total	7	3.6653500		<.0001*
UPV (m/s)	Model	2	959428.00	479714	1774.090
	Error	5	1352.00	270	Prob. > F
	Total	7	960780.00		<.0001*

Table VI-10. Effect test.

	Model term	Estimation	standard Error	t ratio	Prob. > |t|
CS(MPa)	Constante	57.255	0.456158	125.52	<.0001*
	BSS(cm^2/g)	1.55	0.456158	3.40	0.0193*
	D (%)	9.135	0.456158	20.03	<.0001*
	BSS(cm^2/g)*D(%)				
FS(MPa)	Constante	6.9925	0.014534	481.10	<.0001*
	BSS(cm^2/g)	0.3675	0.014534	25.28	<.0001*
	D (%)	0.5675	0.014534	39.05	<.0001*
	BSS(cm^2/g)*D(%)				
UPV (m/s)	Constante	4388	5.813777	754.76	<.0001*
	BSS(cm^2/g)	57.5	5.813777	9.89	0.0002*
	D (%)	341.5	5.813777	58.74	<.0001*
	BSS(cm^2/g)*D(%)				

a) Compressive strength (CS)

Figures VI-9 and VI-10, illustrated the graphical results of compressive strength of SCC concrete at 28 days with different content and finesse of granulated blast furnce slag. According to the effect test, Table VI-10, p-values are lower than 0.05 thus, revealing that all of the independent variables considered contrariwise the interaction is not statistically significant. (p-values bigger than 0.05).

From figures VI-9 -a,VI-9-b, it can be noted that an increase in the Blaine Specific Surface (BSS), led to increasing the compressive strength, While, the increase in the content of

granulated blast furnce slag has a slight influence on the compressive strength. The interaction plots of compressive strength are presented in Figure VI-10-b. The intersection of the two lines Indicates that interaction of factors has no considerable effect on this response. The empirical equation for the compressive strengthis given in equation (Eq VI-4).

$$\mathbf{CS(MPa)} = \mathbf{57.255} + \mathbf{9.135}\frac{\mathbf{BSS-3000}}{\mathbf{1000}} + \mathbf{1.55}\frac{\mathbf{D-7.5}}{\mathbf{2.5}} \qquad \text{(Eq VI-4)}$$

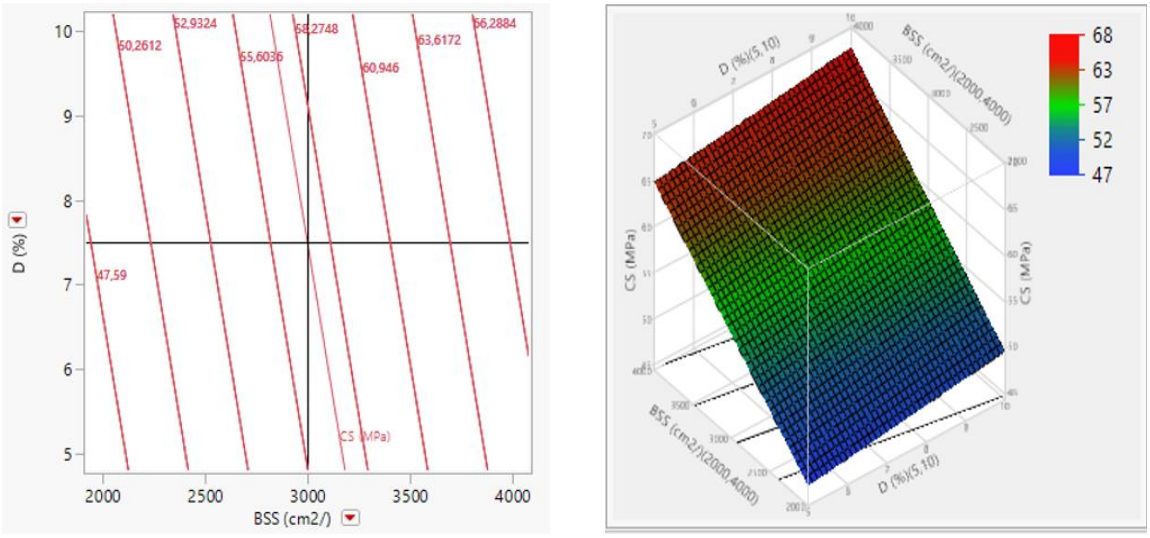

(a) (b)

Figure VI-9. (a) Isoresponse curves and (b) response surfaces of compressive strength at 28 days.

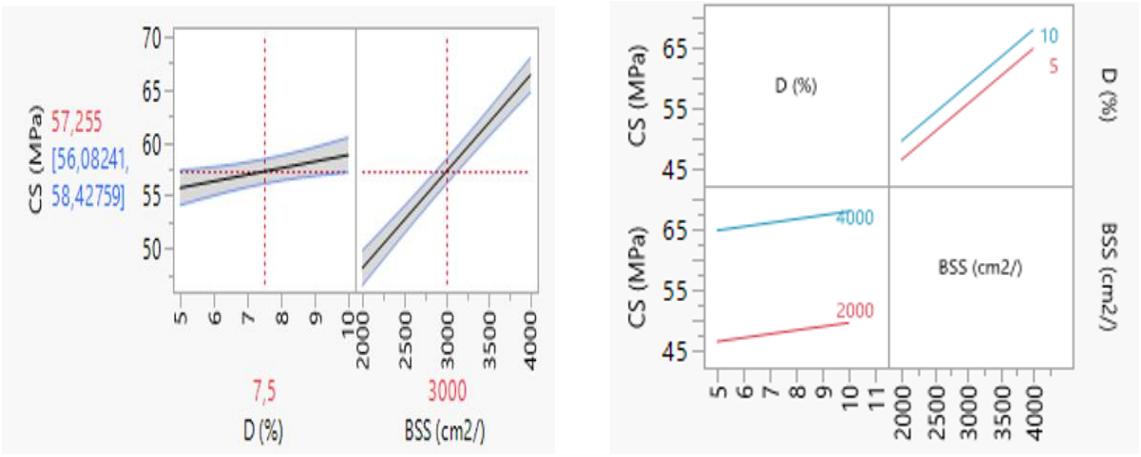

(a) (b)

Figure VI-10. (a) Main effect plots and (b) interaction plots of compressive strength at 28 days.

b) Flexural strength (CS)

Figure VI-11 (a) and (b) show the iso-response and surface response for flexural strength SCC specimens. The Iso-response figure shows that the flexural strength increases from 6.09 to 7.72 with increasing granulated blast furnce slag BSS.It can be also noted from the surface response that the increase in the (BSS), led to increasing the flexural strength.While, the increase in the content of granulated blast furnce slag has a small influence.

Figure VI-12-a (Main effect) describe the effect of the two factors on the flexural strength it may be noted that the BSS of granulated blast furnce slag reproduces a stronger positive effect on the flexural strength, in the same context, the granulated blast furnce slag content has a small positive effect on this response. These results are dependable with the estimated coefficients (table VI-10) and equation (Eq VI-5) ;

Figure VI-12-b shows interaction plots of flexural strength, it can be observed that the intersection of the two lines Indicates that interaction of factors has no considerable effect on this response.

$$\mathbf{FS(MPa)} = \mathbf{6.9992} + \mathbf{0.567}\frac{\mathbf{BSS-3000}}{\mathbf{1000}} + \mathbf{0.367}\frac{\mathbf{D-7.5}}{\mathbf{2.5}} \qquad \text{(Eq VI-5)}$$

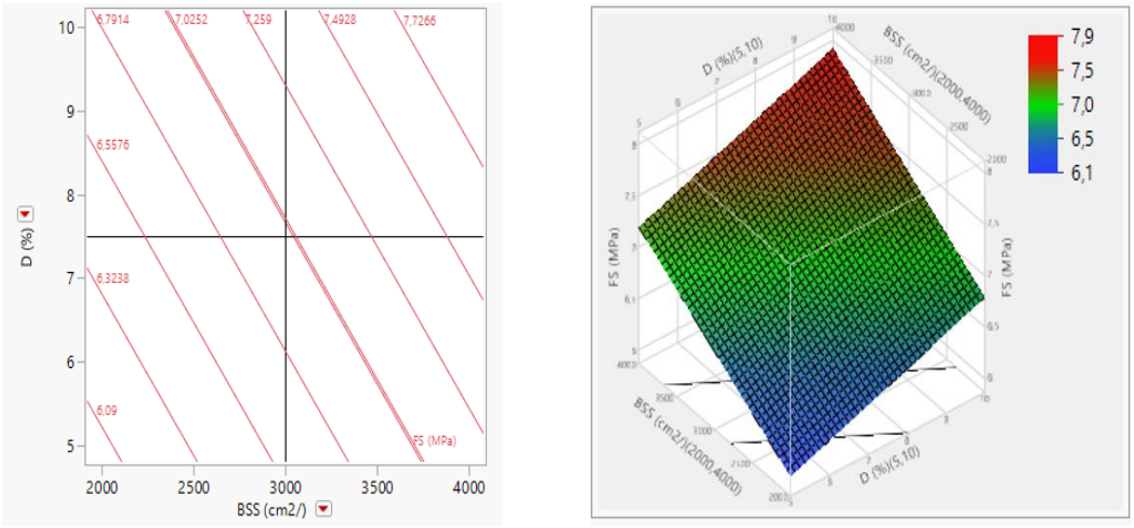

(a) (b)

Figure VI-11. (a) Isoresponse curves and (b) response surfaces of flexural strength (a) Main effect plots and (b) at 28 days.

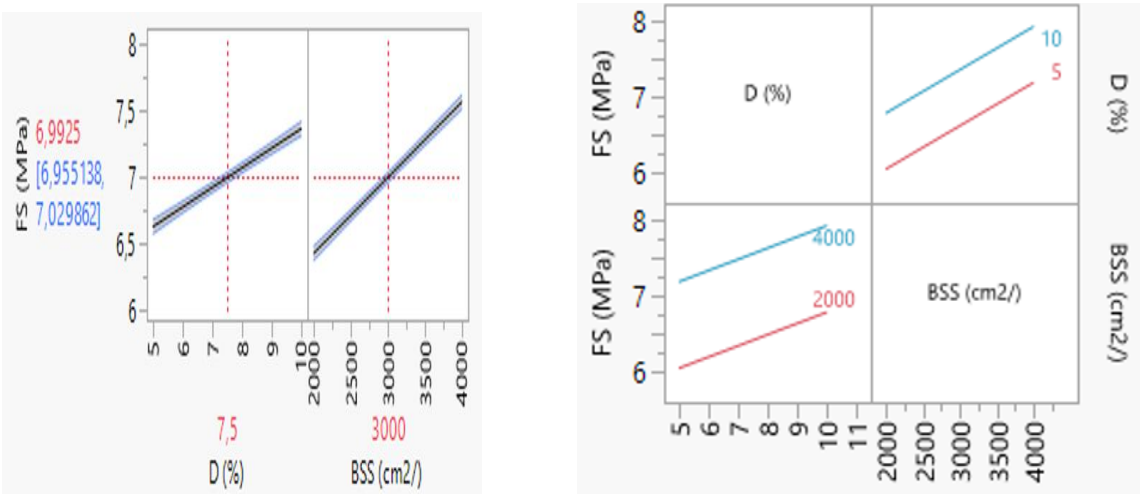

(a) (b)

Figure VI-12. (a)Main effect plots and (b) interaction plots of flexural strength at 28 days.

c) Ultrasonic Pulse Velocity (UPV) - NDT test

Figure VI-13 (a) and (b) show the iso-response and surface response show clearly that the increase of BSS of granulated blast furnce slag increases the Ultrasonic Pulse Velocity, remarkably.Indeed, the content of powder presents a little effect on the response.

The optimum conditions of UPV were 10% granulated blast furnce slagand the fineness 4000 cm^2/g.

in the same context, and according to the test effect table VI-10 above, it has been observed that the BSS of granulated blast furnce slag is the most influencing factor in the Ultrasonic Pulse Velocity, while the content shows a second-order effect; contrariwise the interaction does not affect the response. These results were confirmed by the main effect and interaction plots figure VI-14.

The mathematical model of Ultrasonique Pulse Velocity is written in equation (Eq VI-6).

$$\mathbf{UPV}\left(\frac{\mathbf{cm2}}{\mathbf{g}}\right) = \mathbf{4388} + \mathbf{341.5}\frac{\mathbf{BSS-3000}}{\mathbf{1000}} + \mathbf{57.5}\frac{\mathbf{D-7.5}}{\mathbf{2.5}} \qquad \text{(Eq VI-6)}$$

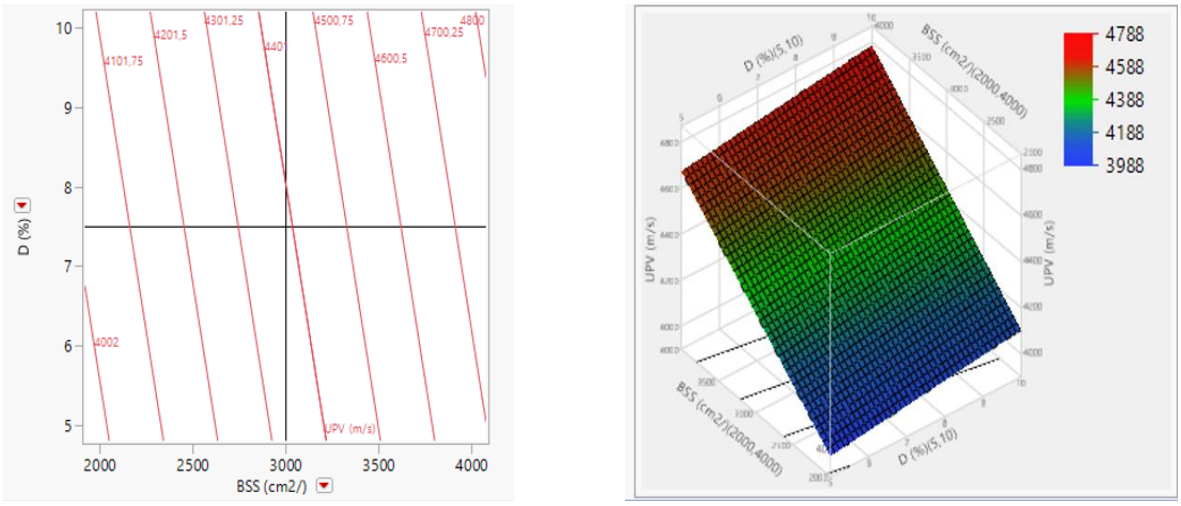

(a) (b)

Figure VI-13. (a) Isoresponse curves and (b) response surfaces of UPV (m /s) at 28 days.

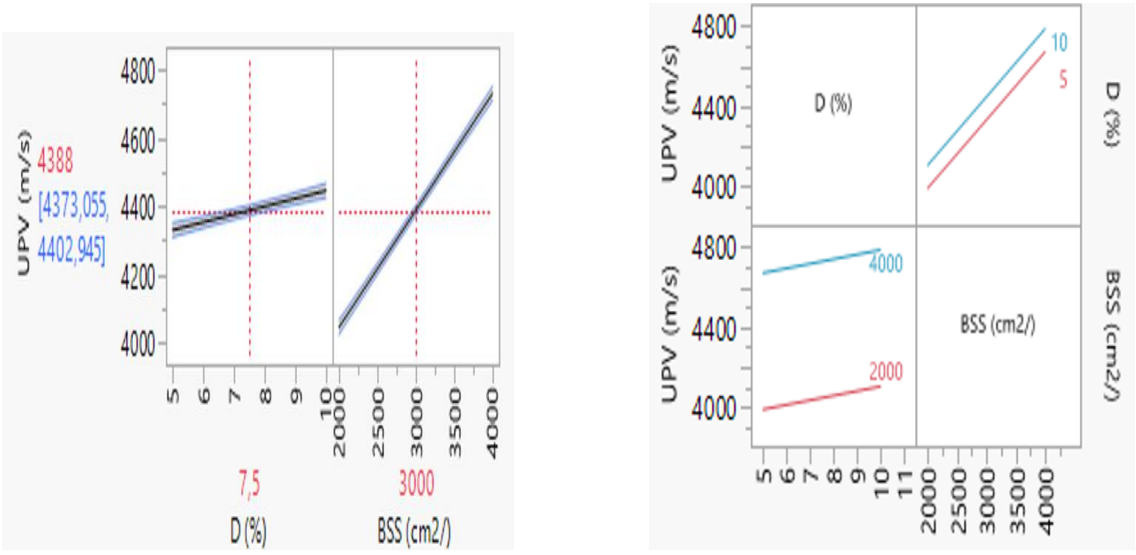

(a) (b)

Figure VI-14. (a) Main effect plots and (b) interaction plots of UPV (m /s) at 28 days.

TableVI-11. Summary statistical analysis of mathematical models at hardened state.

Part N°01	Property (Rs – Response)	Model		Determination coefficient (R^2)	Equation Number
Inert addition (limestone filler)	**CS(MPa)**	Constante BSS(cm^2/g) D(%) BSS(cm^2/g)* D(%)	$CS(MPa) = 74.9 + 7.47\frac{BSS-3000}{1000} + 2.32\frac{D-15}{5} + 0.855\frac{BSS-3000}{1000}.\frac{D-15}{5}$	0.997	Eq VI-1
	FS(MPa)	Constante BSS(cm^2/g) D(%) BSS(cm^2/g)* D(%)	$FS(MPa) = 8.12 + 0.885\frac{BSS-3000}{1000} + 0.125\frac{D-15}{5} - 0.258\frac{BSS-3000}{1000}.\frac{D-15}{5}$	0.998	Eq VI-2
	UPV(m/s)	Constante BSS(cm^2/g) D(%) BSS(cm^2/g)* D(%)	$UPV\left(\frac{cm2}{g}\right) = 4881.5 + 66\frac{BSS-3000}{1000} - 18.16\frac{D-15}{5} + 1.5\frac{BSS-3000}{1000}.\frac{D-15}{5}$	0.997	Eq VI-3
Active addition (Slag)	**CS(MPa)**	Constante BSS(cm^2/g) D(%)	$CS(MPa) = 57.255 + 9.135\frac{BSS-3000}{1000} + 1.55\frac{D-7.5}{2.5}$	0.988	Eq VI-4
	FS(MPa)	Constante BSS(cm^2/g) D(%)	$FS(MPa) = 6.9992 + 0.567\frac{BSS-3000}{1000} + 0.367\frac{D-7.5}{2.5}$	0.997	Eq VI-5
	UPV(m/s)	Constante BSS(cm^2/g) D(%)	$UPV\left(\frac{cm2}{g}\right) = 4388 + 341.5\frac{BSS-3000}{1000} + 57.5\frac{D-7.5}{2.5}$	0.998	Eq VI-6

VI.4 Conclusion

Through the experimental tests and the modeling of our study program, we were initially able to characterize the self-compacting concrete based on inert (limestone) and active granulated blast furnace slag (S) as mineral input in the cement matrix at the fresh and the hardened state. This has been done by destructive and (NDT) methods.The modeling utilizing experimental design plans method (JMP) in order to study the effect of interaction of the specific surface of blaine (SSB) and the percentage of the dosage (D) factors. The statistical analysis of the experimental results in correlation with predicted ones, and the outcome of this analysis allows mathematical models based on such parameters (Fineness and dosage) to be proposed for the mechanical responses (CS, FS and UPV). These equations for the present study are given in the table VI-11 above.

Chapter VII. Computational fluid dynamics CFD (FLOW 3D).

VII.1 Computational Fluid Dynamics

Computational Fluid Dynamics (CFD). Which is the process of solving fluid dynamics problems numerically using a computer.

Some researchers have used CFD in the health field to simulate surgery, blood movement and even the cardiac cycle (Menut and al, 2016 ; 2017).

Other researchers have used CFD in the mechanical field, in the study of air movement ; in the design of vehicles, planes and ships (Preda and al, 2022) (Salehi and al, 2022) (Takahashi and al, 2015). Also, CFD deals with the study of ventilation systems whether it is the ventilation of rooms and dirt, buildings, long tunnels or even the ventilation of cities (Nguyen and al, 2022). Currently CFD is increasingly used in the field of civil engineering, especially to simulate the flow of concrete in the formwork of structures.

The use of CFD numerical methods to solve fluid dynamic problems is due to the fact that most of these problems can not be treated by the traditional analytical method.

VII.1.1 The CFD principles

We apply Newton's second law (fundamental principle of dynamics) for a particle of a fluid ;

$$\sum F_{ext} = m \,.\vec{a} \qquad \text{(EqVII-1)}$$

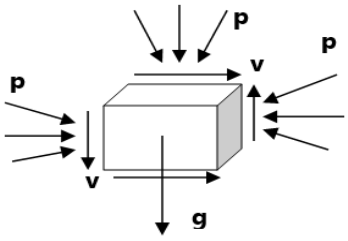

Figure VII-1. ∑ Fext.

We obtain the Navier-Stocks equation ;

$$\rho.\frac{DV}{Dt} = -\nabla p + \rho g + \mu \nabla 2.v \qquad \text{(Eq VII-2)}$$

$\vec{m.a}$: Pressure force ; Force of gravity ; Force of viscosity

The Navier -Stokes equations are nonlinear partial differential equations that describe Newtonian fluids motion.

The Navier-Stokes equation was established in 1821-1822 by the French engineer, mathematician and economist Claude Louis Marie Henrie Navier and the British mathematician and physicist George Gabriel Stokes. These equations are part of the Millennium Prize problems of the Clay Institute of Mathematics. The failure to solve this equation analytically is due to the random flow of fluids, it is impossible to predict their motion hence the use of CFD numerical solution is necessary.

The CFD calculation is based on the Eulerian description, where we define at any point the velocity of the fluid at a given time and the continuity equation of the volume of fluid method (VOF); introduced by C W Hirt and B D Nichols in 1981.

$$\frac{DC}{Dt} + \boldsymbol{V}.\boldsymbol{\nabla C} = \mathbf{0} \qquad \text{(Eq VII-3)}$$

C ; Volume fraction.

V ; Velocity.

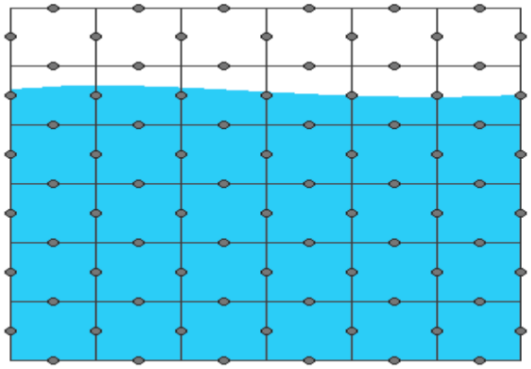

Figure VII-2. VOF method.

The velocity is calculated by the volume of fluid (VOF) method by solving Navier -Stokes equations (NSE) at each time step, the tracking of the fluid movement is done by the advection of the velocity.

VII.1.2 Steps in modeling the flow of SCC in the L-box by Flow 3D

a) Materials identification ;

- The SCC is considered as an elasto-viscoplastic fluid where a shear threshold is required to initiate their flow ; before the shear rate reaches this threshold the fluid behaves as an elastic solid but once it exceeds this threshold the viscosity increases and the SCC behaves as a fluid in a plastic state.
- The thixotropy of SCC is neglected.
- The SCC is subject to internal factors ; viscosity and external factors ; gravity.
- Activated the general moving object technique GMO ; in order to implicitly simulate the motion of the moving boundaries such as the L-box trap and the aggregate grains if we consider that the SCC is a heterogeneous fluid.
- Define the coefficient of restitution.
- Define the coefficient of friction between either, the grains or the fluid and the L-box.

b) The input parameters of SCC are cited as follows;

Density, viscosity, yield stress, and shear modulus of the SCC.

c) Drawing the model ;

The model must be drawn accurately because a small shift in the model can cause the result to fail. The drawing can be done either by flow 3d or import from autocad or other drawing software in **ST**ereo-**L**ithography (STL) form.

d) The mesh ;

- The discretization of the system in CFD numerical modeling is done by a mesh.
- The mesh must cover the entire model and can be divided into several mesh blocks to fit the model.
- It is necessary to determine the size of the mesh grids in such a way that there is no element of the model larger than the size of the grids; otherwise this element will not be taken into account in the simulation.
- The smaller the grid size, the more time the simulation takes and the more accurate the result will be ; thus the simulation time depends on the processor capacity of the computer used.

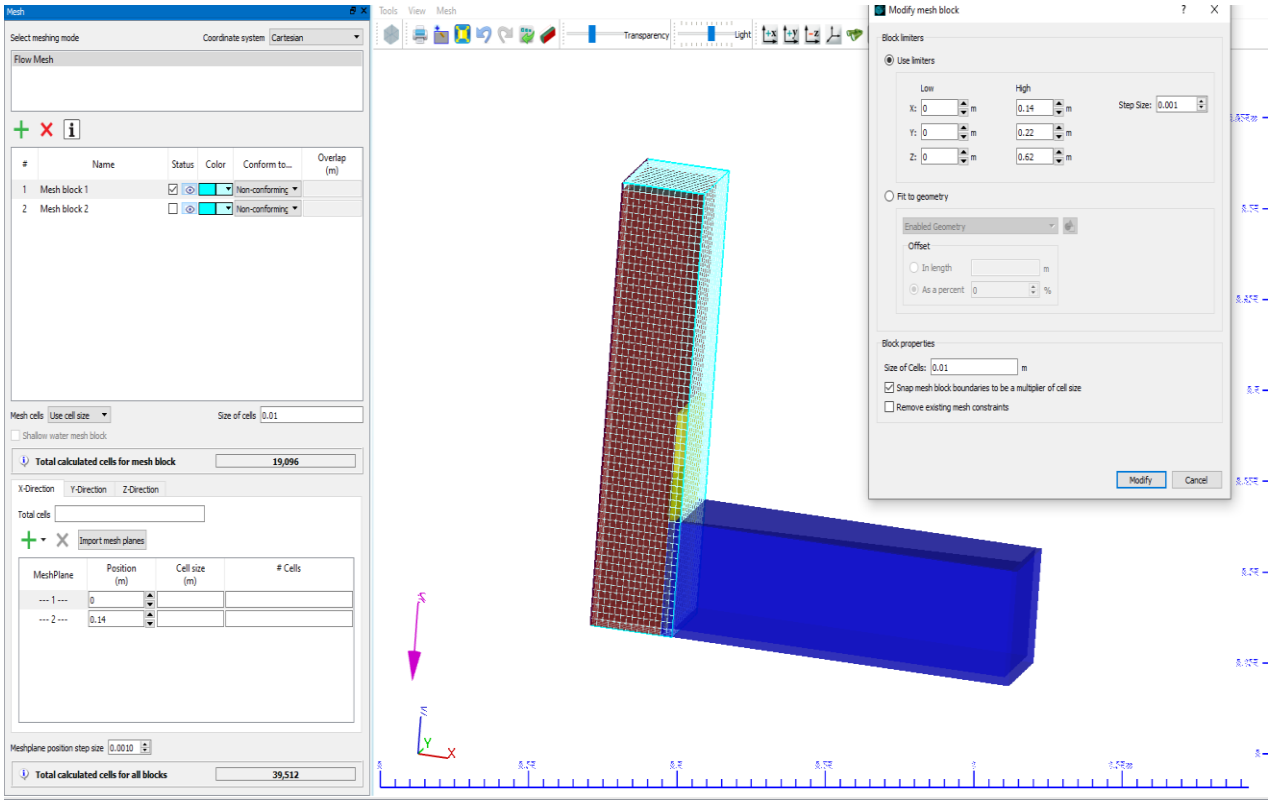

Figure VII-3. Mesh block 1.

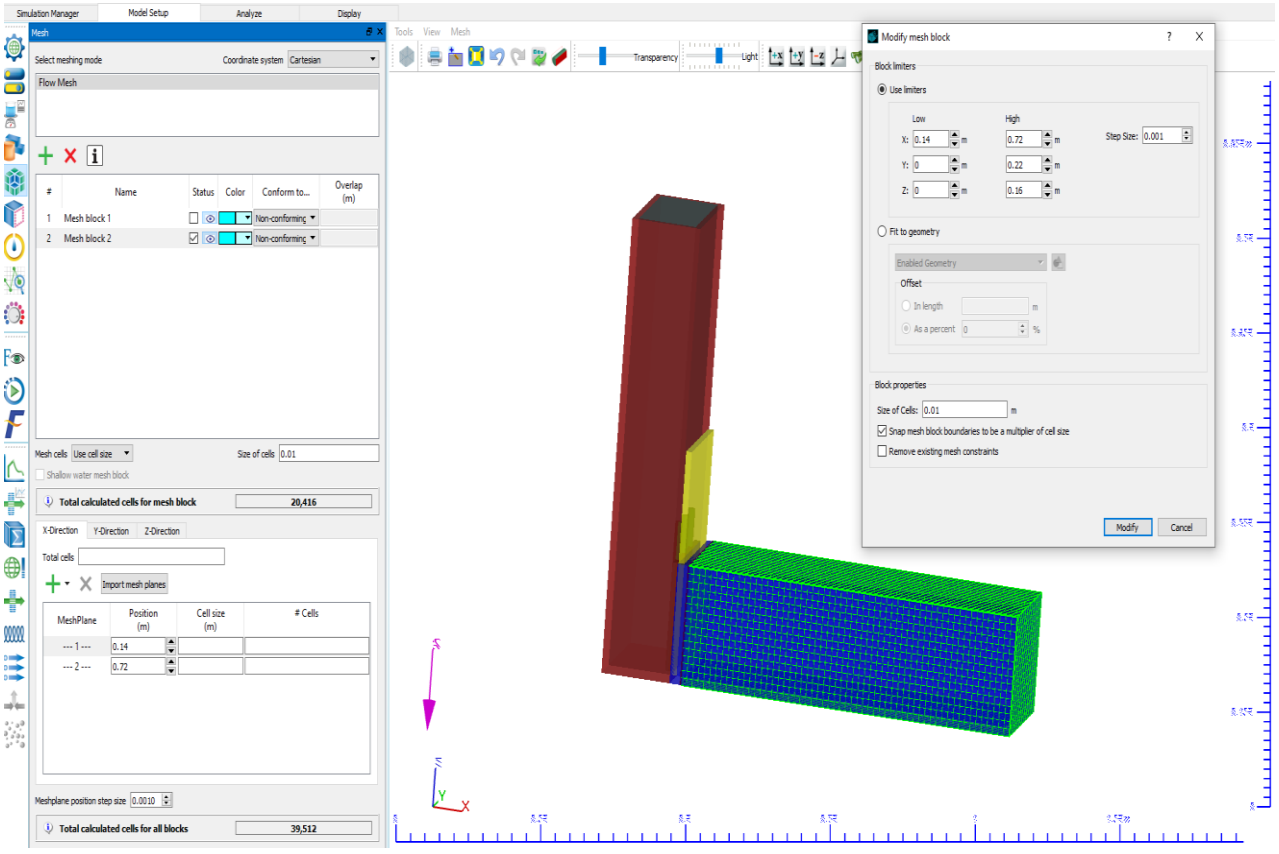

Figure VII-4. Mesh block 2.

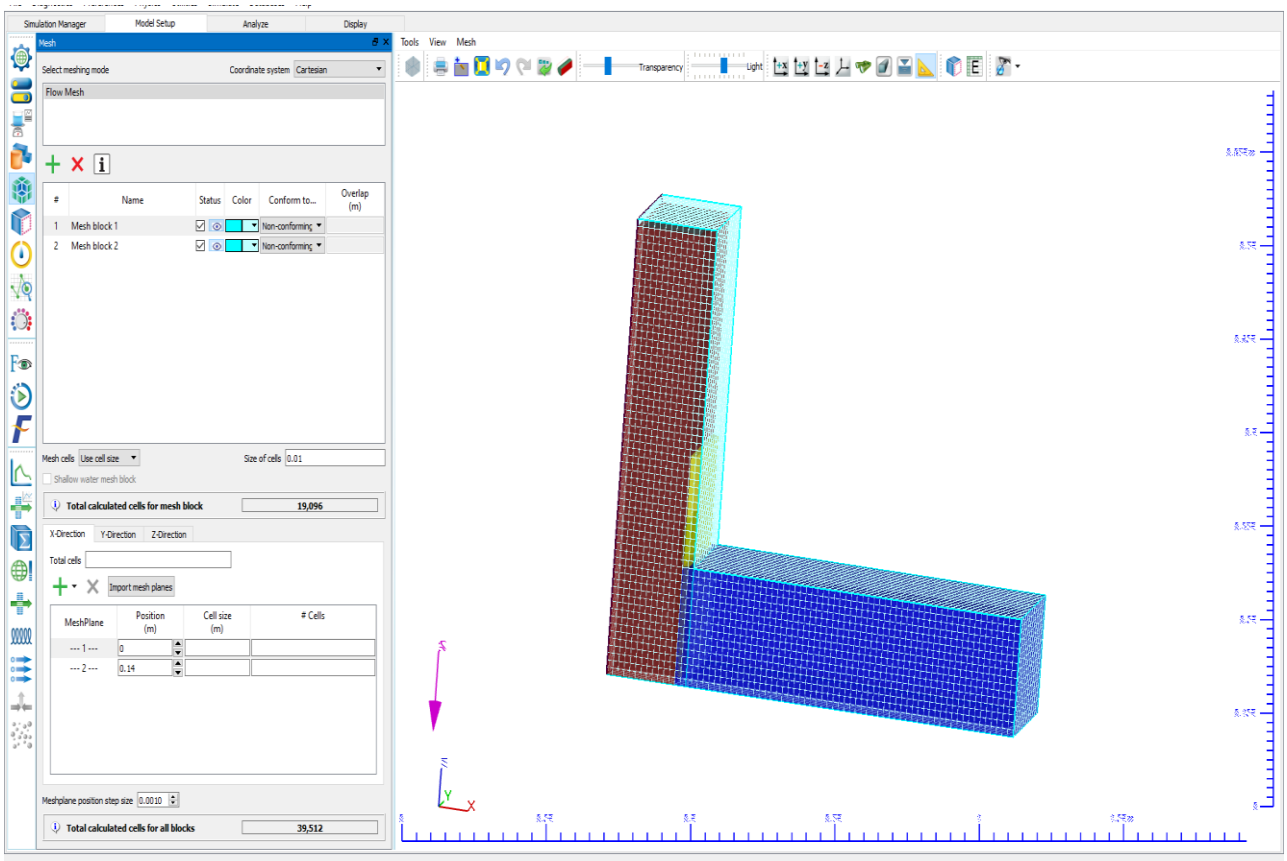

Figure VII-5. Mesh block 1 and 2.

e) Initial conditions ;

Define the initial position of the SCC before their flow ; before the opening of the L-box hatch.

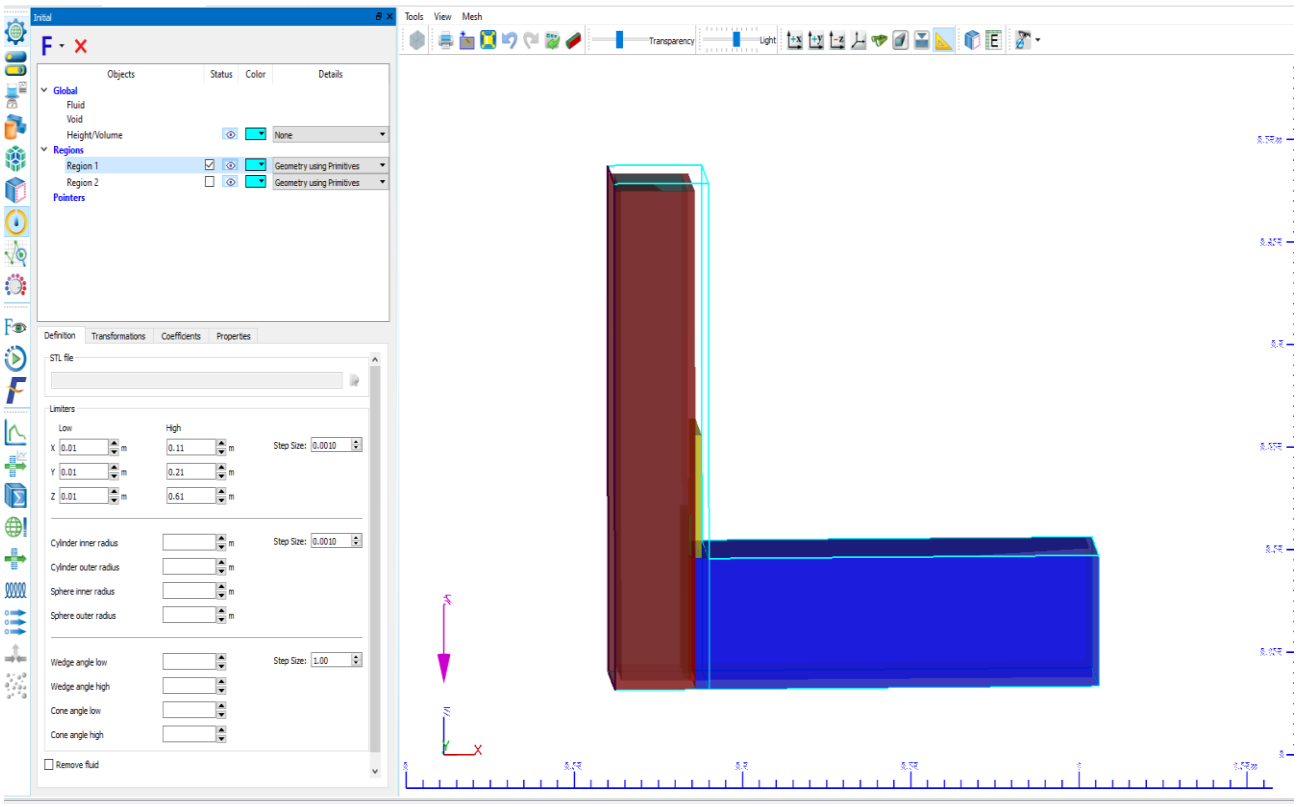

Figure VII-6. Fluid region.

f) Boundary conditions ;

The boundary conditions of the system is defined by their geometry.

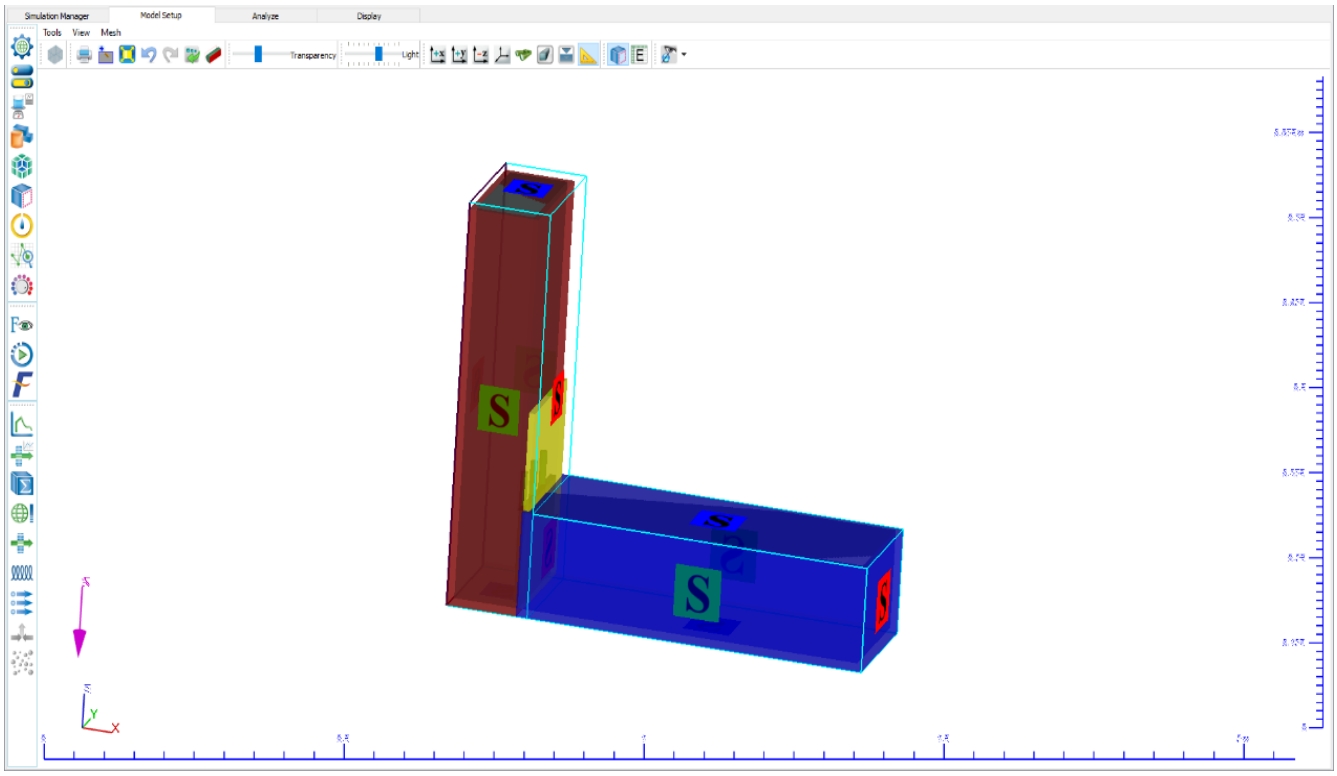

Figure VII-7. Boundary conditions.

i) The parameters output at each time step (output) can be cited below as;

- The distance traveled by the fluid.
- The velocity of the fluid.
- The shear rate of the fluid.
- The pressure.
- The numerical simulation of the Concrete flow in 2d and 3d.

VII.1.3 State of the art on flow modeling of SCC

According to the literature there are several approaches to model the flow of SCC in the fresh state, few researchers have considered the SCC in the modeling as a heterogeneous material in two phases aggregate and fluid in suspension this kind of modeling is used in the case of the study of dynamic granular segregation (Hosseinpoor and al, 2017a ; 2017b).

Some researchers have used particle-only methods where the SCC is discretized into particles without considering the fluid part; such as Discrete Element Method (DEM), Particle Finite Element Method (FEM) and Smoothed Particle Hydrodynamics (SPH) (Hosseinpoor, 2016).

Other researchers have considered SCC in modeling as a homogeneous material based only on the fluid; the latter method is the most used because of its ease and simplicity (Hosseinpoor, 2016).

VII.1.4 Conclusion

Numerical simulations of the flow of SCC in the fresh state depend on the computational capabilities of the available computing tools. But, numerical methods remain the fastest, least expensive and most accurate compared to experimental tests.

Numerical simulations of SCC aim at predicting their flow states and studying the influence of different parameters such as density, rheology of these types of concrete or even external parameters at the fresh state of such SCC.

VII.2 . Modeling of the SCC flow in the L-box

1. Numerical simulations of the flow of SCC in the L-box are established by Flow 3D software using dynamic flow models. The results of the numerical simulations are compared with the experimental results.

Table VII-1. Characteristic of SCC fly ash mixtures.

	SCC 01	SCC 02	SCC 03	SCC 04	SCC 05	SCC 06	SCC 07	SCC 08	SCC 09	SCC 10
Density **[kg/m^3]**	2350	2350	2350	2303	2305	2308	2260	2260	2260	2260
Viscosity **[Pa.s]**	49	36	34	33	25	18	5	10	15	20
Yield stress **[Ps]**	67	63	61	40	37	34	25	25	25	25
Shear modulus **[Ps]**	100	100	100	100	100	100	100	100	100	100

2. A parametric study is considered through numerical simulations; in order to evaluate the effect of rheological parameters (plastic viscosity and yield stress), shear modulus**,** density and arrangement of reinforcements, gate speed as well as the tribology on the stability of the SCC.

Table VII-2. Characteristic of SCC fly ash mixtures for the parametric study.

	Effect of plastic viscosity	Effect of yield stress	Effect of shear modulus	Effect of density	Effect of bars	Effect of gate speed	Effect of tribology
Density **[kg/m^3]**	2300	2300	2300	[2000,2500]	2300	2300	2300
Viscosity **[Pa.s]**	[5,70]	40	40	40	40	40	40
Yield Stress **[Pa]**	60	[5,70]	60	60	60	60	60
Shear modulus **[Pa]**	100	100	[50,1000]	100	100	100	100
Number of bars	3 horizontal	3 horizontal	3 horizontal	3 horizontal	[3 ,18] vertical [3.18] horizontal	3 horizontal	3 horizontal
Gate speed **[m/s]**	0.03	0.03	0.03	0.03	0.03	[0.03, 0.08]	0.03
Tribology	-1	-1	-1	-1	-1		[-1,-0.8]

VII.2.1 Correlation between modeling results and experimental test results

Table VII-3. Results of the SCC fly ash based mixtures.

	SCC 01	SCC 02	SCC 03	SCC 04	SCC 05	SCC 06	SCC 07	SCC 08	SCC 09	SCC 10
Density **[kg/m^3]**	2350	2350	2350	2303	2305	2308	2260	2260	2260	2260
Viscosity **[Pa.s]**	49	36	34	33	25	18	5	10	15	20
Yield stress **[Pa]**	67	63	61	40	37	34	25	25	25	25
Shear modulus **[Ps]**	100	100	100	100	100	100	100	100	100	100
The time of arrival at the end of the box (Experimental result) **[s]**	5.4	4.4	4.75	2	1.8	1.2	0.35	0.38	0.39	0.4
The time of arrival at the end of the box (Modeling results) **[s]**	5.8	4.19	3.9	3.59	2.7	1.9	0.69	0.99	1.5	2.1
H2/H1 (Experimental result)	0.55	0.57	0.58	0.7	0.72	0.74	0.81	0.8	0.8	0.8
H2/H1 (Modeling results)	0.55	0.62	0.7	0.76	0.82	0.87	0.88	0.98	0.97	0.88

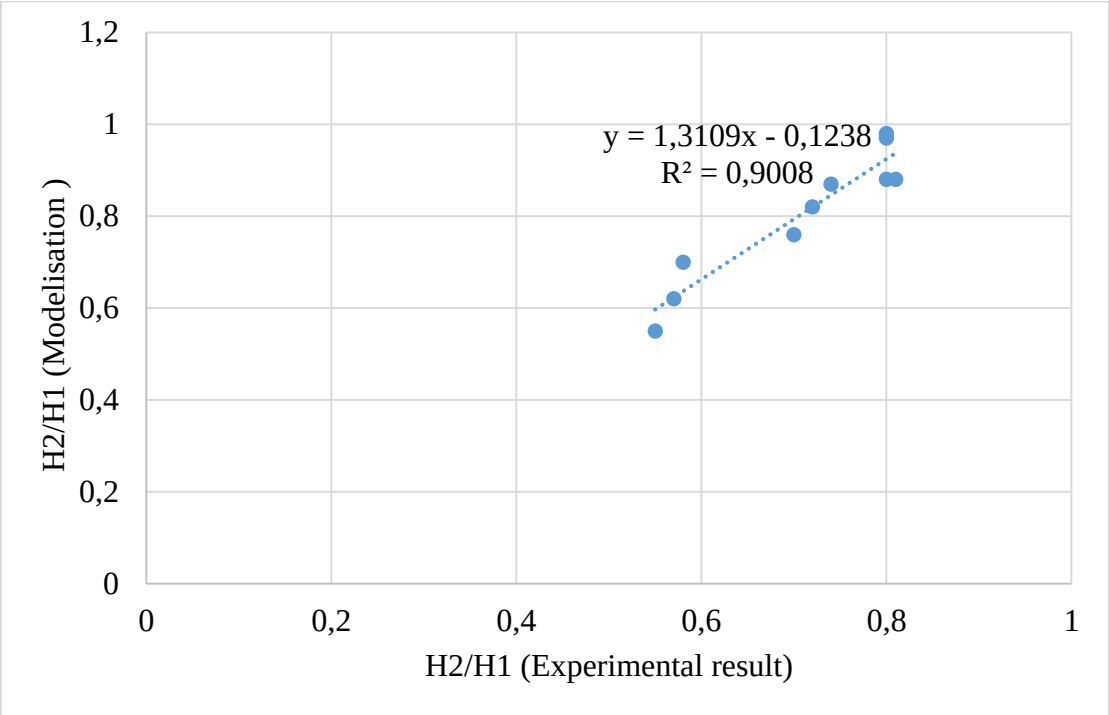

Figure VII-8. H2/H1 modelisation Vs experimental results.

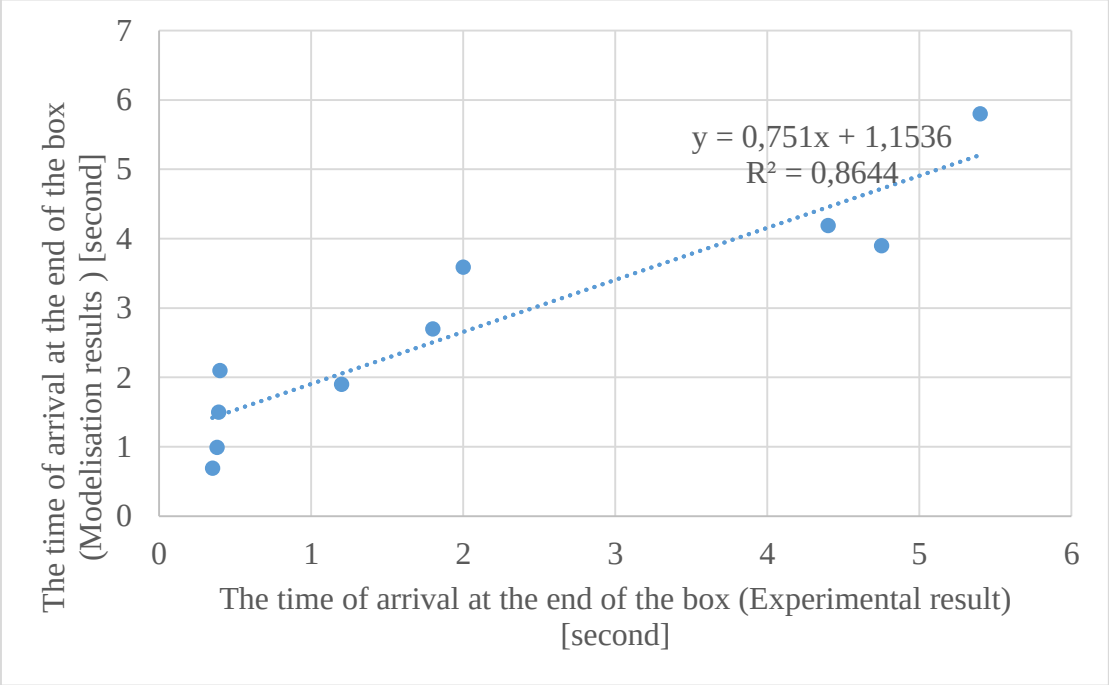

Figure VII-9. The modeling arrival time Vs the experimental results.

From figure VII-8 and VII-9 ; It could be deduced that the numerical simulations are in agreement with the experimental results with an R^2 of 0.90 and 0.86 for the H2/H1 ratio and the time to reach the end of the box, respectively.

This implies that the present numerical model is reliable for carrying out a parametric study to see the influence of each parameter and to predict the flow behavior of SCC in primarly phases and without resorting to the tedious task in the laboratory.

VII.2.2 Parametric study and prediction of the flow of SCC

VII.2.2.1 Internal parameters

a) Effect of viscosity ;

Table VII-4. Viscosity parameter effect results.

	Density **[kg/m^3]**	Yield stress **[Pa]**	Shear modulus **[Pa]**	Viscosity **[Pa.s]**	H2/H1 **ratio**	Time Flow **[s]**
SCC01	2300	60	100	5	0.88	0.69
SCC02	2300	60	100	10	0.69	0.99
SCC03	2300	60	100	15	0.72	1.6
SCC04	2300	60	100	20	0.77	2.29
SCC05	2300	60	100	25	0.76	2.9
SCC06	2300	60	100	30	0.67	3.5
SCC07	2300	60	100	35	0.61	4.09
SCC08	2300	60	100	40	0.59	4.7
SCC09	2300	60	100	45	0.54	5.2
SCC10	2300	60	100	50	0.5	5.8
SCC11	2300	60	100	55	0.55	6.39
SCC12	2300	60	100	60	0.5	7
SCC13	2300	60	100	65	0.51	7.49
SCC14	2300	60	100	70	0.52	8.09

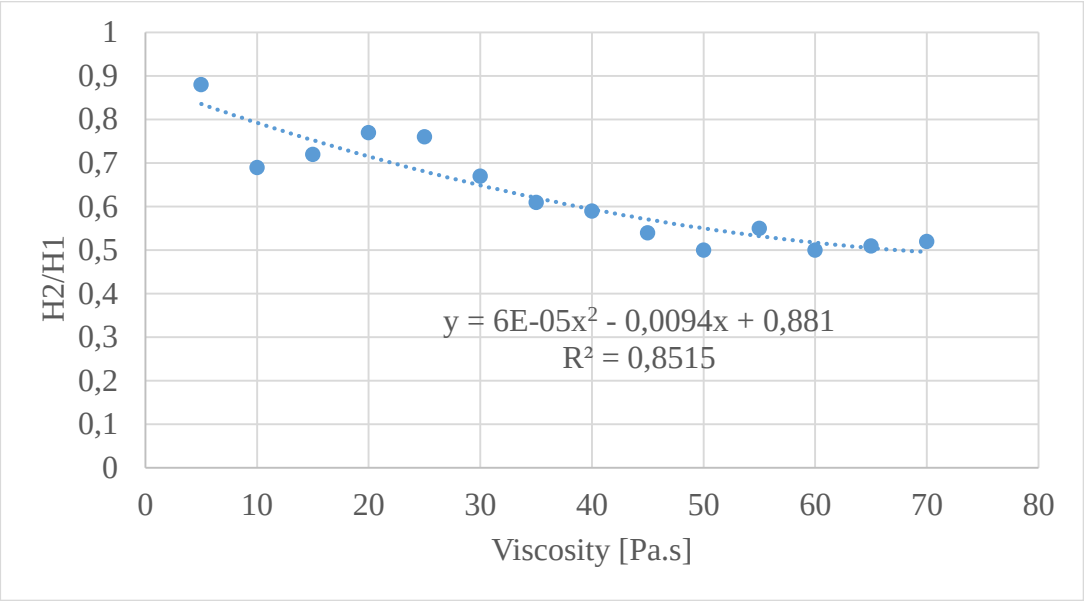

Figure VII-10. Effect of viscosity on H2/H1 ratio.

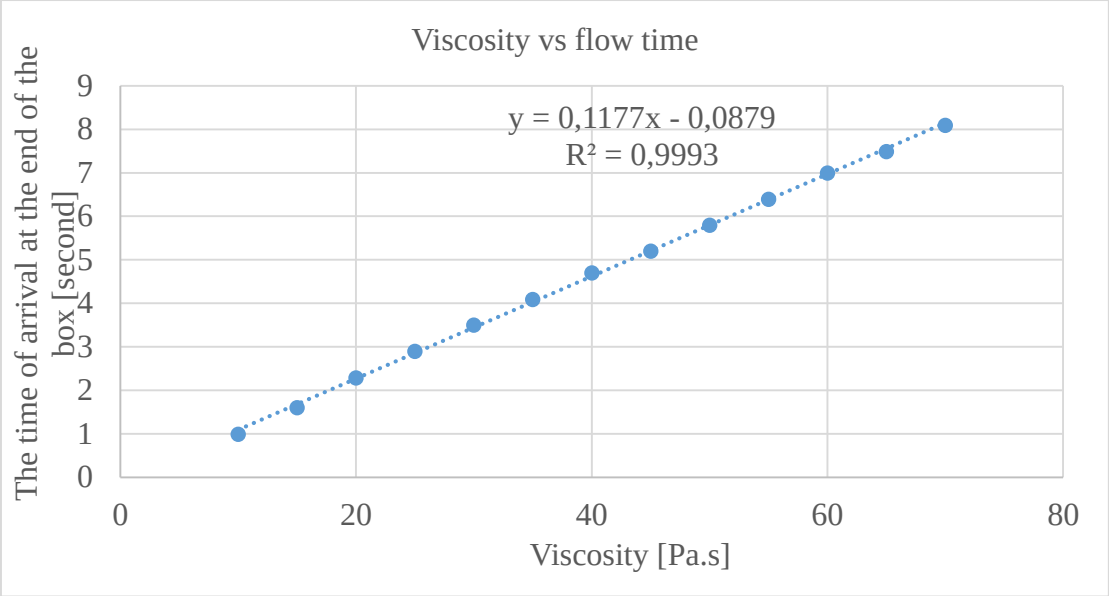

Figure VII-11. Effect of viscosity on the time of arrival at the end of the box.

According to the two figures VII-10 and VII-11, it could be deduced that the increase in viscosity causes a reduction in the dynamic stability by the reduction in H2/H1 and a reduction in the capacity of passage by the increase in the time to arrive at the end of the box. This is in accord with other research study (Hosseinpoor and al, 2017a).The viscosity range that gives us acceptable results extends from 5 Pa.s to 25 Pa.s.

The numerical equations for the prediction of H2/H1 and the time of arrival at the end of the L box as a function of the viscosity respectively are as follows ;

$y = 6E\text{-}05x^2 - 0{,}0094x + 0{,}881$ (Eq VII-4)

$y = 0{,}1177x - 0, 0879$ (Eq VII-5)

b) Effect of yield stress ;

Table VII-5. Yield stress result.

	Density **[kg/m³]**	Viscosity **[Pa.s]**	Shear modulus **[Pa]**	Yield stress **[Pa]**	H2/H1 **ratio**	Time Flow **[s]**
SCC01	2300	40	100	5	0.92	3.9
SCC02	2300	40	100	10	0.89	3.9
SCC03	2300	40	100	15	0.87	3.99
SCC04	2300	40	100	20	0.79	4.09
SCC05	2300	40	100	25	0.81	4.09
SCC06	2300	40	100	30	0.7	4.2
SCC07	2300	40	100	35	0.73	4.29
SCC08	2300	40	100	40	0.72	4.3
SCC09	2300	40	100	45	0.71	4.4
SCC10	2300	40	100	50	0.69	4.5
SCC11	2300	40	100	55	0.64	4.6
SCC12	2300	40	100	60	0.59	4.7
SCC13	2300	40	100	65	0.54	4.8
SCC14	2300	40	100	70	0.53	4.9

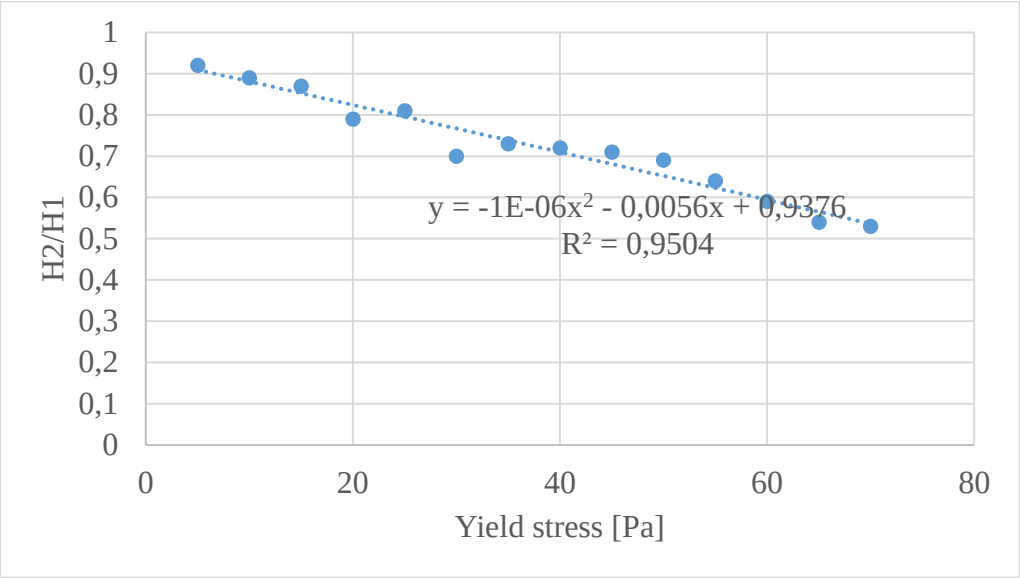

Figure VII-12. Effect of yield stress on H2/H1.

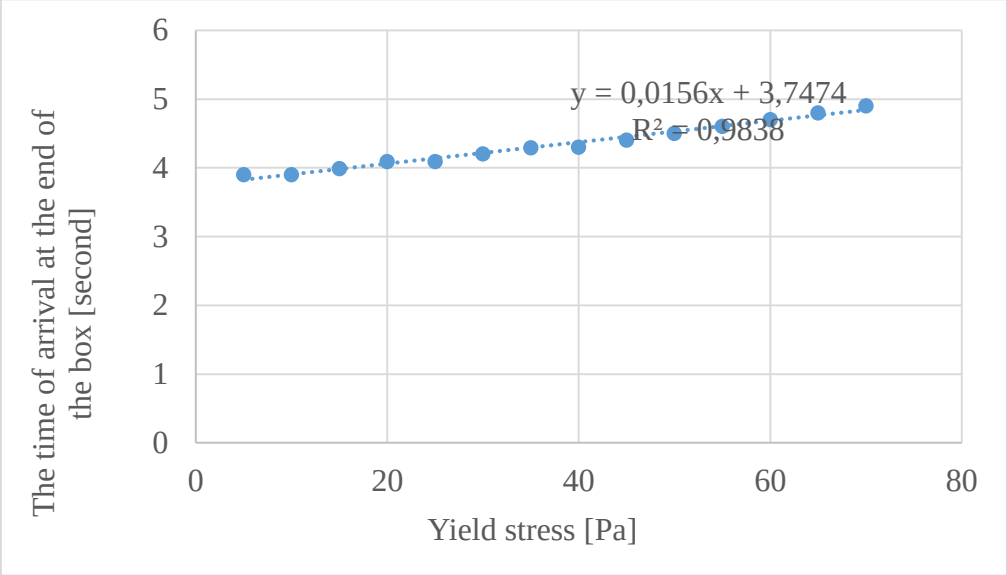

Figure VII-13. Effect of yield stress on the time of arrival at the end of the box.

From the two figures VII-12 and VII-13, it can be deduced that the increase in yield stress causes a reduction in the dynamic stability by the reduction in H2/H1 and a reduction in the capacity of passage by the increase in the time of arrival at the end of the box. This is in agreement with other research studies (Hosseinpoor and al, 2017a). The yield stress range that gives us acceptable results extends from 5 Pa to 25 Pa.

The numerical equations for the prediction of H2/H1 and the time of arrival at the end of the box as a function of the yield stress are respectively ;

$y = -1E\text{-}06x^2 - 0{,}0056x + 0{,}9376$ (Eq VII-6)

$y = 0{,}0156x + 3{,}7474$ (Eq VII-7)

c) Effect of the shear modulus ;

Table VII-6. Shear modulus result.

	Density **[kg/m³]**	Viscosity **[Pa.s]**	Yield stress **[Pa]**	Shear modulus **[Pa]**	H2/H1 **ratio**	Time Flow **[s]**
SCC01	2300	40	60	50	0.59	4.7
SCC02	2300	40	60	100	0.59	4.7
SCC03	2300	40	60	200	0.57	4.69
SCC04	2300	40	60	300	0.57	4.69
SCC05	2300	40	60	400	0.55	4.7
SCC06	2300	40	60	500	0.59	4.69
SCC07	2300	40	60	600	0.58	4.7
SCC08	2300	40	60	700	0.57	4.69
SCC09	2300	40	60	800	0.61	4.69
SCC10	2300	40	60	900	0.58	4.7
SCC11	2300	40	60	1000	0.58	4.7

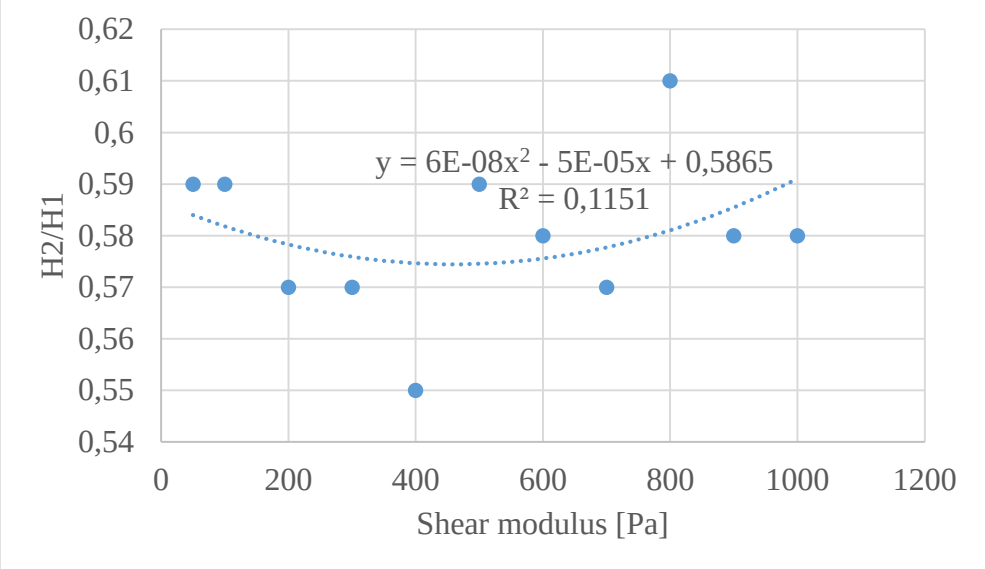

Figure VII-14. Effect of Shear modulus on H2/H1.

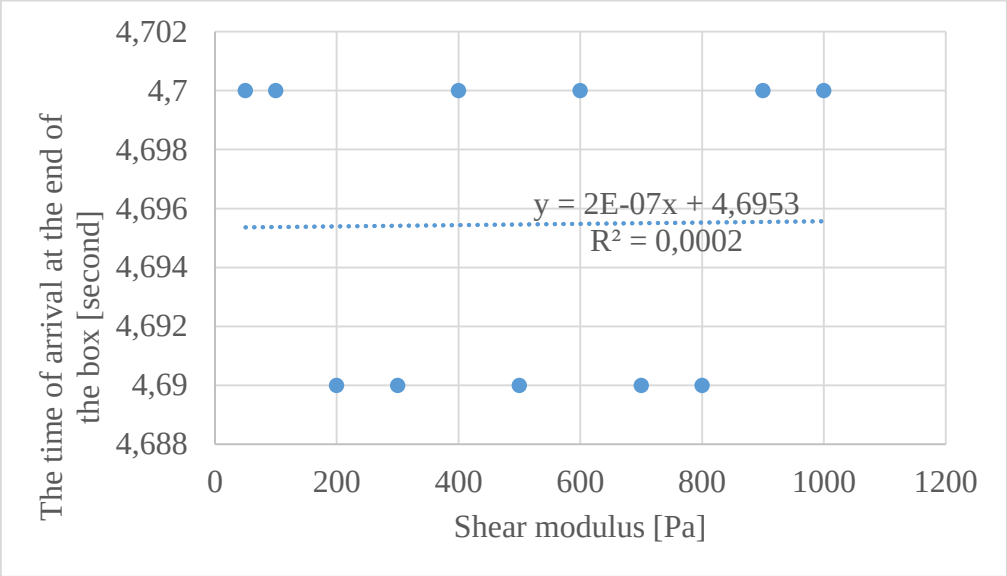

Figure VII-15. Effect of Shear modulus on the time of arrival at the end of the box.

From the two figures VII-14 and VII-15, it can be deduced that the shear modulus has no influence on the dynamic stability and the passage capacity.

The numerical equations for the prediction of H2/H1 and of the arrival time at the end of the box as a function of the shear modulus are respectively ;

$y = 6E\text{-}08x^2 - 5E\text{-}05x + 0{,}5865$ (EqVII-8)

$y = 2E\text{-}07x + 4{,}6953$ (Eq VII-9)

d) Effect of density ;

Table VII-7. Density result.

	Viscosity **[Pa.s]**	Yield stress **[Pa]**	Shear modulus **[Pa]**	Density **[kg/m³]**	H2/H1 **ratio**	Time Flow **[s]**
SCC01	40	60	100	2000	0	5.6
SCC02	40	60	100	2300	0.85	4.7
SCC03	40	60	100	2500	0.63	4.2

It can be deduced that the increase in density leads to a reduction in dynamic stability by the reduction in H2/H1 and a reduction in the passage capacity by the increase in the time of arrival

at the end of the box. This is in agreement with other studies carried out previuously (Hosseinpoor and al, 2017a).the density that gives us acceptable values is that of 2300 kg/m^3.

The numerical equations for the prediction of H2/H1 and of the arrival time at the end of the box as a function of density are respectively as fllows ;

$y = -8E\text{-}06x^2 + 0{,}0367x - 41{,}853$ (Eq VII-10)

$y = -0{,}0028x + 11{,}216$ (Eq VII-11)

Table VII-8. Summary of mathematical equations model prediction of the flow.

Parameter study	**Model**		**Determination coefficient (R^2)**	**Equation Number**
Viscosity	H2/H1	$y = 6E\text{-}05x^2 - 0{,}0094x + 0{,}881$	0.851	Eq VII-4
	Time of arrival at the end of the L box (s)	$y = 0{,}1177x - 0{,}0879$	0.999	Eq VII-5
Yield stress	H2/H1	$y = -1E\text{-}06x^2 - 0{,}0056x + 0{,}9376$	0.950	Eq VII-6
	Time of arrival at the end of the L box (s)	$y = 0{,}0156x + 3{,}7474$	0.983	Eq VII-7
Shear modulus	H2/H1	$y = 6E\text{-}08x^2 - 5E\text{-}05x + 0{,}5865$	0.115	Eq VII-8
	Time of arrival at the end of the L box (s)	$y = 2E\text{-}07x + 4{,}6953$	0	Eq VII-9
Density	H2/H1	$y = -8E\text{-}06x^2 + 0{,}0367x - 41{,}853$	1	Eq VII-10
	Time of arrival at the end of the L box (s)	$y = -0{,}0028x + 11{,}216$	0.997	Eq VII-11

VII.2.2.2 External parameters

a) Effect of the reinforcement bar ;

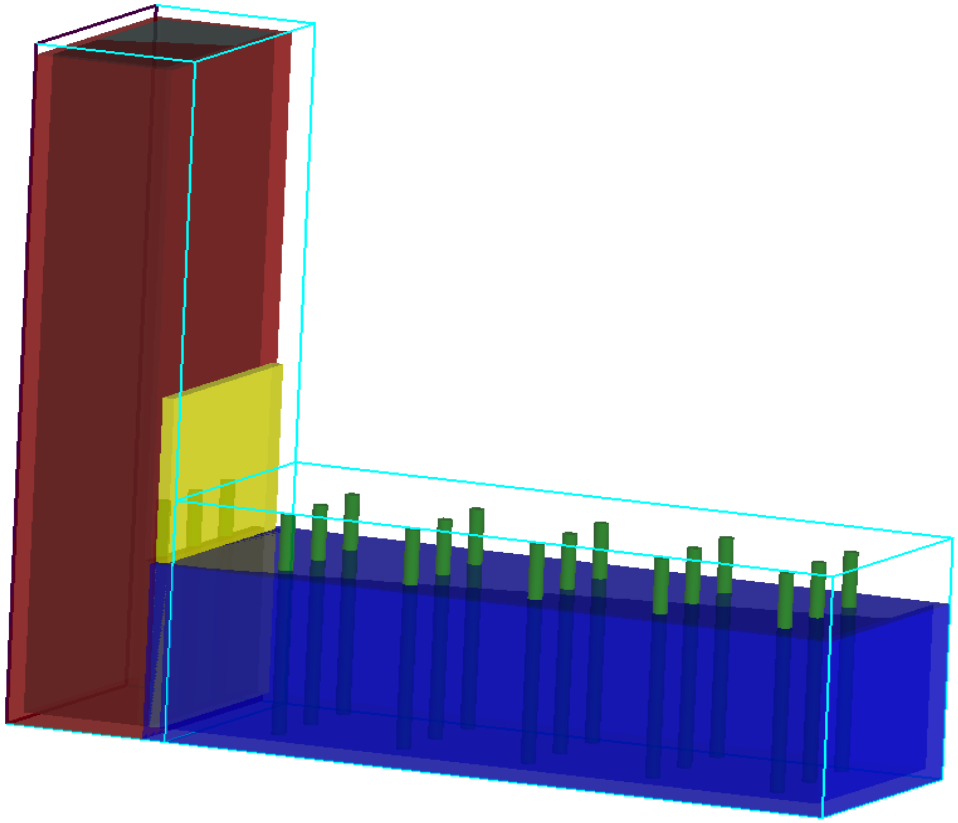

Figure VII-16. Reinforcement bars position in the horizontal part.

Table VII-9. Reinforcement bars density effect results in the horizontal part.

	Viscosity **[Pa.s]**	Yield stress **[Pa]**	Shear modulus **[Pa]**	Density **[kg/m^3]**	Number of bars	H2/H1 **ratio**	Time Flow **[s]**
SCC01	40	60	100	2300	0	0.67	4.3
SCC02	40	60	100	2300	3x1	0.58	4.7
SCC03	40	60	100	2300	3x2	0.55	5.2
SCC04	40	60	100	2300	3x3	0.53	5.99
SCC05	40	60	100	2300	3x4	0.5	6.79
SCC06	40	60	100	2300	3x5	0.58	7.4
SCC07	40	60	100	2300	3x6	0.56	7.9

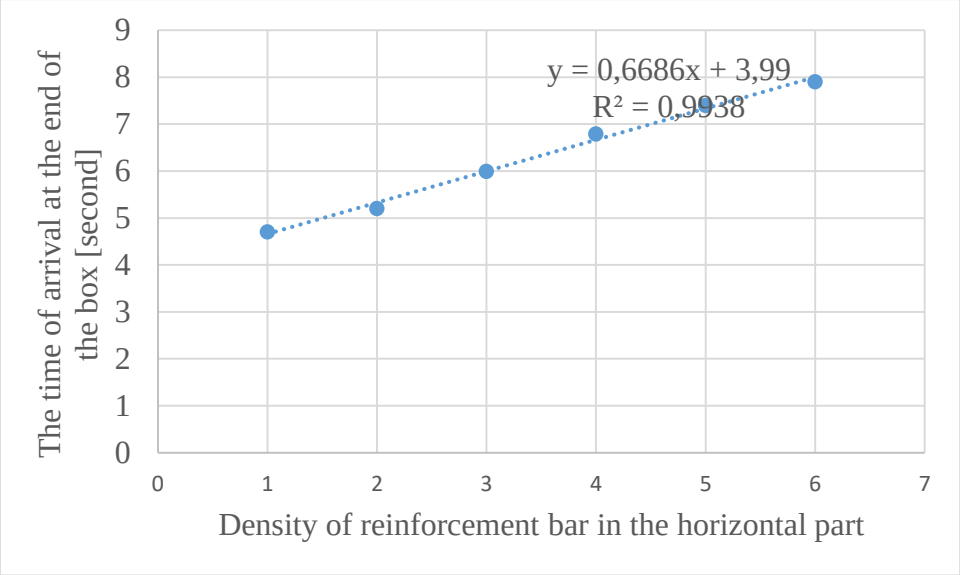

Figure VII-17. Reinforcement bars density effect in the horizontal part on the time of arrival at the end of the box.

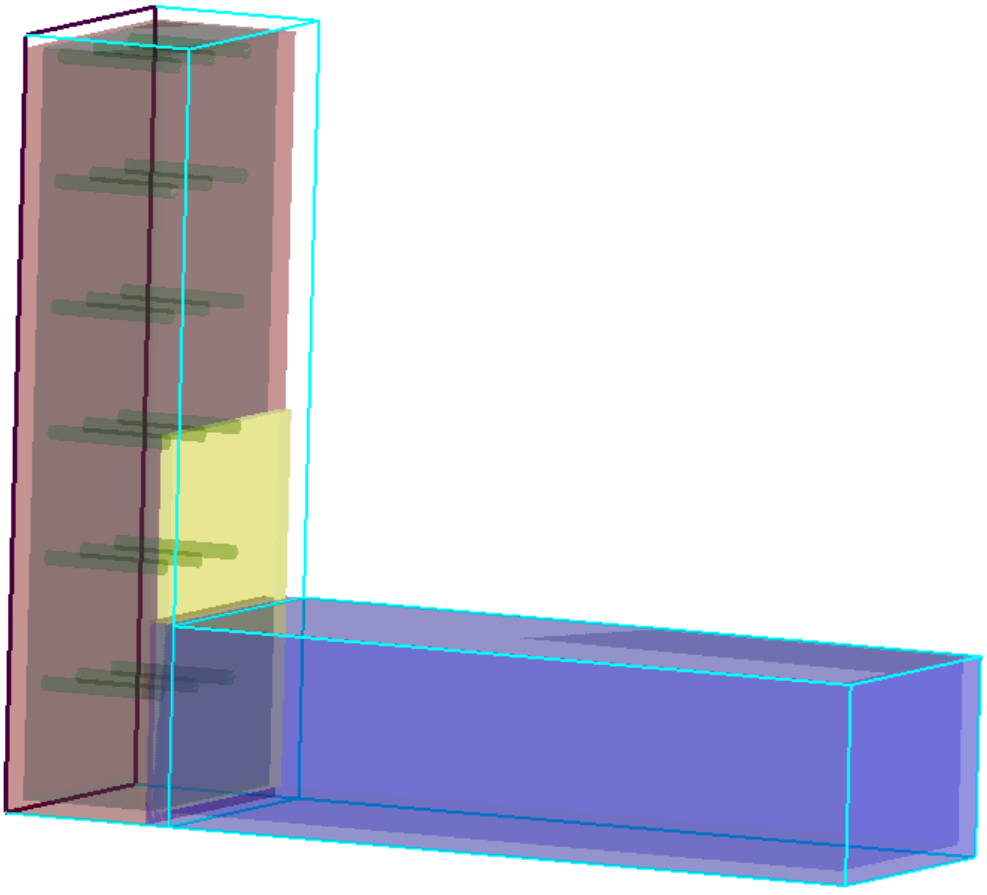

Figure VII-18. Reinforcement bars position in the vertical part.

Table VII-10. Reinforcement bars density results in the vertical part.

	Viscosity **[Pa.s]**	Yield stress **[Pa]**	Shear modulus **[Pa]**	Density **[kg/m^3]**	Number of bars	H2/H1 **ratio**	Time Flow **[s]**
SCC01	40	60	100	2300	0	0.61	4.5
SCC02	40	60	100	2300	3x1	0.67	4.69
SCC03	40	60	100	2300	3x2	0.64	4.9
SCC04	40	60	100	2300	3x3	0.58	4.99
SCC05	40	60	100	2300	3x4	0.68	5.2
SCC06	40	60	100	2300	3x5	1.11	5.19

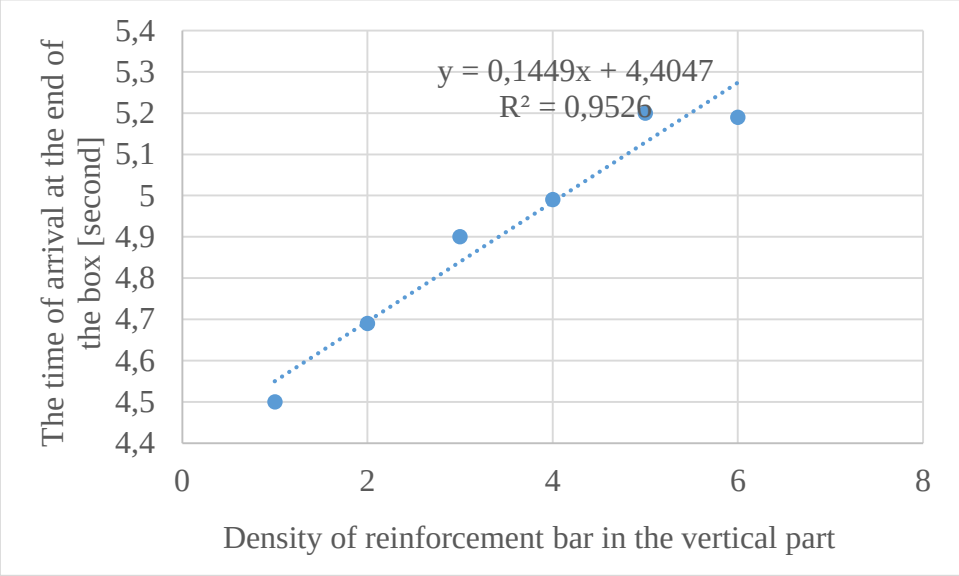

Figure VII-19. Reinforcement bars density effect in the vertical part on the time of arrival at the end of the box.

From figure VII-17and VII-19 ; it can be deduced that the increase in the reinforcement bars decreases the dynamic stability and the passage capacity. This is in agreement with other studies (Hosseinpoor and al ; 2017b) ; Nevertheless, the density of the reinforcement bars has a greater influence on the horizontal dynamic stability than on the vertical dynamic stability.

b) Effect of the gate speed ;

Table VII-11. Gate speed results.

	Viscosity **[Pa.s]**	Yield stress **[Pa]**	Shear modulus **[Pa]**	Density **[kg/m^3]**	Speed of the gate **[m/s]**	H2/H1 **ratio**	Time Flow **[s]**
SCC01	40	60	100	2300	0.03	0.61	6
SCC02	40	60	100	2300	0.04	0.57	5.59
SCC03	40	60	100	2300	0.05	0.57	5.3
SCC04	40	60	100	2300	0.06	0.58	5.19
SCC05	40	60	100	2300	0.07	0.56	5.1
SCC06	40	60	100	2300	0.08	0.87	5

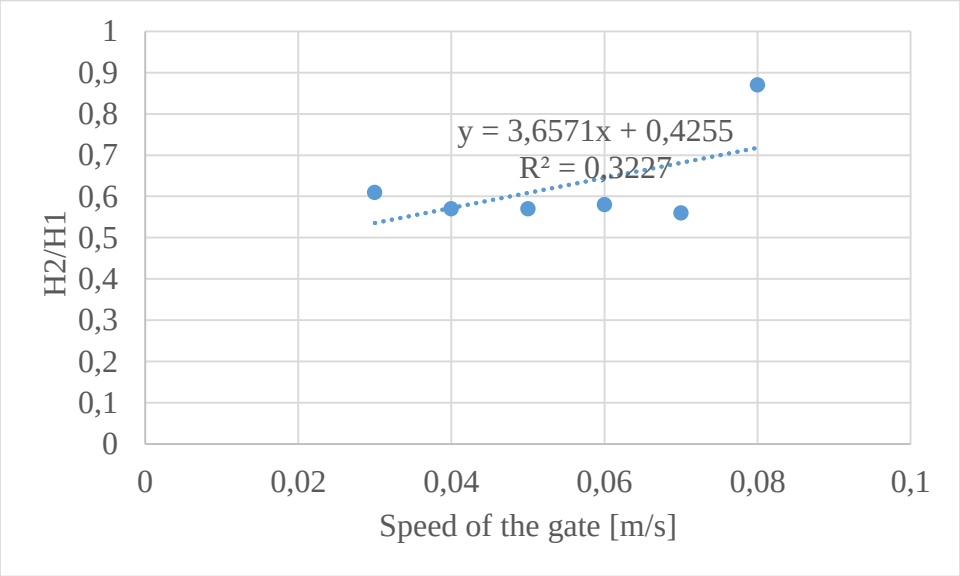

Figure VII-20. Effect of the speed of the gate on H2/H1.

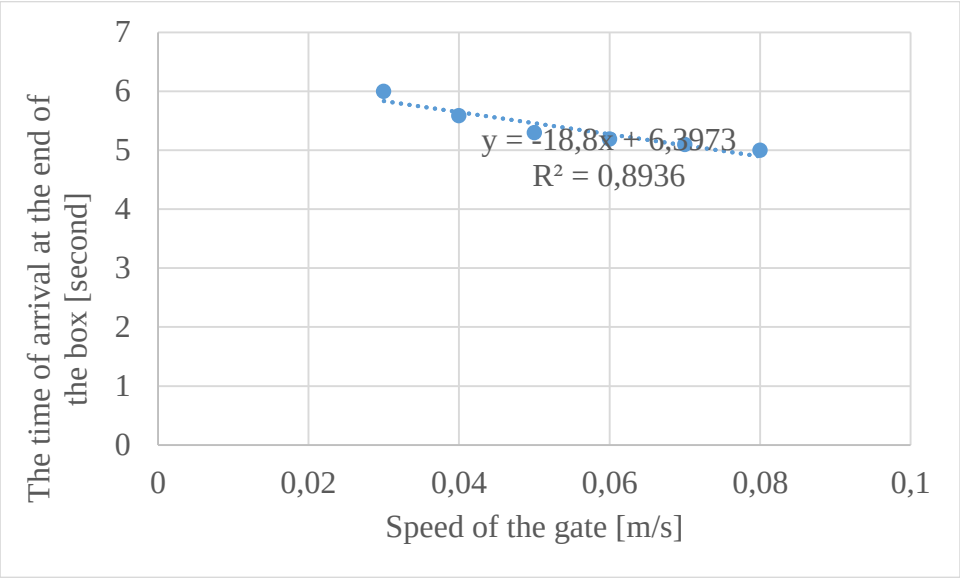

Figure VII-21. Effect of speed of the gate on the time of arrival at the end of the box.

From figure VII-20 and VII-20 ; we deduce that the speed of the gate of the L box has no effect on the dynamic stability. Morever, therefore the uncertainty of the experimenter does not have a strong effect on the behavior of the flow.

c) Effect of the tribology ;

Table VII-12. Tribology result.

	Viscosity **[Pa.s]**	Yield stress **[Pa]**	Shear modulus **[Pa]**	Density **[kg/m^3]**	Tribiology	H2/H1 **ratio**	Time Flow **[s]**
SCC01	40	60	100	2300	-1	0.59	4.7
SCC02	40	60	100	2300	-0.9	0.59	4.7
SCC03	40	60	100	2300	-0.8	0.59	4.7

From table VII-12, It could be deduced we deduce that the tribology has no effect on the dynamic stability and the passage capacity; therefore for the flow in small areas the friction coefficient of the walls of the flow device has no influence.

VII.3 Conclusion

At the end we have modeled the flow of the self-compacting concrete in L box. The effect of the internal parameter (viscosity, elastic limit, density and shear modulus) and of the external

parameter (density of the reinforcement, speed of the door L box and tribology) on the flow behavior of self-compacting concretes have been investigated using such tool of (FLOW 3D). The main correlating equations for predicting the flow behavior are proposed as outcome of this study according to these parameters are proposed in the table VII.8 above.

General conclusion

The present research study on the use of limestone additions, and granulated blast furnace slag emphasizes the valuation of such recovery of mineral waste in its technical, economic and ecological side advantages. Also, our contribution proposed new mathematical numerical equation models for mechanical response assessment of SCC formulation based on this additives.

In the first stage (experimental part); the study aims to characterize SCC based on inert limestone [L] and active mineral additions (slag) [S] in fresh and hardened state where three grades of fineness are employed for each type. Then the evaluation of the static stability utilizing a non-destructive test by a large-scale device (column) and by measurement of the electrical conductivity of the TDR methods is undertaken.

In a second approach (modeling part) ; modeling by experimental plans of SCC based on inert limestone [L] and active mineral additions (slag) [S], mathematical models issued from the statistical analysis are derived for predicted mechanical surface responses and the observed experimental test results in correlation relationship using Non Destructive tets (NDT). Then, the modeling by a CFD program to model the flow of SCC beside a parametric study is performed.

The present research study on the use of limestone additions, and granulated blast furnace slag emphasizes the valuation of such recovery of mineral waste in its technical, economic and ecological side advantages. Also, our contribution proposed new mathematical numerical equation models for mechanical response assessment of SCC formulation based on this additives.

For more precision we use the large scale static stability by the measurement of the electrical conductivity based on the TDR method for fear that the evaluation of the static stability in a reduced model does not simulate real conditions. Also the proposed models plays the role of a numerical laboratory where it allows us to simulate the flow of the SCC without resorting to the tedious test in the laboratory.

Based on experimental and numerical modeling in the present study the following conclusions could be drawn;

- The limestone filler and granulated blast furnace slag incorporation improves the rheological properties mainly, fluidity, the dynamic stability and the static stability (limited segregation) of the SCC.

- Contents up to 20 % of limestone addition and up to 10% of granualated blast furnace slag additionin the formulation of SCC enhance the mechanical performances (compressive and flexural strengths).
- Higher Blaine Specific Surface (BSS) of limestone or granulated blast furnace slag in the formulation of SCC has a benefic effect on the compressive strength, flexural strength and Ultrasonic Pulse Velocity.
- The non-destructive method of UPV could be a reliable mean to determine the mechanical performances for a better SCC quality assessment.
- Based on the statistical analysis it could be concluded that both the Blaine Specific Surface (BSS) and the content of limestone filler or the granulated blast furnace slag have their effect on the mechanical resistance but the SSB is the most influent.
- The numerical modeling by the JMP method gives a good correlation of predicted mechanical surface responses and the observed experimental test results at a determined coefficient is superior to 0.99. The outcome of the present statistical analysis, let us to suggest a numerical models to predict the compressive strength (CS), the flexural strength (FS) as well as the Ultra Pulse Velocity (UPV) at the age of 28 days, taking into account the interaction of two parameters (dosages (%) and fineness grade BSS) of limestone filler and the granulated blast furnace slag based formulated Self Compacting Concrete. The mathematical equation models are reported in equations **(table VI-11).**
- Granular discontinuity of the SCC can cause dynamic instability and blockage but it could keep the filling capacity ability. However, this granular discontinuity of SCC decreases the static stability and rise up the bleeding phenomenon.
- Granular discontinuity of SCC decreases static stability and increases bleeding.
- Viscosity modifying agent improves dynamic and static stability.
- Increasing paste volume decreases static stability and increases bleeding.
- The increase in coarse aggregate content improve the dynamic stability and the static stability and reduce the bleeding.
- The increase in the viscosity , the yield stress and the density causes a reduction in the dynamic stability and In the capacity of passage in confined reinforced area.
- The shear modulus has no influence on the dynamic stability and the passage capacity.
- The increase in the reinforcement bars decreases the dynamic stability and the passage capacity, but the density of the reinforcement bars has a greater influence on the horizontal dynamic stability than on the vertical dynamic stability.

- the speed of the gate of the L box and the tribology has no effect on the dynamic stability.
- The numerical equations as outcome for the present research work for the prediction of L-box test values of H2/H1 and the time of arrival at the end of the box are reported in mathematical equations models **(table VII-8).**

Perspectives;

Based on this present thesis research outcome, future research studies could be proposed;

- The characterization and modeling by experimental plans of self-compacting concretes based on inert limestone and active mineral additions (slag), to predict the durability properties.
- Establish a CFD numerical model using Flow 3D software to simulate the static stability test (the column).
- Modeling by a CFD program of the flow of self-compacting concrete in the large-scale beam to study the vertical and horizontal dynamic stability.

References

Ashteyat, Ahmed M, Rami H. Haddad, and Muhannad Ismeik, (2014), « Prediction of mechanical properties of post-heated self-compacting concrete using non-destructive tests », European journal of environmental and civil engineering,vol 18, n 1, p 1-10.

Ahmed, Ali Ahmed Abdalrahman, (2015), « Production of High Strength Concrete », doctoral thesis, Sudan University of Science and Technology.

Amini K, (2016), « Effect of binder composition on time-dependentstability and robustness characteristics of self-consolidating mortar subjected to prolonged agitation », Construction and Building Materials, p. 12.

Aïssoun B. M, S.-D. Hwang, and K. H. Khayat, (2016), « Influence of aggregate characteristics on workability of super workable concrete », Materials and Structures, vol. 49, no 1-2, p. 597-609.

Al qadi, A N S, Mahmoud BA Alhasanat, Dahamsheh Ahmad AL, Al Zaiydneen Sleiman, (2016), « Using of box-benken method to predict the compressive strength of self compacting concrete containing Wadi Musa bentonite », Jordan. Am. J. Eng. AppliedSci, vol. 9, p. 406-411.

Al qadi, Arabi ns, (2017), « Estimating contours and desirability of the j-ring test on self-compacting concrete », Proceedings of IEEEFORUM International Conference, 23rd July, 2017, Mumbai, India.

Alyousef R, Benjeddou O, Soussi C, Khadimallah M A, Mustafa Mohamed A, (2019), « Effects of incorporation of marble powder obtained by recycling waste sludge and limestone powder on rheology, compressive strength, and durability of self-compacting concrete », Advances in Materials Science and Engineering, 2019: 1-15.

Allali I, Belagraa L, Beddar M, and Kessal O, (2020), « Study of the effect of silica fume on the mechanical response of à self compacting concrete using non destructive testing methods (NDT) », Academic Journal of Civil Engineering, vol 38, no 2, p 180-183.

Alani, Nibras Y., Al-Jumaily, Ibrahim A, and Hilal, Nahla, (2021), « Effect of nanoclay and burnt limestone powder on fresh and hardened properties of self-compacting concrete», Nanotechnology for Environmental Engineering, vol. 6, no 1, p. 1-26.

References

Al-Oran, Abdallah Adnan Abdallah, Safiee, Nor Azizi, and Nasir, Noor Azline Mohd, (2022), « Fresh and hardened properties of self-compacting concrete using metakaolin and GGBS as cement replacement », European Journal of Environmental and Civil Engineering, vol. 26, no 1, p. 379-392.

Baron J, Assocuation Technique de l'industrie des Liants Hydrauliques et Ecole Française du Béton, (1999), Les béton : bases et données pour leur formulation (3e tirage). Eyrolles.

Bonen D, and Shah S P, (2005), « Fresh and hardened properties of self-consolidating concrete ». Progress in Structural Engineering and Materials, 7(1), 14-26.

Beeralinge gowda B, Gundakalle, V D, (2007), « The effect of addition of limestone powder on the properties of self-compacting concrete », International Journal of Innovative Research in Science, Engineering and Technology (An ISO 3297: 2007 Certified Organization), 2(9).

Belghit Chahine, (2009), « contribution à la formulation d'un béton autoplaçant a base de materiaux locaux effet du laitier granulé micronisé sur l'ouvrabilité », Magister's Memoir, 2009 at the university of Badji Moukhtar –Annaba- .

Bouakkaz Mohammed El Amin, (2012), « Caractérisation du béton par les méthodes non destructives – application de la methode de frequence de resonance », magister's memoir, University of Abou Bekr Belkaid – Tlemcen.

Bouziani Tayeb, (2013), « Assessment of fresh properties and compressive strength of self-compacting concrete made with different sand types by mixture design modelling approach », Construction and Building Materials, vol. 49, p. 308-314.

Bensalem S, Amouri C, Houari H, and Belachia M, (2014), « Elaboration and characterization of self-compacting concrete based on local by-products », International Journal of Engineering, Science and Technology, Vol 6, N°1, p 98-105.

Belagraa Larbi, (2015), « Formulation et caractérisation d'un béton recyclé local », doctoral thesis, 2015 à the university of Mohamed Boudiaf - M'sila.

References

Benaicha M, O. Jalbaud, X Roguiez, A Hafidi Alaoui, and Y Burtschell, (2015), « Prediction of Self-Compacting Concrete homogeneity by ultrasonic velocity », Alexandria Engineering Journal, vol. 54, no 4, p. 1181-1191.

Bederina M, Hadjoudja M, Dheilly RM, Makhloufi Z, Quéneudec M, (2016), « Combined effect of sand grain size and contents of wood and filler on the physico mechanical properties and the microstructure of light weight sand concrete », Journal of adhesion science and Technology, vol 30, no 13, p 1391-1412.

Benjeddou O, Soussi C, Jedidi, M, Benali M, (2017), « Experimental and theoretical study of the effect of the particle size of limestone fillers on the rheology of self compacting concrete », Journal of Building Engineering, 10: 32-41.

Benaicha M, Belcaid A, Alaoui, AH, Jalbaud O, Burtschell Y, (2019), « Effects of limestone filler and silica fume on rheology and strength of self-compacting concrete », Structural Concrete, 20 (5) : 1702-1709.

Belouadah, M., Rahmouni, Z.E., Tebbal, N., Hicham, M.E.H, (2021), « Evaluation of concretes made with marble waste using destructive and non-destructive testing », In Annales de Chimie-Science des Matériaux, 45(5): 361-368.

Benjeddou, Omrane, Alwetaishi, Mamdooh, Tounsi, Morched, (2021), « Effects of limestone filler fineness on the rheological behavior rofcement–Limestone filler grouts », Ain Shams Engineering Journal, vol. 12, no 4, p. 3569-3578.

Bharathi, K P P, Adari, S K , and Pallepamula, Urmila, (2022), « Mechanical properties of self-compacting concrete using steel slag and glass powder », Journal of Building Pathology and Rehabilitation, vol 7, no 1, p 1-10.

Cotto-Ramos, Anamarie, (2020), « Experimental design of concrete mixtures using recycled plastic, fly ash, and silica nano particles », Construction and Building Materials, vol 254, p 119207.

References

Cui W, W Yan, H Song, and X Wu, (2020), « DEM simulation of SCC flow in L-Box set-up: Influence of coarse aggregate shape on SCC flowability », Cement and Concrete Composites, vol. 109, p. 103558.

Cristofaro M T, S Viti, and M Tanganelli, (2020), « New predictive models to evaluate concrete compressive strengthusing the SonRebmethod », Journal of Building Engineering Vol 27, p 100962.

Çelik, Zinnur, Bingöl, Ahmet Ferhat, and Ağsu, Ayhan Soner, (2022), « Fresh, mechanical, sorptivity and rapid chloride permeability properties of self-compacting concrete with silica fume and fly ash. Iranian Journal of Science and Technology, Transactions of Civil Engineering », vol. 46, no 2, p. 789-799.

Dreux G and Festa J, (1995), « Nouveau Guide du Béton », 7éme édition, EYROLLES, Paris, France, ISBN2-212-10230-5.

Djebri Noura, (2018), « Formulation et caractérisation d'un béton autoplaçant fibré à base de matériaux locaux exposé aux hautes températures », doctoral thesis, 2018 at the university of Mohamed Boudiaf - M'sila.

Daoud, Osama Mohamed Ahmed and Mahgoub, O. S, (2020), « Effect of limestone powder on self-compacting concrete », FES Journal of Engineering Sciences, vol. 9, no 2, p. 71-78.
De larrard F, (2000), « Structures granulaires et formulation des bétons », Ouvrage du Laboratoire Central des Ponts et Chaussées, p. 249-254.

El hilali, (2009), « Etude expérimentale de la rhéologie et du comportement des bétons autoplaçants (BAP) ; Influence des Fines Calcaires et des Fibres Végétales », doctoral thesis, 2009 at the university of Cergy-Pontoise.

Erdem S, (2014), « X-ray computed tomography and fractal analysis for the evaluation of segregation resistance, strength response and accelerated corrosion behaviour of self-compacting lightweight concrete », Construction and Building Materials, vol. 61, p. 10-17.

References

Esmaeilkhanian B, K H Khayat, A Yahia, and D Feys, (2014), « Effects of mix design parameters and rheological properties on dynamic stability of self-consolidating concrete », Cement and Concrete Composites, vol. 54, p. 21-28.

Elsayed, Mahmoud, Tayeh, Bassam A., Aisheh, Yazan I, Abu, (2022), « Shearstrength of eco-friendly self-compacting concrete beams containing ground granulated blast furnaceslag and flyash as cement replacement », Case Studies in Construction Materials, vol. 17, p. e01354.

Fang, Chuanxin, and Samuel Labi (2020), « Image-processing technology to evaluate static segregation resistance of hardened self-consolidating concrete », Transportation research record 2020.1 (2007): 1-9.

Faraj, Rabar H, Mohammed, Azad A, and Omer, Khalid M, (2022), « Modeling the compressive strength of eco-friendly self-compacting concrete incorporating ground granulated blast furnace slag using soft computing techniques ». Environmental Science and Pollution Research, p. 1-20.

Goupy, Jacques L, (1990), « Étude comparative de divers plans d'expériences », Revue de statistique appliquée, vol. 38, no 4, p. 5-44.

Goodier Chris I, (2003), « Development of self-compacting concrete », Proceedings of the Institution of Civil Engineers-Structures and Buildings, vol. 156, no 4, p. 405-414.

Giuseppe Faella, Guadagnuolo Mariateresa, Donadio Alfonso, Ferri Luca, (2011), « Calibrazion esperimental edelmetodo SonReb per costruzioni della Provincia di Casertadegli anni’60’80." Proceedings of the 14 th Anidis Conference, Bari, Italia.

Ghoddousi P, A AShirzadi Javid, and J Sobhani, (2014), « Effects of particle packing density on the stability and rheology of self consolidating concrete containing mineral admixtures », Construction and Building Materials, vol. 53, p. 102-109.

Gökçe, H Süleyman, and Ö. Andiç-Çakır, (2018), « A new method for determination of dynamic stability of self-consolidating concrete: 3-Compartment sieve test », Construction and Building Materials, p 305-312.

Hassan El-Chabib, and Moncef Nehdi, (2006), « Effect of Mixture Design Parameters on Segregation of Self-Consolidating Concrete », ACI Mater. J., vol. 103, no 5.

References

Hannachi S, and Guettache M N, (2011), « Le contrôle non destructif des ouvrages en béton, Evaluation de la résistance du béton a la compression sur site: application de la méthode combinée», Sciences & Technologie B, Sciences de l'ingénieur, p. 09-14.

Hosseinpoor Masoud, (2016), « Numerical simulation of fresh scc flow in wall and beam elements using flow dynamics models », doctoral thesis, 2016 at University of sherbrooke Canada.

Hosseinpoor Masoud, H Khayat Kamal, Yahia Ammar, Mesbah Habib A, (2016), « Homogeneous Analysis of Self-Consolidating Concrete (SCC) Casting in Reinforced Beam Using Computational Fluid Dynamics (CFD) », Washington DC, USA 15-18 May 2016 Edited by Kamal H. Khayat, p 549.

Hosseinpoor Masoud, Kamal H Khayat, and Ammar Yahia, (2017), « Numerical simulation of self-consolidating concrete flow as a heterogeneous material in L-Box set-up : coupled effect of reinforcing bars and aggregate content on flow characteristics », Materials and Structures, Vol 50, N° 2, p 1-15.

Hosseinpoor Masoud, Kamal H. Khayat, and Ammar Yahia, (2017), « Numerical simulation of self-consolidating concrete flow as a heterogeneous material in L-Box set-up: Effect of rheological parameters on flow performance », Cement and Concrete Composites, Vol 83, p 290-307.

Habibi, Alireza, Ghomashi, Jian, (2018), « Development of an optimum mix design method for self-compacting concrete based on experimental results », Construction and Building Materials, vol. 168, p. 113-123.

Hamla, Wafa, Dalila Benamara, Ammar Noui, (2022), « Statistical modeling of physical and mechanical responses of roller-compacted sand concrete made with ternary sand using the experimental design method », Construction and Building Materials, vol 345, p 128354.

Hilal Nahla N, Alobaidi Yusra M, Al-Hadithi Abdulkader Ismail, (2022), « Viability of cellulose nano fibre powder and silica fume in self-compacting concrete rheology, hardened properties, and microstructure », Journal of King Saud University - Engineering Sciences.

References

Navarrete I, M. Lopez, (2017), « Understanding the relationship between the segregation of concrete and coarse aggregate density and size », Construction and Building Materials, vol. 149, p. 741-748.

John H, Bungey, Michael G Grantham, (2006), «Testing of concrete in structures», Crc-Press.

Khan R A, Sharma A, (2016), « Effect of lime powder and metakaolin on fresh and hardened properties of self compacting concrete », Journal of Materials and Engineering Structures «JMES», 3(4) : 161-166.

Kherraf Leila, (2018), « Effets de l'interaction ciment-polyadditions-adjuvant sur les propriétés des bétons », doctoral thesis, 2018 at the university of 20 Aout 1955 - Skikda.

Daddy Kabagire, (2018), « Modélisation expérimentale et analytique des propriétés rhéologiques des bétons autoplaçants », doctoral thesis, 2018 at university ofsherbrooke Canada.

Kenai Said, (2018), « Non-destructive testing and evaluation of concrete structures», cours at Algerian American Foundation summer university, USTHB.

Koura B.-I. O., M. Hosseinpoor, and A. Yahia, (2020), « Coupled effect of fine mortar and granular skeleton characteristics on dynamicstability of self-consolidating concrete as a diphasic material », Construction and Building Materials, vol. 263, p. 120131.

Karimipour, Arash, Jahangir, Hashem, and Eidgahee, Danial Rezazadeh, (2021), « A thorough study on the effect of redmud, granite, limestone and marble slurry powder on the strengths of steel fibres-reinforced self-consolidation concrete : Experimental and numerical prediction ». Journal of Building Engineering, vol. 44, p. 103398.

Karakurt, Cenk, Dumangöz, Mahmut, (2022), « Rheological and Durability Properties of Self-Compacting Concrete Produced Using Marble Dust and Blast Furnace Slag », Materials, vol. 15, no 5, p. 1795.

Kavitha, Sajjala and Ashwini, D. G, (2022), « Experimental Investigations on Durability Characteristics of Bamboo Fiber Reinforced Self-Compacting Concrete with GGBS and Alccofine », ECS Transactions, 2022, vol 107, no 1, p 7661.

References

Lin Shen, Leslie Struble, and David Lange, (2005), « Testing static segregation of SCC. » SCC2005, Proceedings of the 2nd North American conference on the design and use of SCC.

Lin Shen, Leslie Struble, and David Lange, (2009), « Modeling Dynamic Segregation of Self-Consolidating Concrete », ACI Materials Journal, vol. 106, no 4.

Libre, N A, R Khoshnazar, and M Shekarchi, (2010), « Relationship between fluidity and stability of self-consolidating mortar incorporating chemical and mineral admixtures », Construction and Building Materials, p. 10.

Lin Shen, H. B. Jovein, and M. Li, (2014) « Measuring static stability and robustness of self-consolidating concrete using modified Segregation Probe », Construction and Building Materials, vol. 70, p. 210-216.

Laifa Walid, (2015), « contribution à l'étude des effets du laitier cristallisé et des fibres de diss sur les propriétés des bétons autoplaçants », doctoral thesis, at the university of Badji Mokhtar à Annaba.

Lin Shen, Jovein Hamed Bahrami, and Wang, Qian, (2016), « Correlating aggregate properties and concrete rheology to dynamic segregation of self-consolidating concrete ». Journal of Materials in Civil Engineering, vol. 28, no 1, p. 04015067.

Liu, Miaomiao, Carlos Jimenez-Bescos, and John Calautit, (2022), « CFD investigation of a natural ventilation windtower system withsolid tube banks heatre covery for mild-cold climate », Journal of Building Engineering, Vol45, p 103570.

Lee Jaewon, Sunghyun CHO, Hyungtae CHO, Moon I, Kim J. (2022), « CFD modeling on natural and forced ventilation during hydrogen leaks in a pressure regulator process of a residential area », Process Safety and Environmental Protection, Vol161, p 436-446.

Mehdipour I, M. S. Razzaghi, K. Amini, and M. Shekarchi, (2013), « Effect of mineral admixtures on fluidity and stability of self-consolidating mortar subjected to prolonged mixing time », Construction and Building Materials, vol. 40, p. 1029-1037.

References

Menut, Marine, Bou-Said, Benyebka, Le Berre, Hélène Walter, (2016), « Characterization of the aorticarch behaviour and CFD simulations validaded with 4D Cardiovascular MRI », In : 22d congress of the European Society of Biomechanics. p. 1 p.

Menut Marine, Bou-Said Benyebka, Le Berre Hélène Walter, Escriva Xavier, Yann, (2017), « Patient-specific CFD simulations using MPTT rheological model with 4D cardiovascular MRI validation », 23 rd Congress of the European Society of Biomechanics.

Mesbah H. A, A. Yahia, Khayat K H, (2011), « Electrical conductivity method to assess static stability of self-consolidating concrete », Cement and Concrete Research, vol. 41, no 5, p. 451-458.

Mohammad Musa Alami, (2014), « Development of a new test method to evaluate dynamic stability of self-consolidating concrete», Thesis of master, İzmir Institute of Technology.

Mesbah A H, Abelkrim Laraba, Ammar Yahia. (2016), « Flowability and Stability Performance of Self-Consolidating Concrete in Full-Scale Beam », 8th International RILEM Symposium on Self-Compacting Concrete, Washington, DC, United States. Conference Proceedings.

Mohan, Ardra and Mini, K. M, (2018), « Strength and durability studies of SCC incorporating silica fume and ultra fine GGBS », Construction and Building Materials, vol. 171, p. 919-928.

Mohammed, Aseel Madallah, Asaad, Diler Sabah, and Al-Hadithi, Abdulkader I, (2022), « Experimental and statistical evaluation of rheological properties of self-compacting concrete containing flyash and ground granulated blast furnace slag », Journal of King Saud University-Engineering Sciences, vol. 34, no 6, p. 388-397.

Naji. S, K. H. Khayat, M. Karray, (2017), « Assessment of staticstability of concrete using shear wavevelocity approach », ACI Materials Journal, vol. 114, no 1.

Nili, Mahmoud, Razmara, M. Nili, (2017), « Proposing new methods to appraise segregation resistance of self-consolidating concretebased on electrical resistivity », Construction and Building Materials, vol. 146, p. 192-198.

References

Nili M, M. Razmara, (2018), « Proposing a New Apparatus to Assess the Properties of Self-Consolidating Concrete », Journal of Testing and Evaluation, vol. 48, no 4, p. 3188-3201.

Nepomuceno, Miguel CS, and Luís FA Bernardo, (2019), « Evaluation of self-compacting concrete strengthwith non-destructive tests for concrete structures », Applied Sciences vol 9 no 23 p 5109.

Nguyen, Y. Quoc, and al, (2022), « CFD Analysis of Different Ventilation Strategies for a Room with a Heated Wall », Buildings, Vol 12, N° 9, p 1300.

Okamura H, Ouchi M, (1999), « Self-compacting concrete, Development, present use and future », RILEM PRO7, p. 3-14.

Okamura H, Ozawa K, Ouchi M, (2000), « Self-compacting concrete », Structural Concrete, n° 1, p. 3-17.

Okamura H, and Ouchi M, (2003), « Self-Compacting Concrete », Journal of Advanced Concrete Technology, 1(1), 5-15.

Petrou M. F, K. A. Harries, F. Gadala-Maria, V. G. Kolli, (2000), « A unique experimental method for monitoring aggregate settlement in concrete », Cement and Concrete Research, p. 8.

Paki Turgut, Kazim Turk, Hasan Bakirci, (2012), « Segregation control of SCC with a modified L-box apparatus », Magazine of concrete research, p 707–716.

Panesar, D. K, B. Shindman, (2012), « The effect of segregation on transport and durability properties of self consolidating concrete », Cement and Concrete Research, vol. 42, no 2, p. 252-264.

Preda C, R M Bleotu R. M, Pinca-Bretotean C, (2022), « Study and thermal analysis of vanes shape design for brake disc in automotive industry », Journal of Physics : Conference Series. Vol. 2212. No. 1. IOP Publishing.

References

Qin, Daqiang, Dong, Chunru, Zong, Zhenyu, (2022), « Shrinkage and Creep of Sustainable Self-Compacting Concrete with Recycled Concrete Aggregates, Fly Ash, Slag, and Silica Fume ». Journal of Materials in Civil Engineering, vol. 34, no 9, p. 04022236.

Roussel Nicolas, (2008), « Thixotropie des bétons modernes: Modélisation et application », Laboratoire Central des Ponts et Chaussées, Paris, France : p1-9.

Revilla-Cuesta Víctor, Skaf Marta, Serrano-Lopez, Ortega-Lopez Vanesa, (2021), « Models for compressive strength estimation through non-destructive testing of highly self-compacting concrete containingr recycled concrete aggregate and slag-based binder », Construction and Building Materials, vol 280, p 122454.

Rautaray, Subodha Kumar, Bera, Dillip Kumar, Rath, A K, (2022), « The Effects of Ground Granulated Blast-Furnace Slag Blending with Fly Ash Based Self Compacting Geo-polymer Concrete on the Workability and Strength Properties at Ambient Curing », In : Recent Developments in Sustainable Infrastructure (ICRDSI-2020) Structure and Construction Management. Springer, Singapore, p 567-579.

Rahman, O. Abdel and Soliman, A, (2023), « Properties of Sustainable Self-CompactingMortar Incorporating Limestone Filler », In : Canadian Society of Civil Engineering Annual Conference. Springer, Singapore, p 571-579.

Sedran T, (1999), « Rhéologie et rhéométrie des bétons. Applications aux bétons autonivellants », thesis of LCPC.

Sedran T, De larrard F, (1999), « Optimization of self-compacting concrete thanks to packing model », RILEM PRO7, p. 321-332.

Sonebi Mohammed, (2004), « Medium strength self-compacting concrete containing fly ash: Modelling using factorial experimental plans », Cement and Concrete research, vol. 34, no 7, p. 1199-1208.

References

Solis-Carcaño, Rómel, Moreno, Eric I, (2008), « Evaluation of concrete made with crushed limestone aggregate based on ultrasonic pulse velocity », Construction and Building Materials, vol 22, no 6, p.1225-1231.

Spangenberg Jon, Roussel N, Hattel J H, Sarmiento E V, Zirgulis G, and Geiker M R, (2012), « Patterns of gravity induced aggregate migration during casting of fluid concretes », Cement and Concrete Research., vol 42, no 12, p. 1571-1578.

Shekireb sihem, (2015) « Valorisation De La Poudre De Verre Dans Le Béton Autoplaçant », Master's thesis, Sherbrooke (Québec) Canada.

Singh, Navdeep , Singh S P, (2018), « Evaluating the performance of self compacting concretes made with recycled coarse and fine aggregates using non destructive testing techniques », Construction and Building Materials, vol. 181, p. 73-84.

Skender Z, Bali A, Kettab R, (2021), « Self-compacting concrete (SCC) behaviour incorporating limestone fines as cement and sand replacement », European Journal of Environmental and Civil Engineering, 25(10) : 1852- 1873.

Salehi, Saeed, Håkan Nilsson, (2022), « Effects of uncertainties in positioning of PIV plane on validation of CFD results of a high-head Francis turbine model », Renewable Energy Vol 193, p57-75.

Solouki, Abbas, Piergiorgio Tataranni, Cesare Sangiorgi, (2022), « Mixture Optimization of Concrete Paving Blocks Containing Waste Silt », Sustainability, vol14, n 1, p 451.

Tregger Nathan, Gregori A, Ferrara L, S Shah, (2012), « Correlating dynamic segregation of self-consolidating concrete to the slump-flow test », Construction and Building Materials, p 499-505.

Takahashi Yuki, Fujimori Y, Hu F, Shen X, Kimura N, (2015), « Design of trawlotter boards using computational fluid dynamics », Fisheries Research, Vol161, p 400-407.

Tenza-Abril, A J, D Benavente, C Pla, F Baeza-Brotons, J Valdes-Abellan, A MSolak, (2020), « Statistical and experimental study for determining the influence of the segregation phenomen

on on physical and mechanical properties of lightweight concrete », Construction and Building Materials, vol. 238, p. 117642.

Tripathi Deep, Kumar R, Mehta PK, (2022), « Evaluation of a sustainable self compacting concrete using destructive and non-destructive testing », Materials Today:Proceedings, vol 58, p. 830-835.

Van Khanh B, Denis Montgomery, (1999), « Mixture porportioning method for self-compacting high performance concrete with minimum paste volume », RILEM PRO7, p. 373-384.

Velrajkumar G, Muralikrishnan R, Mohan A, (2022), « Performance of GGBFS and silica fume on self compacting geopolymer concrete using partial replacements of R-Sand », Materials Today : Proceedings, vol. 59, p. 909-917.

Vivek, S S, (2022), « Performance of ternary blend SCC with ground granulated blast furnace slag and metakaolin ». Materials Today : Proceedings, vol. 49, p. 1337-1344.

WescheK, (1955), « Possibilities for the application of ultra sounds in concrete testing ». Bautechnik, vol 32, p 151-155.

Wong H H C, Kwan A K H, (2008), « Packing density of cementitious materials: part 1 measurement using a wetpacking method », Materials and Structures, vol. 41, no 4, p. 689-701.

Yan, Wenlong, Gang Wu, Zhiqiang Dong, (2019), « Optimiztion of the mix proportion for desertsand concrete based on a statistical model », Construction and Building Materials, vol 226, p 469-482.

Wang, Qing, Yao, Boyu, HE, Jianqiang, (2022), « Impact of condensed silica fume on splitting tensile strength and brittleness of high strength self-compacting concrete », Structural Concrete, vol. 23, no 1, p. 604-618.

Yim, H J, Y H Bae, J. H. Kim, (2020), « Method for evaluating segregation in self-consolidating concrete using electrical resistivity measurements », Construction and Building Materials, vol. 232, p. 117283.

References

Yang, Song, Zhang, Jingbin, AN, Xuehui, (2021), « Effects of fly ash and limestone powder on the paste rheological thresholds of self-compacting concrete » Construction and Building Materials, vol. 281, p. 122560.

Yang Song, Ai Zubin, Zhang Chao, Dong Shun, Ouyang Xun, Liu Rong, Zhang Ping, (2022), « Study on Optimization of Tunnel Ventilation Flow Field in Long Tunnel Based on CFD Computer Simulation Technology », Sustainability, vol 14, N°18, p 11486.

Yuce, Bahadir Erman, Peter Vilhelm Nielsen, and Pawel Wargocki, (2022), « The use of Taguchi, ANOVA, and GRA methods to optimize CFD analyses of ventilation performance in buildings », Building and Environment, vol 225, p 109587.

Zhao Hui, Sun Wei, WU Xiaoming, Gao Bo, (2015), « The properties of the self-compacting concrete with fly ash and ground granulated blast furnace slag mineral admixtures », Journal of Cleaner Production, vol. 95, p. 66-74.

Zhang Zedi, XiaoJia, Zhang Qing, (2021), « A state-of-the-art review on the stability of self-consolidating concrete », Construction and Building Materials, vol. 268, p. 121099.

Zied Benghazi, (2021), « Amélioration des proprietés rhéologiques et mécaniques des bétons autoplaçants à base de matériaux locaux. », doctoral thesis, 2021, at he university of M'sila.

Zhanggen Guo, Zhang Jing, Jiang Tao, Jiang Tianxun, Chen Chen, Bo Rui, Sun Yan, (2022), « Development of sustainable self-compacting concrete using recycled concrete aggregate and flyash, slag, silica fume », European Journal of Environmental and Civil Engineering, vol. 26, no 4, p. 1453-1474.

References

Standards

Règles B.A.E.L, (1991), Régles techniques de conception et de calcul des ouvrages et constructions en béton armé, suivant la méthode des états limites, édition EYROLLES, France.

« RILEM draft recommendation, for in situ concrete strength determination by combined non-destructive methods », (1993), Materials and Structures, vol 26, p 43-49.

EFNARC, (2002), « Self compacting concrete».

AFGC, (2008), « Recommandations pour l'emploi des Bétons Auto-Plaçants » ASSOCIATION FRANÇAISE DE GÉNIE CIVIL. Recommandations pour l'emploi des bétons auto-plaçants: ecommendations for use of self-compacting concrete.

NF EN 12620+A1, (2008), « Granulats pour béton ».

NF EN 12350-9, (2010), « Essai d'étalement a l'entonnoir ».

NF EN 12350-10, (2010), « Essai dela boite en L ».

NF EN 12350, (2010), « Essai de stabilité au tamis ».

EN NF 934-2+A1, (2012), « Adjuvants pour bétons, mortier et coulis - Partie 2 : adjuvants pour béton - Définitions, exigences, conformité, marquage et étiquetage ».

NF EN 12350-8, (2019), « Essai d'étalement au-cône ».

NF EN 197-1, (2020), « Composition des ciments courants ».

NF EN 12350-9, (2010), « Essaid'étalement a l'entonnoir ».

NF EN 12350-10, (2010), « Essai de la boite en L ».

NF EN 12350-12, (2010), « Essaid'écoulement a l'a l'anneau ».

NF EN 12350, (2010), « Essai de stabilité au tamis ».

NF EN 206+A2/CN, (2020), « Classification des bétons ».

References

ASTM C1712-20, (2020), « Test method for rapid assessment of static segregation resistance of self-consolidating concrete using penetration test ».

ASTM C1611/C1611M-18, (2021), « Standard test method for slump flow of self-consolidating concrete ».

ASTM C1610/C1610M-19, (2021), « Standard test method for static segregation of self-consolidating concrete using column technique ».

NF EN 12390-6, (2012), « détermination de la résistance en traction par fendage d'éprouvettes ».

NF EN 12390-3, (2019), « Résistance à la compression des éprouvettes ».

NF EN 12390-5, (2019), «Résistance à la flexion des éprouvettes ».

NF EN 12504-2, (2021), « essais non destructifs - Détermination de l'indice de rebondissement ».

NF EN 12504-4, (2021), « détermination de la vitesse de propagation des ultrasons ».

Annex

ALCAL UF5

Fiche Technique

Le gisement El-khroub occupe la partie sud ouest du massif Oum Settas au sud-est de Constantine, il est constitué de calcaire d'origine *néritique caractérisé* par une grande pureté chimique et une blancheur élevée.

Caractéristiques chimiques

$CaCO_3$	99,61%
CaO	55,94%
SiO_2	0,04%
Na_2O	0,05%
AL_2O_3	0,03%
MgO	0,20%
Fe_2O_3	0,02%
K_2O	0,01%
P_2O_5	0,01%
TIO_2	0,01%
SO_3	0,02%
Perte au feu	43,67%
Ph	9

Caractéristiques physiques

Dureté (Mohs):	3
Poids spécifique:	2,7
Densité apparente non tassée:	0,80g /cm³
Blancheur (ELREPHO 070):	L*≥96, a* ≤+0.50, b*≤+3.5
Prise d'huile (NF.T30.022):	21g/100g de poudre
Humidité à l'ensachage:	0,02%
Indice de réfraction:	1,71%

Les elements toxiques:

Cyanure	0,045 µg / gr
Mercure	0,35 µg / gr
Arsenic	0,08 µg / gr
Fluor	0,02mg / gr

Répartition granulométrique

Inférieur à 3 µm : 13% Diamètre médian : 6,62µm Inférieur à 20µm : 98,35%

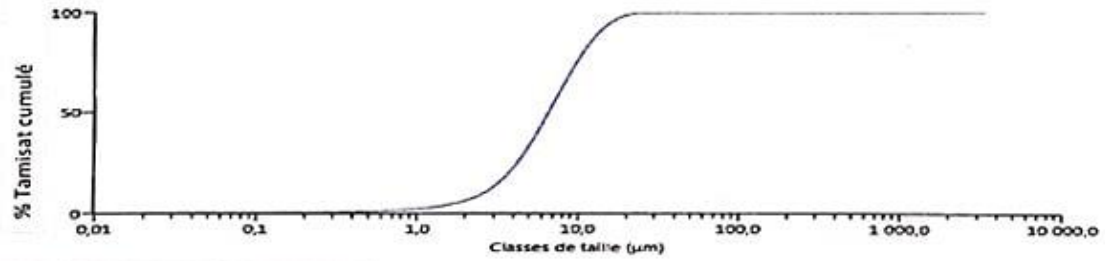

diffraction laser (3000)

Les valeurs figurants dans cette fiche technique sont des valeurs caractéristiques moyennes de la production

Conditionnement

Big-bag (1tonne)
Palettes houssées (48 sacs de 25kg)

Principales utilisations

Peinture mate et satinée en phase aqueuse et phase solvant.
Peinture en poudre hydrodispersible
Peinture routière et Peinture industrielle
P V C plastifié
Caoutchouc et plastique industriel
Différentes colles
Composites
Etanchiété, isolation
Câblerie
boue de forage

DG : ZI Gué de Constantine Alger tél : 021 83 93 86 / 021 83 93 87 / Fax: 021 - 83 93 84 / Site WEB ENG (W W W.eng-spa.dZ)
Usine Carbonate de Calcium El -khroub W. Constantine Tél: 031 95 41 76 / 95 41 14 Fax: 031 95 41 13 E-mail : elkhroubcaco3 @ eng.dz

mai-18

ALCAL UF10

Fiche technique

Le gisement El-khroub occupe la partie sud ouest du massif Oum Settas au sud-est de Constantine, il est constitué de calcaire d'origine néritique caractérisé par une grande pureté chimique et une blancheur élevée.

Caractéristiques chimiques

$CaCO_3$	99,61%
CaO	55,94%
SiO_2	0,04%
Na2O	0,05%
AL2O3	0,03%
MgO	0,20%
Fe2O3	0,02%
K2O	0,01%
P2O5	0,01%
TiO2	0,01%
SO3	0,02%
Perte au feu	43,67%
Ph	9

Caractéristiques physiques

Dureté (Mohs):	3
Poids spécifique :	2,7
Densité apparente non tassée:	0,90
Blancheur (ELREPHO 070):	L* ≥ 95 ; a*≤ 0,55 ; b*≤4
Prise d'huile (NF.T 30.022):	19g/100g de poudre
Humidité à l'ensachage:	0,02%
Indice de réfraction:	1,71

Les éléments toxiques:

Cyanure	0,045 µg / gr
Mercure	0,35 µg / gr
Arsenic	0,08 µg / gr
Fluor	0,02mg / gr

Répartition granulométrique

Inférieur à 5µm :23% Diamètre médian : 9,09 µm Inférieur à 40µm : 99%

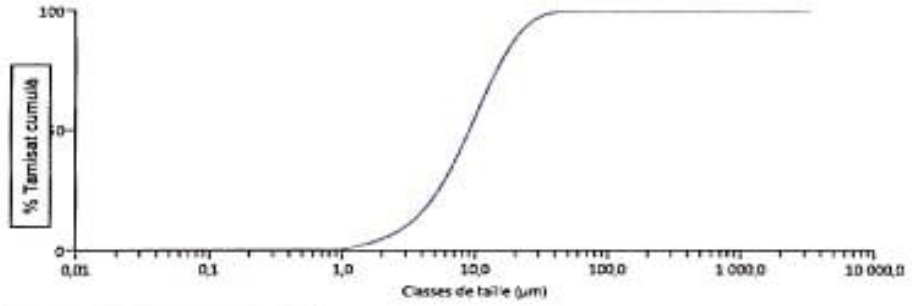

diffraction laser (3000)

Conditionnement

Big-bag (1tonne)
Palettes houssées (48 sacs de 25kg)

Principales utilisations

Peinture mate à phase aqueuse et phase solvant
Peinture en poudre hydrodispersible
Polyesters
Colle
Pâte à chewin-gum
Caoutchouc
Céramique sanitaire
Fabrication de craie
Pâte à modeler
boue de forage

DG : Z.I Gué de Constantine Alger tél: 021 83 93 86 / 021 83 93 87 /Fax: 021 - 83 83 84 / Site WEB ENG (W W W.eng-epa.dz)
Usine Carbonate de Calcium El -Khroub W. Constantine. Tél: 031 95 41 76 / 95 41 14. Fax: 031 95 41 13 E-mail : elkhroubcaco3 @ eng.dz

mai-10

Annex

ALCAL F20

Fiche technique

Le gisement El-khroub occupe la partie sud ouest du massif Oum Settas au sud-est de Constantine, il est constitué de calcaire d'origine néritique caractérisé par une grande pureté chimique et une blancheur élevée.

Caractéristiques chimiques

CaCO3	99,61%
CaO	55,94%
SiO2	0,04%
Na2O	0,05%
AL2O3	0,03%
MgO	0,20%
Fe2O3	0,02%
K2O	0,01%
P2O5	0,010%
TiO2	0,010%
SO3	0,0200%
Perte au feu	43,67%
Ph	9

Caractéristiques physiques

Dureté (MOHS) :	3
Poids spécifique :	2,7
Densité apparente non tassée :	1,16
Prise d'huile (NF.T 30.022):	18g/100g de poudre
Humidité à l'ensachage :	0,001%
Indice de réfraction :	1,71

Répartition granulométrique

Inférieur à 10µm : 20%

Inférieur à 200µm : 99%

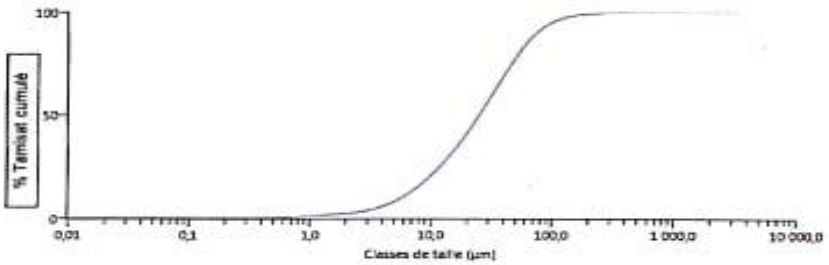

diffracion laser (3000)

Les valeurs figurants dans cette fiche technique sont des valeurs caractéristiques moyennes de la production

Conditionnement

Big-bag (1tonne)
Palettes houssées (48 sacs de 25kg)

Principales utilisations

Poudre et crème à récurer
Améliorant de pain
Détergent
Faïence
Etanchéité
boue de forage

DG : Z.I Gué de Constantine Alger tel: 021 83 83 86 / 021 83 83 87 Fax: 021 - 83 83 84 / Site WEB ENG (W W W.eng-spa.dz)
Usine Carbonate de Calcium El-khroub W. Constantine Tél: 031 95 41 79 / 95 41 14 Fax: 031 95 41 13 E-mail : elkhroubcaco3 @ eng.dz

mai-18

BUILDING TRUST

NOTICE PRODUIT
Sika® ViscoCrete® TEMPO 12

SUPERPLASTIFIANT / HAUT RÉDUCTEUR D'EAU

NF

INFORMATIONS SUR LE PRODUIT

Sika® ViscoCrete® TEMPO 12 est un superplastifiant/haut réducteur d'eau polyvalent de nouvelle génération à base de polycarboxylates.

DOMAINES D'APPLICATION

Sika® ViscoCrete® TEMPO 12 permet la fabrication de tout type de béton de consistance plastique à autoplaçante.

- Béton autoplaçant ou autonivelant
- Béton à long maintien d'ouvrabilité sans effet retard de prise
- Béton à faible rapport E_{eff}/C
- Béton à haute ou très haute performance
- Béton pompé sur de très longues distances
- Bétonnage par temps chaud
- Béton pour ouvrages fortement ferraillés
- Chapes autonivelantes

CARACTÉRISTIQUES / AVANTAGES

De part sa formulation spécifique, Sika® ViscoCrete® TEMPO 12 est particulièrement recommandé pour les ciments à faible ou moyenne teneur en sulfates alcalins. Sa capacité à conférer un long maintien d'ouvrabilité lui permet de s'adapter facilement à des ciments faiblement demandeurs en adjuvants.
Son caractère polyvalent permet de s'adapter à tout type de matériaux et à une large gamme de ciments.

AGRÉMENTS / NORMES

Marquage CE et NF selon la norme NF EN 934-2 tab 3.1 et 3.2.

DESCRIPTION DU PRODUIT

Conditionnement	▪ Fût de 217 L ▪ CP de 1000 L ▪ Vrac
Aspect / Couleur	Liquide brun clair
Durée de Conservation	12 mois dans son emballage d'origine intact.
Conditions de Stockage	A l' abri du gel. En cas de gel accidentel, le produit retrouve ses qualités d'origine une fois dégelé lentement et réhomogénéisé.
Densité	1,060 ± 0,020
Valeur pH	5,5 ± 1,0
Extrait Sec	29,5 ± 1,4% (méthode halogène selon NF 085) 29,5 ± 1,4% (NF EN 480-8)
Teneur Totale en Ions Chlorure	≤ 0,1 %
Équivalent Oxyde de Sodium	≤ 1 %

Notice Produit
Sika® ViscoCrete® TEMPO 12
Février 2018, Version 01.01
021301011000000110

RENSEIGNEMENTS SUR L'APPLICATION

Dosage Recommandé	Plage de dosage : 0,1 à 5,0% du poids du liant ou du ciment selon la fluidité et les performances recherchées.

INSTRUCTIONS POUR L'APPLICATION

Sika® ViscoCrete® TEMPO 12 est ajouté, soit en même temps que l'eau de gâchage, soit en différé dans le béton préalablement mouillé avec une fraction de l'eau de gâchage.

VALEURS DE BASE

Toutes les valeurs indiquées dans cette Notice Produit sont basées sur des essais effectués en laboratoire. Les valeurs effectives mesurées peuvent varier du fait de circonstances indépendantes de notre contrôle.

RESTRICTIONS LOCALES

Veuillez noter que du fait de réglementations locales spécifiques, les données déclarées pour ce produit peuvent varier d'un pays à l'autre. Veuillez consulter la Notice Produit locale pour les données exactes sur le produit.

ÉCOLOGIE, SANTÉ ET SÉCURITÉ

Pour obtenir des informations et des conseils sur la manipulation, le stockage et l'élimination en toute sécurité des produits chimiques, les utilisateurs doivent consulter la fiche de données de sécurité (FDS) la plus récente contenant les données physiques, écologiques, toxicologiques et autres données relatives à la sécurité. Nos FDS sont disponibles sur www.quickfds.com et sur le site www.sika.fr

INFORMATIONS LÉGALES

Les informations, et en particulier les recommandations concernant les modalités d'application et d'utilisation finale des produits Sika sont fournies en toute bonne foi et se fondent sur la connaissance et l'expérience que Sika a acquises à ce jour de ses produits lorsqu'ils ont été convenablement stockés, manipulés et appliqués dans des conditions normales, conformément aux recommandations de Sika. En pratique, les différences entre matériaux, substrats et conditions spécifiques sur site sont telles que ces informations ou recommandations écrites, ou autre conseil donné, n'impliquent aucune garantie de qualité marchande autre que la garantie légale contre les vices cachés, ni aucune garantie de conformité à un usage particulier, ni aucune responsabilité découlant de quelque relation juridique que ce soit. L'utilisateur du produit doit vérifier par un essai sur site l'adaptation du produit à l'application et à l'objectif envisagés. Sika se réserve le droit de modifier les propriétés de ses produits. Notre responsabilité ne saurait d'aucune manière être engagée dans l'hypothèse d'une application non conforme à nos renseignements. Les droits de propriété détenus par des tiers doivent impérativement être respectés. Toutes les commandes sont soumises à nos conditions générales de vente et de livraison en vigueur. Les utilisateurs doivent impérativement consulter la version la plus récente de la Notice Produit correspondant au produit concerné, accessible sur internet ou qui leur sera remise sur demande.

SIKA FRANCE S.A.S.
84 rue Edouard Vaillant
93350 LE BOURGET
FRANCE
Tél.: 01 49 92 80 00
Fax: 01 49 92 85 88
www.sika.fr

Annex

Construction

Notice Produit
Édition octobre 2015
Numéro 257
Version n° 2015-349
SIKA® STABILIZER 400

SIKA® STABILIZER 400

Agent de stabilité pour mortiers et bétons

Présentation

Sika® Stabilizer 400 est un agent de stabilité qui permet d'augmenter la résistance à la ségrégation des bétons et des mortiers, et de réduire les phénomènes de ressuage après gâchage.
Sika® Stabilizer 400, en agissant sur la consistance du mélange, permet d'augemnter la robustesse des bétons fluides et des BAP vis-à-vis des variations dans le dosage en eau.
Sika® Stabilizer 400, en améliorant l'enrobage des agrégats au sein de la pâte de ciment, protège les pompes à béton et les conduites de transport de l'usure excessive.
Sika® Stabilizer 400 facilite le pompage des mortiers et bétons contenant des fibres métalliques.

Domaines d'application

Sika® Stabilizer 400 est surtout indiqué pour les bétons à teneur en fines variable, à faible teneur en ciment, et dans tous le cas où la composition granulométrique du béton ne permet pas d'assurer un empilement optimal pour contrer la ségrégation.

Sika® Stabilizer 400 convient pour les utilisations suivantes:
- Bétons à teneur en fines variables
- Bétons formulés avec des granulats concassés
- Bétons autoplaçants avec ou sans fibres métalliques
- Chapes autonivelantes avec ou sans fibres métalliques
- Coulis d'injection
- Bétonnage de comblement

Caractères généraux

Sika® Stabilizer 400 augmente fortement la cohésion interne du béton et améliore l'enrobage des agrégats au sein de la pâte de ciment.
Sika® Stabilizer 400 permet ainsi la production courante de BAP en diminuant la sensibilité des formules aux variations dans la formulation: variations de dosages en eau ; teneur en fines des agrégats ; aléas du chantier...
Sika® Stabilizer 400 est totalement compatible avec les adjuvants traditionnels (plastifians, superplastifians, accélerateurs, rétardateurs, entraîneurs d'air).

De plus, il permet d'améliorer la mise en place sur chantier :

- Élimination des défauts de compactage
- Mise en œuvre plus économique
- Pompage aisé du béton

Sika® Stabilizer 400 ne contient ni chlorures ni autres substances favorisant la corrosion de l'acier et peut de ce fait être utilisé sans restriction pour ouvrages en béton armé et précontraint.

Caractéristiques

Coloris: Brun

Conditionnement

- Fût de 220 kg
- Container perdu de 1000 kg
- Vrac

Construction

Stockage	A l'abri du gel.
Conservation	Sika® Stabilizer 400 peut geler, mais une fois dégelé lentement et réhomogénéisé, il retrouve ses qualités d'origine. Délai de conservation en emballage intact : 6 mois.
Données techniques	
Densité	1,025 ± 0,020
pH	8,0 ± 1.0
Teneur en $Na_2O_{éq}$	≤ 0,2 %
Teneur en Cl^-	≤ 0,1%
Conditions d'application	
Dosage	Plage d'utilisation recommandée 0,1 à 2 % du poids de liant selon les performances recherchées. Ce dosage peut être augmenté jusqu'à 4% pour des applications spéciales.
Mise en œuvre	Le produit peut être utilisé en combinaison avec d'autres adjuvants, dès la formulation du béton, ou en complément de l'adjuvantation des formules existantes. Cependant, d'une manière générale, il est toujours conseillé de valider toute nouvelle formulation par des essais préliminaires.
Préparation du mélange	Sika® Stabilizer 400 est ajouté au mélange ciment/gravier à la centrale à béton après l'eau de gâchage et après l'éventuel ajustage de la quantité d'eau. Ne pas ajouter au mélange sec. L'ajustage ultérieur de la quantité d'eau a une influence minimale sur la consistance du béton ; l'eau de gâchage est directement absorbée par l'effet stabilisant du Sika® Stabilizer-400. Sika® Stabilizer 400 modifie légèrement la viscosité du béton frais, le mélange est stabilisé et ne ressue pas même s'il contient trop d'eau.
Précautions d'emploi	En cas de contact avec la peau, laver abondamment à l'eau. Consulter la fiche de données de sécurité accessible sur Internet www.sika.fr.

Mentions légales

Sika France S.A.S.
84, rue Edouard Vaillant – BP 104
93351 Le Bourget Cedex
France
Tel. : 01 49 92 80 00
Fax : 01 49 92 80 21